STUDIES ON SOME MIXED MONOMOLECULAR FILM PROPERTIES OF n-LONG CHAIN ALCOHOLS, n-ALKOXY ETHANOLS AND PROPANOLS

A Thesis Submitted to The

University of Poona

For The Degree of

DOCTOR OF PHILOSOPHY

(IN CHEMISTRY)

BY

VITTHAL SHRINIWAS KULKARNI

PHYSICAL CHEMISTRY DIVISION
NATIONAL CHEMICAL LABORATORY
PUNE 411 008. (INDIA)

JANUARY 1984

C O N T E N T S

ACKNOWLEDGEMENTS

The entire work of this thesis has been carried out under the guidance and encouragement of Dr. S.S. Katti, Assistant Director, Physical Chemistry Division, National Chemical Laboratory, Pune. By appending a customary note of acknowledgement, I will be doing great injustice to my teacher Dr. S.S. Katti, who more than richly deserves the gratitude of his students for many years to come.

My sincere thanks are also due to my colleagues, friends and relatives who rendered the help and inspired me at all stages of the work.

Mr. Dhake and Mr. Koshy made their skill and time available for the art-work of the figures and for the typing of the text respectively. I am extremely thankful to both of them for their kind help.

I am grateful to the Director, NCL, Pune for kindly permitting me to submit this work in the form of a thesis.

I am also thankful to CSIR, New Delhi, for the monetary support in the form of a research fellowship.

Vitthal S Kulkarni

Pune [VITTHAL S. KULKARNI]

January 23, 1984

Certified that work incorporated in the thesis "Studies on Some Mixed Monomolecular Film Properties of n-Long Chain Alcohols, n-Alkoxy Ethanols and Propanols" submitted by Shri Vitthal S. Kulkarni was carried out by the candidate under my supervision. Such material, as has been obtained from other sources has been duly acknowledged in the thesis.

[Dr. S.S. Katti]
Research Guide.

ABSTRACT OF THE THESIS

Measurements on some monomolecular film properties viz. surface viscosity (μ), surface pressure (π), area per molecule (A) and collapse pressure (π_c) were undertaken on various mixed monolayers at air-water interface at 25°C, with a view to understand the nature of the various two dimensional phase changes, intermolecular interactions between the two film forming components, miscibility and non-ideality.

From the literature survey it was observed that chain-chain van der Waals interactions play a vital role in miscibility and non-ideality in mixed monolayers. Therefore, a study was undertaken on mixed monolayers, where two components have the same polar group but large difference in hydrocarbon chain length. The surface viscosity - film pressure (μ-π) , film pressure area (π-A) isotherms and collapse pressure of following systems were studied.

1) Hexadecanol ($C_{16}H_{33}OH$) with Docosanol ($C_{22}H_{45}OH$)

2) Hexadecoxy ethanol ($C_{16}H_{33}OC_2H_4OH$) with Docosanoxy ethanol ($C_{22}H_{45}OC_2H_4OH$)

3) Hexadecoxy propanol ($C_{16}H_{33}OC_3H_6OH$) with Docosanoxy propanol ($C_{22}H_{45}OC_3H_6OH$).

All the mixed monolayers exhibited non-Newtonian surface viscosity. The μ-π curves can be explained in general as follows: The surface viscosity is low at low film pressures since the film molecules are randomly oriented. As the film is compressed, the molecules are brought together, chain-chain interactions start operating. The surface viscosity increases and is predominant at Lc → I transition. As the film is further compressed, the molecules rearrange themselves vertical to water surface. During this process the surface viscosity increase rapidly with pressure. The further compression of the film leads either to decrease in viscosity or remains constant because the hydrogen bonding between the film molecules and water sub-phase becomes weak and dipole-dipole repulsive forces become dominant.

The deviations from ideal behaviour are observed in the plots of fluidity ($\phi = 1/\mu$) against mole fraction, indicating all the three systems are miscible and non-ideal.

Various flow parameters have been calculated at two transitions (Lc → I and I → LS) using Joly's theory. The state "i" is assigned to Lc → I transition and "i-1" to I → LS transition. Free energy of activation for viscous flow ΔF_i (ΔF_{i-1}), relaxation time τ_i (τ_{i-1})

intermolecular interaction energy $W_{i-k}(0.94r_i)$ ($W_{i-k-1}(0.94r_{i-1})$) have been calculated. The free energy of activation for viscous flow at other than transition point $\Delta F_{(g)}$ has also been calculated for one typical system. The values of different parameters for mixed monolayers are of the same order of magnitude in all the systems. This indicates that the quasi-hexagonal network model suggested by Joly for a single component monolayers is also applicable to mixed monolayers. The variation of $\Delta F_{(g)}$ with the shear rate also confirms the non-Newtonian behaviour in mixed monolayers. The miscibility in mixed monolayers has been confirmed from π-A isotherms.

The plots of area (A), excess free energy of mixing (ΔG^E), compression modulus (K_s) and collapse pressure (π_c) against mole fraction indicate non-ideality and miscibility in these systems. The positive and negative deviations observed in area versus mole fraction curves are explained by using Cadenhead-Muller-Landau model.

Studies on π-A isotherms of mixed monolayers of polyvinyl stearate with eicosanol, hexadecoxy ethanol, octadecoxy ethanol, docosanoxy ethanol, hexadecoxy propanol

and docosanoxy propanol have been undertaken at 25°C with a view to understand miscibility, non-ideality and ultimately stability of these mixed films.

In the above systems polyvinyl stearate and all other long chain compounds are vertically oriented. The plots of area (A), compression modulus (K_s), excess free energy of mixing (ΔG^E) and collapse pressure indicate miscibility and non-ideality in all the systems. This indicates strong intermolecular interactions between the two components. The collapse pressures of mixed monolayers are higher than pure components exhibiting higher stability.

The mixed monolayers of polyvinyl acetate with docosanoxy ethanol at 1:1 molar ratio shows two distinct collapse pressures indicating immiscibility because of horizontal-vertical nature of the system. Thus our study supports the views expressed by Gabrielli and his co-workers regarding orientation and compatibility.

Area in π-A isotherms can be expressed in two units (viz. m^2/mg and/or $Å^2$/monomer unit) in mixed monolayers where one of the components is a polymer. We have shown that area against mole fraction curves may not truly differentiate an ideal and non-ideal behaviour. Therefore, to avoid confusion, the collapse pressure data is important to understand the behaviour of the binary systems.

KEY TO NOTATIONS AND ABBREVIATIONS

π Surface pressure or film pressure (in dynes/cm).

π_c Collapse pressure (subscripts 1, 2 and m correspond to component 1, 2 and the mixture respectively).

π^{eq} Equilibrium surface pressure between two phases (transition pressure)

A Area per molecule in $\mathring{A}^2$

ΔF Free energy of activation for viscous flow for a kinetic unit.
(subscripts i and i-1 correspond to respective states)

$\Delta F'$ Free energy of activation for viscous flow for a kinetic unit when a second displacement occurs before removed lateral molecules can occupy the initial positions (subscripts i and i-1 correspond to respective states; $\Delta F > \Delta F'$).

$\Delta F_{(g)}$ Free energy of activation for viscous flow for a kinetic unit at a given shear rate.

ΔV Surface potential

μ Surface viscosity in surface poise (subscripts o and ∞ correspond to zero and infinite shear rate).

$\mu' = \mu_{(g)}$ Surface viscosity at a given shear rate

μ_1 Surface dipole moment

ϕ Surface fluidity (the subscripts o and ∞ indicate the fluidity at corresponding shear rate).

τ Relaxation time in sec., the mean time which is required by a disturbed kinetic unit to reoccupy its normal position (subscripts i and i-1 correspond to respective states).

p_i The probability that a molecule from the state i removed from its initial position will not reoccupy its normal position before a second molecule goes beyond it.

g Shear rate

r_i Distance between two neighbouring molecules in the state i.

r Specific resistance to evaporation (subscripts 1, 2 and 12 correspond to components 1, 2 and the mixture respectively).

n Proportion of molecules in the state i-1 compared with the total number of molecules per square cm.

a Partial molar area (superscripts α, β indicate respective phases).

x Mole fraction of the component (subscripts 1 and 2 correspond to component 1 and 2 respectively).

ΔG^E Excess free energy of mixing

m Mass of one kinetic unit

$W_{i-k}(0.94\ r_i)$ Interaction energy between one kinetic

unit and all its neighbours assumed to be in the state "i-k" at a distance of 0.94 r_i (the subscripts i, i-k, i-k-1 and 0.94 r_i, r_i, r_{i-k} represent respective states and the distances).

k	Boltzman's constant
T	Temperature in ^{o}K.
R	Gas constant
h	Plank's constant
t	Period of rotation of the inner ring (sec.)

C_{16}-OH	Hexadecanol
C_{20}-OH	Eicosanol
C_{22}-OH	Docosanol
C_{16}-OC_2H_4OH	Hexadecoxy ethanol
C_{18}-OC_2H_4OH	Octadecoxy ethanol
C_{22}-OC_2H_4OH	Docosanoxy ethanol
C_{16}-OC_3H_6OH	Hexadecoxy propanol
C_{22}-OC_3H_6OH	Docosanoxy propanol
PVS	Polyvinyl stearate
PVA_c	Polyvinyl acetate

C H A P T E R - I

INTRODUCTION AND LITERATURE SURVEY

INTRODUCTION

The discovery of monolayer was a great landmark in the history of chemistry. The monolayer concept is universally accepted as one of the basic ideas of physical sciences. It has wide applications in various industries and other socio-economic fields.

The spreading of oil on water was known in antiquity. However, it was Benjamin Franklin [1] in 1757, first observed the calming effect of the oil on the rough sea. The oils then available, of course, were of animal or vegetable origin which are now recognized as polar compounds generally mixtures of glycerides. Benjamin Franklin reported that

" . . . the oil, though not more than a teaspoonful, produced an instant calm over a space several yards square, which spread amazingly, and extended itself gradually till it reached the lee side, making all that quarter of the pond, perhaps half an acre, as smooth as a looking glass".

This report has been described as "the first recorded scientific experiment" in surface chemistry [2]. Miss Pockels [3,4] had developed a technique for the measurement of surface tension as a function of area of oil contaminated water surface. This work was published in the prestigeous journal Nature in 1891. This technique is valid even today as has been mentioned by Gaines [5].

Taking the hints from Pockel's work, Lord Rayleigh in 1899 reported for the first time that the oil films on the water surface were in fact "monomolecular" [c.f. 8 in ref.5].

Devaux [6] introduced simple but elegant experimental method for studying various film forming compounds and noted that these films behave sometimes as solid and sometimes as fluids. Hardy in 1912 [7] found that non-polar oils do not spread in the same way as animal or vegetable oils.

Finally it was Irving Langmuir who developed experimental and theoretical concepts which form the base for modern understanding of sizes and shapes of molecules in monolayer and their orientation at the interface [8]. He proved that long chain fatty acid molecules occupy the cross-sectional area about 20 $\mathring{A}^2$ per molecule, independent of the chain length. He concluded that the films were not only one molecule thick but also were oriented at the water surface, with polar functional group immersed in the water and the long non-polar chain directed nearly vertically up from the surface (Schematically shown in Fig. 1.1).

This technique, introduced by Langmuir for studying monomolecular films, has been named after him as "Langmuir Film Balance".

Langmuir's experiments provided strong support for molecular orientation at the surface and forces between

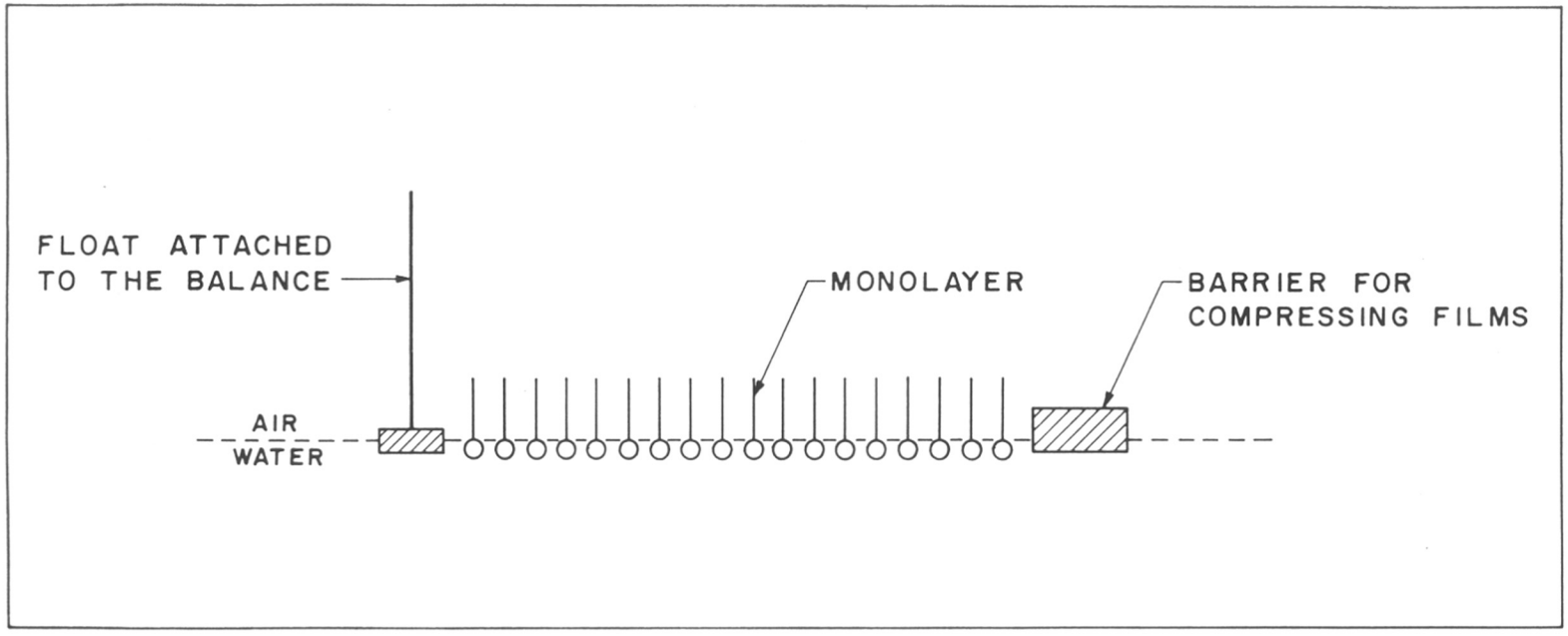

FIG. 1·1 : SCHEMATIC DIAGRAM OF A MONOLAYER IN LANGMUIR FILM PRESSURE BALANCE.

them. This was developed independently by Langmuir [8] and Harkins [9].

In the next decade, many of the scientists from various parts of the world started reporting their work on monolayers of various compounds. N.K. Adam, Rideal, Schulman in England, Devaux, Marcelin, Dervichian, Gustalla and Joly in France, Frumkin and Trapeznikov in USSR and Gorter in the Netherlands were actively engaged in studying monomolecular films of various compounds.

Since 1945 the monolayer research has spread throughout the world and many of the scientists are contributing their ideas to advance the knowledge. The monolayer technique has now found wide applications which have been summarised in short in Table I.

The detailed account of the historical development of monolayer studies has been given in the literature [2,5,10-13].

The monolayer technique has been considerably developed today and it is possible to measure various film properties fairly accurately. The various properties used to study the monomolecular films have been listed in Table II. The study on measurements of these properties gives various intermolecular interactions, two dimensional phases and general nature and behaviour of the monolayer. In case of mixed monolayers,

TABLE I

Applications	References
1. Foams and emulsions: Dispersions of liquids and gases in other liquids are of great practical importance. Such dispersions are almost always stabilized by interfacial films. Surface viscosity and elasticity are important parameters in stabilization of dispersed systems. Studies on basic properties, such as surface pressure, surface potential and surface viscosity give the information regarding the behaviour of monolayers on molecular scale. Such data can be related to practical problems such as lubrication, detergency, rust prevention and ore floatation. Long chain compounds in particular fatty acid salts have been identified as most effective lubricants.	13, 14-18
2. Analytical: One of the sensitive analytical tools provided by monolayers is estimation of the very small amount of compounds needed to form monolayers. Hughes and Rideal used the technique to calibrate the sensitive microbalance.	19
3. Biological membranes: Langmuir has clearly established that molecular alignment in monolayers is closely related to the functional behaviour of	20

TABLE I (contd.)

	Applications	References
	membranes Since then lipid monolayers have found paramount significance for membrane studies. This area now represents the most developing segment of Biophysics.	
4.	Evaporation control: The efforts since 1920 on water evaporation control by insoluble monolayers have shown that long chain compounds of fatty alcohols and alkoxy ethanols are the best evaporation retardants. The experimental studies on mixed monolayers of these long chain compounds are found to be promising water evaporation retardants towards the stability of the films.	21-23
5.	Monolayer coating: The methods that coat the solids with suitable phospholipids and then polymerize the lipids into a membrane like coating are being developed. The resulting coated solids have many properties that are determined not by bulk material but by properties of the outer phospholipid membrane.	24
6.	Langmuir-Blodgett films: The recent development in LB films has shown the evidence that these films will have promising applications in electronic industry as super conductors. Many physicists are being attracted by these techniques.	25,26

TABLE I (contd.)

Applications	References
7. Studies on electron transfer: Studies have already been reported on electron transfer in dye monolayers. Such studies may be of significance in elucidating the mechanism of photosynthesis.	13
8. Two dimensional crystals: To determine the structure of biological macromolecules by electron microscopy two dimensional crystals are required. Recently Uzgiris and Kornberg have attempted successfully to develop two dimensional crystals of biological macromolecules bound on the surface of a lipid monolayer.	27
9. To study the biological processes: Attempts have been made to study the enzyme systems by monolayers of (^{32}P) lecithin. Recently, the intracellular turnover has been studied in which the monolayer technique has been used along with other methods.	28,29
10. Mosquito control: The monomolecular film of isostearyl alcohol containing two oxyethylene groups has been successfully used for the mosquito control. The monomolecular film formed on the water surface, wets the breathing tubes of pupal and larval mosquitoes as they come to the water surface to breath, causing them to drown. The field experiments have been reported to be successful; the commercial production is expected in near future.	30

these properties help us to understand the miscibility and nonideality of the components.

TABLE II

1. Surface viscosity (μ)
2. Surface pressure (π)
3. Surface potential (ΔV)
4. Area per molecule (A)
5. Equilibrium spreading pressure (πe)
6. Collapse pressure (πc)
7. Rate of spreading (dN/dt)
8. Specific resistance to evaporation (r)

The work on monolayer was undertaken in our laboratory in connection with the "water evaporation control" project. Various n-long chain compounds have been studied in the laboratory. Some new compounds having extended polar group, were synthesized from various n-long chain alcohols. These compounds are named as alkoxy ethanols, propanols and butanols having general formula $C_nH_{2n+1}OC_2H_4OH$, $C_nH_{2n+1}OC_3H_6OH$ and $C_nH_{2n+1}OC_4H_8OH$ respectively, where n = 16, 18, 20 and 22. The above compounds not only form condensed monolayers but, some of them are found to be good water evaporation retardants [31,32]. However, the use of pure compounds,

on large scale for evaporation control is uneconomical. The mixed monolayers are sometimes found to be more effective than pure components, as evaporation retardants. Therefore, in the present investigation we have undertaken work on mixed monolayers of various film forming compounds.

Before going into details of the present investigation, it is necessary to understand the general concept of various monolayer properties used in the present investigation.

Plateau [33] first observed the existence of surface viscosity (he termed it as "superficial viscosity") from the difference in damping rates of a compass needle oscillating in the surface and in the bulk of a liquid. However, he was unaware of the contaminants, which are almost always present on surfaces of the liquids. It was Marangoni [34] who recognized that the surface active contaminants were responsible for the effect observed by Plateau. The first precise interpretation of the deformational resistance of the surface films was proposed by Gibbs [35] and was later on developed by Rayleigh.

Based on geometrical and mechanical considerations, Boussinesq [36] has characterized the mechanics of any interface by its static equilibrium tension and two coefficients related to its flow behaviour, viz. the surface shear viscosity and surface dilational viscosity.

In the present investigation we have restricted ourselves to the study of surface shear viscosity. The 'surface shear viscosity', is generally known as "surface viscosity". The coefficient of surface viscosity (μ) as defined by Joly [37] is a small element dx dy of a monolayer, flowing in its plane xy at the velocity u (y) in the direction x, undergoes from adjacent monolayer elements a resisting force (f) which is equal to

$$f = \mu \frac{d^2 u}{dy^2} dx\, dy \qquad (1.1)$$

The dimensions of μ are $M T^{-1}$ instead of $M^{-1}LT^{-1}$ for the bulk viscosity; the c.g.s. units being termed as "surface poise". Before proceeding further it is desirable to survey the literature on surface viscosity.

Moore and Eyring [38] have developed a theory of viscosity of unimolecular films. They have modified the equation for fluidity based on reaction rate theory of viscous flow. They have calculated the free energy of activation for viscous flow in surface film from the data of Myers and Harkins [39] and Langmuir and Schaefer [40]. They observed that the free energy of activation for viscous flow was twice for the flow in liquid bulk. This has been attributed to various types of associations in the films, e.g. intermolecular

association of films and polar group substrate association. They have also given the equations for pressure and temperature effects on surface viscosity. The knowledge of these effects may be used to interpret the structure of the films.

Joly [41-47] has contributed to surface science by further developing the theory of surface viscosity given by Moore and Eyring of monomolecular films.

According to Moore and Eyring's theory [38] as stated by Joly [45] each molecule of a liquid is in a potential trough, each of these corresponding to a possible equilibrium position for the molecules. For the flow of a molecule to occur, the molecule must acquire the energy of activation necessary to pass over the potential barrier which separates it from neighbouring equilibrium position. When this theory is applied to monolayers, it leads to:

$$\sinh \frac{\mu g A}{2kT} = \frac{gh}{2kT} \exp. (\Delta F/kT) \qquad (1.2)$$

The surface viscosity of a liquid is Newtonian when the viscosity coefficient does not depend upon the rate of shear. According to Eyring's theory, flow of a monolayer remains Newtonian as long as the inequality

$$\mu g A << 2kT \qquad (1.3)$$

is obeyed.

In this case eqn. (1.2) is reduced to:

$$\mu = \frac{h}{A} \exp.(\Delta F/kT) \qquad (1.4)$$

Very frequently non-Newtonian behaviour is observed, that is to say one observes that surface viscosity coefficient depends on the velocity gradient 'g' even if the experimental condition satisfies the inequality condition in eqn.(1.3). Therefore in non-Newtonian viscosity the eqn. (1.4) is still valid but the free energy of activation, ΔF, varies with rate of shear. Joly [42] has showed the method of calculation of ΔF with the help of van der Waals forces.

By definition, ΔF, in eqn. (1.4) is the energy necessary for a molecule of the film to pass from one position of equilibrium to another neighbouring position. This energy according to Joly is resolved into two terms: (i) The energy which is required to be supplied to the monomolecular layer for making the hole in it, (ii) the energy required for making a molecule to pass from one equilibrium position to another free neighbouring position.

To understand the viscosity phenomena, Joly has assumed a quasihexagonal network of monolayer molecules. The displacement of one molecule in the 'i' state from its initial position to an adjacent free place in a molecular row parallel to the

flow direction, produces the temporary removal of other molecules in the neighbouring rows. The distance between two neighbouring molecular rows vary locally by 0.866 r_i to 0.94 r_i and it corresponds to a deformation term in activation energy ΔF_i of the quasihexagonal network. If a second displacement occurs before the removed lateral molecules return to their initial equilibrium positions the activation energy for an elementary displacement is no longer ΔF_i but a smaller energy $\Delta F_i'$. The difference $(\Delta F_i - \Delta F_i')$ chiefly corresponds to the fact that there is no new local deformation of the network and no new change in equilibrium form of the neighbouring molecules during the displacement of second kinetic unit. If the probability that an i molecule removed from its initial position will not reoccupy its normal position before a second molecule goes beyond it, is given by p_i then the free energy of activation for any elementary flow is given by

$$\Delta F_{(g)} = \Delta F_i - p_i \ (\Delta F_i - \Delta F_i') \qquad (1.5)$$

Thus for a film whose molecules are initially in the same state 'i' μ_i is to be replaced by μ_i' in the following equation:

$$\mu_i' = \frac{h}{A} \exp \frac{\Delta F_i - p_i (\Delta F_i - \Delta F_i')}{kT} = \mu_i \exp - \frac{p_i(\Delta F_i - \Delta F_i')}{kT}$$

(1.6)

In the case of a flow with a velocity gradient g the molecules of a row parallel to the flow direction are overtaken g times per sec. by the molecules of neighbouring row. If τ_i is considered as relaxation time, which is the mean time required by a disturbed kinetic unit to reoccupy its normal position, p_i is given by

$$p_i = \exp(-1/g\,\tau_i) \tag{1.7}$$

Molecules pass from the state i to i-k during the deformation of the network; τ_i may be regarded as measure of the mean life time of the local aggregate formed by molecules in the state i-k but with a lattice parameter $0.94\ r_i$ rather than r_{i-k}. To the first approximation τ_i is given as

$$\tau_i \simeq 0.94\ r_i \cdot \sqrt{(2\pi m/kT)} \cdot \exp.[(W_{i-k}(0.94\ r_i))/kT] \tag{1.8}$$

where m is the mass of one kinetic unit*, $W_{i-k}(0.94\ r_i)$ is the value per kinetic unit of interaction energy between one kinetic unit and all its neighbours assumed to be in the

---

* By definition, elements that move without internal deformation are the kinetic units of the deforming system [47]. It has been shown experimentally [45] that there is no slipping between a flowing monolayer and its water substrate. All the neighbouring water molecules close to the polar groups of a molecule of the insoluble monolayer behave as if they were rigidly bound to this molecule. Thus, when the monolayer flows, the kinetic units are not the molecules of the insoluble monolayer but, aggregates made up by each of these molecules and the water molecule bound to it.

state i-k and at a distance 0.94 r_i from it and $\pi = 3.142$ (not to be confused with the film pressure π) one can also write:

$$\log (\mu'_i/\mu_i) = (4/kT)\,[1.1\, W_{i-k}(r_i) - W_i(r_i)]$$

$$\times \exp.\ -[(1.064/g.r_i)\,.\,\sqrt{(kT/2\pi m)}.\exp - (W_{i-k}\,(0.94\, r_i)/kT)] \qquad (1.9)$$

The eqn.(1.9) expresses the variation of μ as a function of velocity gradient (g), whose sense depends upon the sign of "$1.1\, W_{i-k}(r_i) - W_i(r_i)$". In general this expression is negative and the μ decreases with increase in the velocity gradient.

When $g \to 0$; $\mu_i' \to \mu$; the following applies:

$$\mu_{(g=o)} = (h/A_i).\ \exp\,(\Delta F_i/kT) \qquad (1.10)$$

when $g \to \infty$; $\mu_i' \to \mu_i \exp\,[(\Delta F_i - \Delta F_i')/kT]$

in other words:

$$(\Delta F_i - \Delta F_i') = kT.\ \ln\,(\mu_{i\,(g=o)}/\ \mu_i'\ (g=\infty)) \qquad (1.11)$$

Thus using the eqn. (1.7), (1.8), (1.10) and (1.11) one can calculate various flow parameters in the state i and in the same way in the state i-1.

As a consequence of lattice deformation, the apparent molecular area at a constant surface pressure increases with velocity gradient. If A_i is the molecular area at rest, the apparent molecular area $A_{(g)}$ at the shear rate g is

given by [45]:

$$A_{(g)} = (1+0.07\ p_i)A_i \qquad (1.12A)$$

In a general case the monolayer is a mixture of two molecular forms i-1 and i; the mean molecular area at rest is given by:

$$A = (1-n)A_i + nA_{i-1} \qquad (1.12B)$$

where n is the proportion of molecules in the state i-1 compared with total number of molecules in a square centimeter.

Then the equation (1.5) becomes:

$$\Delta F_{(g)} = (1-n)\ \Delta F_i + n\Delta F_{i-1} - p_i(1-n)\ (\Delta F_i - \Delta F_i') - p_{i-1}n.(\Delta F_{i-1} - \Delta F_{i-1}') \qquad (1.13)$$

These equations have been used in the present investigation of mixed monolayers. The results will be described in Chapter III.

Monolayers of stearic acid, oleic acid on 0.01 N HCl and triolein, tribenzoin on distilled water have been studied by Dervichian and Joly [48] by using a slit viscometer. They have observed, that for these films, the rate of the flow is proportional to the length of the slit and to the potential gradient. Joly [49] has shown that the surface viscosities of these monolayers are characterised

by its structure and its resistance to flow offered by the substrate. He has studied the surface viscosities of the above compounds with canals of different widths, with a view to establish the effect of narrow and deep canal and capillary action on the viscosity of the film. He obtained the viscosities of the same order of magnitude as those in three dimensions.

Myers and Harkins [39] determined the viscosities of unimolecular films of C_{14} to C_{20} fatty acids. They claim that the phenomena of penetration of liquids into solids and the rate of spreading of monolayers can be understood with the help of surface viscosity. They have also observed that the surface viscosity depends more on close packing of film molecules rather than number of carbon atoms in the molecule. Intermolecular forces in the film have much greater effects when the film is closely packed than when it is expanded.

Boyd and Harkins [50] studied the viscosity of monolayers of various long chain fatty acids (C_{15} to C_{20}). They observed that in condensed liquid films the increase in logarithm of viscosity is proportional to film pressure. They have also observed that the viscosity of the liquid films increases rapidly with length of the hydrocarbon chain; the liquid or low pressure condensed films exhibit a Newtonian

viscosity; the viscosity of "plastic" film decreases with length of hydrocarbon chain; the "plastic" films exhibit non-Newtonian viscosity and the viscosities of long chain acids are very much less compared to corresponding long chain alcohols. They have also investigated the effect of temperature on viscosity of arachidic acid monolayer and found that viscosity decreases with rise in temperature.

Trapeznikov [51] studied the monolayers of palmitic acid, oleic acid, cetyl alcohol by measuring surface viscosity and elasticity. He noticed the solidification of palmitic acid film when multivalent ions were added to the substrate.

The surface viscosity of monolayers of cholesterol, casein and nerve proteins has been studied using damping of a vane oscillating method by Fourt [52]. From this study he concludes that the formation of bonds within the film molecules convert a fluid film into an elastic film. Further he has found that pH of the substrate play an important role in determining the viscosity and elasticity of protein films.

Nutting and Harkins [53] have determined surface viscosity of stearic acid and n-long chain alcohols containing 15 to 18 carbon atoms at 20 to 25°C on 0.01N H_2SO_4 by using canal method. They have observed linear increase in viscosity with mean film pressure.

Alexander [54] has surveyed the possible methods of measuring changes in interfacial tension, viscosity and potential brought about by spreading an insoluble monolayer at oil-water interface. The data obtained is compared with that obtained for air-water interface.

Copeland et al.[55] have reported super-liquid (LS) phase for octadecanol and found that the viscosity of LS phase behaves abnormally with temperature; the viscosity increases with rise in temperature. The authors explain this abnormality by assuming a certain type of bonding which is extremely sensitive to distance between the molecules in the monolayer. The similar abnormalities observed in bulk viscosity involve only minor change in viscosity; the enormous effects found in surface viscosity seem to be associated with the presence of aqueous sub-phase.

At 8.85°C and 16 dynes/cm the molecular area is 20.0 Å^2 and the viscosity which is that of LS phase is 0.0044 surface poise. If at this pressure the molecular area of this phase is increased to 20.75 Å^2 by increase of temperature, the viscosity increases by a factor of 55 to 0.24. From this observation the authors say that the binding is increased greatly by an increase of molecular area and temperature, both of which should normally decrease it.

Trapeznikov [56] has examined the surface viscosity of higher alcohols as a function of film pressure using damped vibrations of a disc suspended by an elastic wire. He has noticed that surface viscosity increases with increase in chain length and attributed this to van der Waals interactions between the chains.

Mukherjee [57] derived a linear relation between surface viscosity and film pressure which was earlier empirically developed by Boyd and Harkins [50]. Davis [58] studied the surface viscosity of protein films at oil-water and air-water interface. He observed viscosities to be very much higher at oil-water interface than at air-water interface. The cohesion within the polypeptide coil is removed at oil-water interface, therefore the viscosity is increased by as much as ten folds, indicating the molecules have been relatively long.

Jarvis [59] has measured the surface viscosities of monolayers of 14, 16 and 18 carbon chain aliphatic alcohols, amines, acids and amides as a function of film pressure, substrate pH and rate of flow of the film, using a canal viscometer. He observed that surface viscosities of the film vary with the nature of the polar group and with the degree of interaction between polar group and aqueous sub-phase. The viscosity values depend upon the orientation and close-packing of the molecules in the film. In the case of

Newtonian films, the surface viscosity increased with hydrocarbon chain length. However, for non-Newtonian films the behaviour was not so regular. The viscosities of amines and acids showed marked dependence on the pH of the substrate.

Katti and his coworkers [60-67] have studied the surface viscosity along with pressure-area isotherms of various n-long chain alcohols, alkoxy ethanols, propanols, butanols and some of their mixtures at air-water interface. They have constructed a rotating ring type surface viscometer [61]. The various n-long chain compounds studied by them exhibited non-Newtonian surface viscosity. They have calculated various flow parameters using Joly's theory [44]. They have studied the effect of temperature and effect of substrate pH on propanols and butanols [66,67] and have concluded negligible influence of these parameters on the compounds.

Deamer and Cornwell [68] have studied the surface viscosities of octadecanol, dipalmitin, distearin and some unsaturated fatty acids. The stearic acid was studied on different substrates. The data suggest that the unusual properties of calcium stearate and palmitate films are explained by a copolymeric lattice structure. The authors found that calcium has no effect on surface viscosity of cis and trans monoethenoic acid and phospholipid monolayers.

Boyd and Vaslow [69] have studied the surface viscosity of mixed monolayers. They have studied the stearic acid with octadecanol and with arachidic acid, using a torsional viscometer. The addition of octadecanol to stearic acid lowers the transition pressure. The authors have also given a method of finding whether the mixed monolayer is truly miscible or not as expressed below:

$$\phi_{12} = x_1\phi_1 + x_2\phi_2 \qquad (1.14)$$

ϕ_{12} = surface fluidity of the mixed monolayer

ϕ_1 = surface fluidity of the first component

ϕ_2 = surface fluidity of the second component

x_1 and x_2 = mole fractions of respective components.

The above equation will be obeyed if the components are immiscible and any deviation from this equation will indicate a miscibility.

Enever and Pilpel [70,71] have made use of the surface viscosity technique for the study of slow reaction between stearic acid and calcium ions at air-water interface. They have estimated the energy of activation of the reaction as 8 K cal/mole.and free energy of activation for viscous flow of resulting film as 11 K.cal/mole. In their study of mixed monolayers of octadecanol with stearic acid on M/2000 calcium chloride substrate they have found that

the stearic acid molecules react to form calcium stearate whereas octadecanol behaves practically as an inert diluent.

Vilallonga [72] has studied surface viscosity, by *floating canal method along with surface pressure-area and surface potential - area isotherms of dipalmitoyl lecithin monolayer at different temperatures.* The order of magnitude of surface viscosity was 10^{-3} to 10^{-4} surface poise. Logarithm of surface viscosity was found to be in general, a linear function of surface pressure. A distinct change in slope at 12 dynes/cm has been reported by the author, indicating a possible change in structure of flow unit at this pressure.

Trapeznikov and Zaozerskaya [73] have measured the surface viscosity of monolayers of oxyethylated octadecanol with one and two ethylene-oxy groups. They observed decrease in surface viscosity of monolayers under the action of waves. It shows the weakening of cohesion in the monolayer.

Hayashi et al. [74-76] have measured surface viscosity by canal method along with surface pressure and surface potential to study the surface properties of synthetic phospholipids.

They have observed extremely high surface viscosities for all the members of phosphatidyl ethanolamine groups [74]. Further they have studied the thermal phase transitions in monolayers of synthetic phospholipids by surface viscosity measurements [75]. The authors conclude that choline group cannot be introduced into the two dimensional ionic lattice formed by primary amine and phosphate, because of stearic hinderance caused by their different polar group sizes. They have also studied the surface viscosity and film pressure of lecithin, cephalin and its analogs at air-water and oil-water interface [76].

Goodrich et al. [77-79] have designed a new surface viscometer. Here a film covered interface is driven by making contact with a rotating ring inserted into a narrow gap in the wall of a cylindrical vessel. Surface viscosity can be measured by comparing the period of revolution of a floating dust particle inserted into the interface near the cylindrical axis with the rotational period of the rings. The surface viscosity in the range of 10^{-5} to 10^{-1} surface poise can be measured quantitatively at air-water interface. The authors report the experimental data on surface viscosity of stearic acid monolayer at 22°C and at pH = 7 with above mentioned surface viscometer [78]. The surface shear viscosity is very low at low surface concentrations. The

surface viscosity is found to be Newtonian for stearic acid. In continuation of the study, the authors have reported their study on surface viscosity of stearic acid at oil-water interface [79]. The oil phase is cyclohexane whereas aqueous NaCl is another liquid phase. The interfacial viscosity changes from $5x10^{-4}$ surface poise to less than $1x10^{-1}$ surface poise when the pH of the aqueous phase is changed from 5.5 to 9.0.

Neuman [80] has studied film pressure, surface potential, surface viscosity and electron microscopy for stearic acid monolayers on 10^{-4} M $CaCl_2$ subphase over a pH range of 2 to 9. He has explained the results satisfactorily using a new model of Ca^{++} binding.

Hard and Löfgren [81] have done the measurements of surface viscosity on propyl stearate monolayers using a new laser light scattering apparatus. The authors claim, that for the first time the film elasticity and viscosity have been determined from light scattering measurement. They have compared the elasticity obtained from laser light scattering and from conventional π-A curve from Wilhelmy method. Though the order of magnitude of elasticity is the same in both cases, the behaviour is quite different.

Joos [82] has extended the theory of Eyring of viscous flow to mixed monolayer with miscible component.

This treatment allows to calculate surface viscosity of a mixed monolayer if the flow parameters of single components are known. The author has applied the treatment to senegin - digitonin and cholestrol - phospholipid systems.

Surface viscosity in relation to surface potential and ion binding has been studied in lipid monolayers by Colacicco et al. [83]. The authors have determined the surface viscosity by torsion oscillation method. They have experimentally observed that the surface viscosity of dipalmitoyl lecithin is markedly greater on 0.075 M $CaCl_2$ than on 0.15 M NaCl substrate. This may be due to the influence of electrolyte on the water structured around the polar surface of lipid and thus on the extent and strength of the coalescence. The effect may not be due to binding of Ca^{++} onto the ionic groups of lecithin.

Chatelain et al. [84] have studied the perturbations induced in lipid layer by the presence of a spin probe molecule in a model membrane. For this purpose the authors have studied mixed monolayers of a spin probe molecule and lecithin at air-water interface using surface viscosity, pressure-area isotherms and enzyme hydrolysis techniques. The surface viscosity measurements have been made with an oscillating mica floating ring method. The surface viscosity results indicate that the probe induces a more packed organization of lecithin molecules.

Langevin [85] has investigated the monolayer viscoelasticity by light scattering techniques. Several insoluble monolayers have been studied: myristic acid, stearic acid, propyl stearate, and polymer films of polyvinyl acetate, polymethylmethacrylate. The behaviour of longitudinal surface viscosity (k) illustrates the difference between condensed and expanded monolayers.

Crilly and Earnshaw [86] have studied the surface viscosity of glycerol monooleate (GMO) monolayers on 0.1M NaCl aqueous solution using laser light scattering technique. The effect of temperature on viscoelastic behaviour of GMO monolayers has been investigated.

Miyano et al. [87] have compared the phases of insoluble fatty alcohol monolayers between surface pressure-area (π-A), isotherms and shear modulus measurements. They have reported some unusual observations. The authors emphasize the point that the phases of the films cannot be determined solely from π-A diagrams.

Abraham et al. [88] have reported the first observation of a static shear modulus exhibited by monomolecular films of stearyl alcohol ($C_{18}H_{37}OH$) and nonadecanoic acid ($C_{18}H_{37}COOH$) spread on cation free water. They have reported that the values of shear modulus is several orders of magnitude smaller than the theoretically predicted value.

Goodrich et al. [89-93] have published the papers on the theory of absolute surface shear viscosity. The theory takes full account of the hydrodynamic coupling between the internal viscosity of the substrate with the surface viscosity of adsorbed films. The authors show that rotating disk surface viscometer is a poor experimental design for the measurements of surface viscosity. The problem of steady laminar flow in the viscinity of a rotating ring inserted into a semifinite fluid interface is solved when liquid surface is covered with an insoluble film. From the calculations given, the absolute surface viscosity can be calculated from the measured values of the torque [91]. The hydrodynamic problem of two concentric counter-rotating rings, making a knife edge contact with a viscous surface film supported by semi-infinite, viscous substrate has been discussed [92]. The effect of finite thickness of the rings on the flow parameters generated by a rotating ring has been discussed theoretically [93]. According to the authors [93], the lower limit for measuring surface viscosity by Couette surface viscometer for an adsorbed film on water surface is of the order of 10^{-6} g/sec.

Goodrich [94] has reviewed the progress in the theory of measurements of surface shear viscosity.

The author has discussed both Newtonian and non-Newtonian behaviours of the film. Recently Goodrich [95] also has reviewed interfacial rheology as a branch of fluid mechanics. Experimental equipment needed to measure surface rheological properties is discussed. The author stresses that the entirely erroneous results are obtained if the investigator neglects the mechanical coupling of the interface with the adjacent bulk fluids.

From the above survey of literature on surface viscosity, it is clear that many workers have used different types of surface viscometers for the study depending on the suitability of the system. In our laboratory, to study mixed monolayers of n-long chain compounds which exhibits non-Newtonian behaviour we have used a rotating ring type surface viscometer. This viscometer gives fairly accurate data in the range of 10^{-3} to 10^{-1} surface poise. This will be described in detail in the Chapter II.

Surface pressure-area per molecule (π-A) isotherms

The measurement of surface pressure (π) as a function of area per molecule (A) is of immense importance in the study of monolayer behaviour. The surface pressure is defined as a difference in surface tension of water and that of film covered water, i.e.

$$\pi = \gamma_0 - \gamma \qquad (1.15)$$

γ_o = surface tension of water

γ = surface tension of film covered water

π = film pressure (or surface pressure)

Henri Devaux, shortly after 1900, pointed out that molecules in monolayers could exist in different states, analogous to those in three dimensions (solid-liquid-gas). Since then many investigators have reported the existence of a number of different monolayer states or two dimensional phases in various films. There are differences of opinion regarding the existence of the various two dimensional phases whether really occur or an experimental artifact. However, the various phases have been classified and are described in detail by Harkins [96] and Gaines [97] with the help of π-A isotherms.

All the phases may not be observed with any single substance at one temperature. In order to detect different phases, one has to examine the different compounds at various temperatures.

The structure and stability of an insoluble monolayer is governed by delicate balance of forces of attraction and repulsion between the film molecules themselves as well as between film molecules and the substrate molecules. The most important variables in determining monolayer structure are temperature, pressure, pH of substrate and ionic composition of the substrate.

The thermodynamic classification introduced by Ehrenfest is also applicable to monolayer phase transitions [96,98]. The phase transitions which take place in a monolayer are ordinary or first order transitions which involve a discontinuity of molecular area, A, and subsidiary thermodynamic properties, and second order transition which are characterized by a sudden change of the compressibility, K_s, of the monolayer. The first order transition involves a discontinuity of first partial derivative of free energy of the system F with respect to film pressure π.

$$(\partial F/\partial \pi)_{P,T} = A . \qquad (1.16)$$

A change in compressibility without any discontinuity of the area corresponds to a discontinuity of the second partial derivative of F, indicating a second order phase change.

$$(\partial^2 F/\partial \pi^2)_{P,T} = (\partial A/\partial \pi)_{P,T} ; \; K_s = (-1/A)(\partial A/\partial \pi) . \qquad (1.17)$$

In the π-A isotherms, first order transitions are recognized as regions of constant pressure or plateaus, and second order transitions are apparent as changes in slope. A schematic π-A isotherm consisting of various phases is shown in Fig. 1.2, the details of which have been described below.

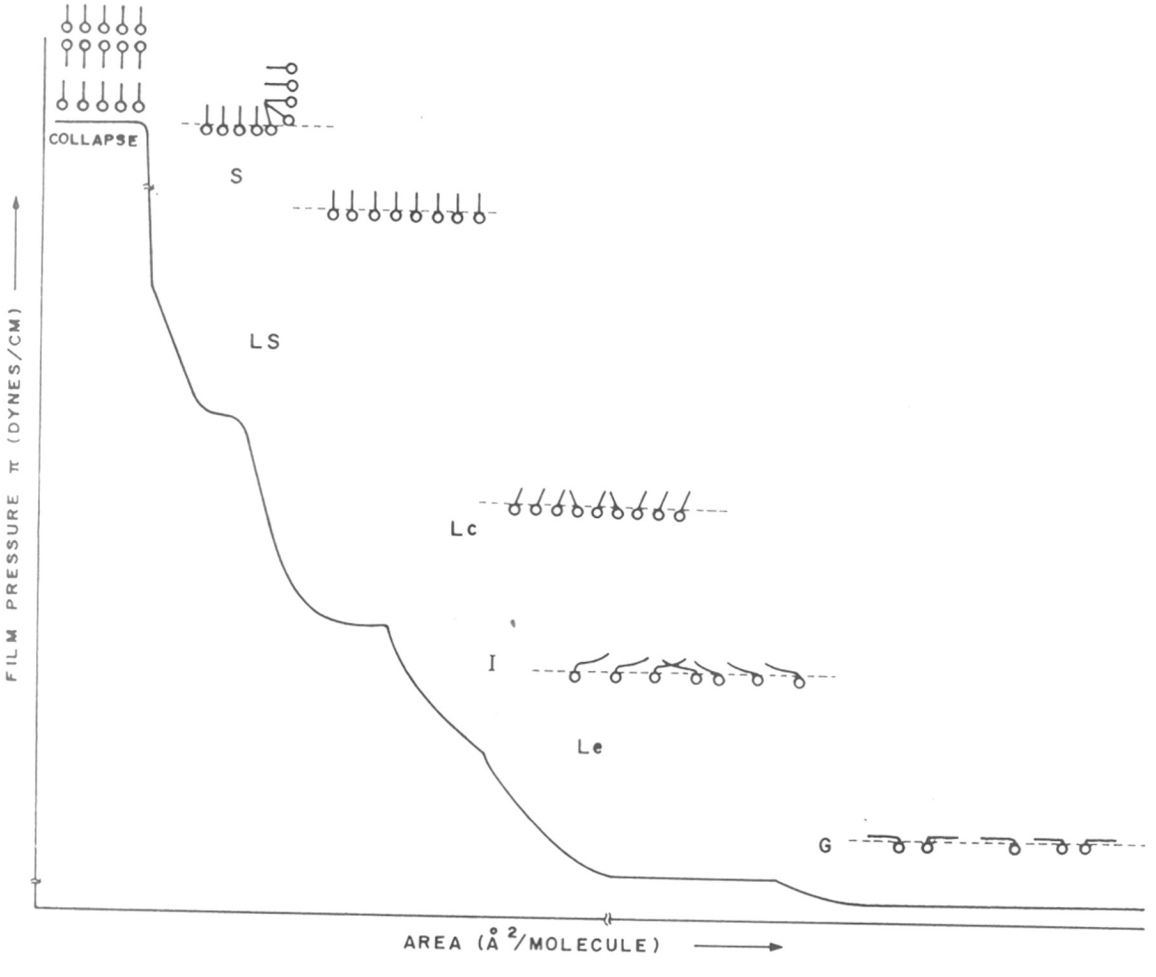

FIG. 1·2 : SCHEMATIC REPRESENTATION OF A SURFACE PRESSURE AREA ISOTHERM.

Gaseous or vapour phase (G): At an extremely large area per molecule (> 100 $\mathring{A}^2$), the film behaves like a gas. The existence was first predicted by Langmuir [8]. The monolayer in this state obey the standard gas equation.

$$\pi A = kT \qquad (1.18)$$

π = film pressure, k = Boltzamann constant

T = temperature in ^{o}K A = area per molecule.

The film molecules lie flat on the water surface in this phase. The surface viscosity is very low in the gaseous phase.

Liquid expanded phase (Le): When the area is decreased, the liquid expanded phase is observed. The film in the liquid expanded phase is still coherent, but the molecules occupy much larger area than the condensed film. This phase shows no direct analogy with three dimensional systems.

The intermediate liquid phase (I): Increase of pressure at constant temperature, decrease of area at constant pressure or decrease of temperature at constant area result in intermediate liquid phase. Harkins [99] feels the transformation may be of second order. The main feature of this phase is its high compressibility especially at large area.

Liquid condensed phase (Lc): The further compression of the film leads to liquid condensed phase. Harkins [100] called it as L_2 type of the film and Adam [101] as a film with "close-packed heads, rearranged on compression". This phase has been referred as "mesomorphous" by Dervichian [102].

Liquid solid phase (LS): This phase has been discovered by Harkins and Copeland [103]. It exhibits remarkable and anomalous properties. This phase shows the fluidity of liquid condensed phase whereas the compressibility of a solid phase. Therefore, it is named as "liquid-solid" phase. Stenhagen and Stenhagen [104] observed the LS phase for long chain carboxylic acids and suggested that the chains are evidently free to undergo both rotation and translation.

Solid phase (S): The liquid condensed phase on further compression leads to a solid phase. This phase is characterised by low compressibility. In this phase the film molecules are arranged vertical to the surface and are close-packed. Most of the long chain fatty acids, alcohols exhibit this phase.

Since the time of Irving Langmuir many investigators all over the world, have undertaken studies on monolayers of various compounds. Adam and Harkins are the pioneers in the field.

Dervichian [102] has established a general correlation between all transformation phenomena observed in surface films and has shown that they correspond closely with the same substance in the bulk. He has made a systematic classification of different types of isotherms. He has detected higher order phase transitions in monolayers by studying the variations of compressibility, viscosity and apparent dipole moment.

Alexander [105] has studied the role of hydrogen bonds in condensed monolayers using π-A and surface potential - area (ΔV-A) isotherms. He has studied various types of organic compounds having different polar groups viz. acetamides, $R.NHCOCH_3$; ureas, $R.NHCONH_2$; amides, $R.CONH_2$; methylamide, $C_{17}H_{35}CONHCH_3$; acetanilides, $R.C_6H_4NHCOCH_3$; aldoximes, R.CH = NOH; acids R.COOH; α-amino acids, $R.CH.NH_2COOH$ (where $R = C_{16}H_{33}$). He has observed that no direct cross hydrogen bonding is possible with alcohols. He is not in favour of the Dervichian's [102] idea of inclined chains in solid condensed region. He has shown enough evidence to predict that the long hydrocarbon chains are vertically oriented in the solid condensed region.

Schulman and Hughes [106] from the study of π-A isotherm, confirmed the views of Adam and Dyer [107] that increasing the chain length has the same effect as

decreasing the temperature. As the chain length is increased, the condensed films show more closer packing.

Barnett and Zisman [108] studied the π-A and μ_1-A isotherms of monolayers of two series of progressively flourinated fatty acids $F(CF_2)_n-(CH_2)_{16}COOH$ and $F(CF_2)_n-(CH_2)_{10}COOH$ spread on water at different pH. In both series, the stability of the monolayers at all the pH values decreased rapidly with progressively shorter perfluoro segments.

Spink [109] studied the π-A and ΔV-A isotherms of monolayers of fatty acids from C_{14} to C_{18} on M/100 NaCl as a function of pH. The contraction observed for partly ionized films is explained in terms of an increased head group interaction rather than an increased interaction between the paraffin chains resulting from rearrangement of molecules.

Healy and Ralston [110] have studied the effect of specific cation on the monolayer of n-octadecanol at 21°C. They have used various substrates viz. 4M $MgCl_2$, 1M $MgCl_2$, 0.01M $MgCl_2$, 4M $CaCl_2$, distilled water, 4M NaCl, 4M KCl, 1M KCl and 0.01M KCl. The presence of the salt in the substrate indicates the expansion of the π-A isotherms.

Deo et al.[111] have studied the π-A isotherms of $C_nH_{2n+1}OH$ and $C_nH_{2n+1}OC_2H_4OH$ where n = 14, 16, 18, 20 and 22.

at different temperatures. The area at zero compression is higher for alkoxy ethanols compared to the alcohols. For solid state, the two areas are nearly equal suggesting the alignment of extended polar group of the former along the carbon chain at high pressures.

Shukla et al. [112] have studied the π-A isotherms of monolayers of diethylene and triethylene glycol monooctadecyl ether and of diethylene glycol monodocosyl ether on water at different temperatures. They have found that reducing the hydrocarbon chain length of alcohols and of their ethylene oxide condensation products or increasing the number of ethylene oxide units added lowers the film expansion temperature.

Lo and Lu [113] have studied the π-A isotherms, equilibrium spreading pressure and specific resistance to evaporation of octadecanol, eicosanol, docosanol and oxyethylene docosanol in the temperature range of 15 to 30°C. They have observed that specific resistance of fatty alcohols increase with increase in chain length. Equilibrium spreading pressure decreases with increase in chain length.

Rosano and La Mer [114] have studied the surface viscosity area, specific resistance to evaporation as a function of film pressure of various compounds viz. ethyl palmitate, ethyl linoleate, ethyl elaidate, ethyl stearate,

arachidic acid, stearic acid, 1-octadecanol, cetyl alcohol and 1,1,13-trihydroperfluorotridecyl alcohol. Some of these films are highly compressible in the liquid phase, as compared to incompressible saturated fatty acids. The compressible films are poor evaporation retardants as compared to incompressible films.

Archer and La Mer [115] studied the resistance to evaporation of water by monolayers of four saturated fatty acids C_{17}, C_{18}, C_{19} and C_{20} as a function of surface pressure, chain length, subphase composition and temperature. In liquid condensed phase evaporation of resistance is independent of surface pressure and the substrate pH; its logarithm is a linear function of chain length. On the other hand in solid phase on alkaline subphase containing calcium ions, the logarithm is a linear function of both chain length and the surface pressure.

Costin and Barnes [116] have studied the effects of various environmental factors and of impurities in materials on the evaporation resistance of alcohol monolayers. They have shown that the evaporation resistance of octadecanol monolayers at low surface pressures is an extremely sensitive test for contamination.

Kellner [117] has studied the effect of temperature difference between liquid substrate and the air above the

film on liquid expanded - liquid condensed phase transition of tetradecanoic acid. He has found negligible effect on the transition pressures. Therefore it may be concluded that the properties of monolayer are almost entirely determined by the substrate surface temperature.

Recently Garfias [118,119] has suggested a model for solid monolayers of fatty alcohols in water. He has presented the model in two stages. First a model for pure water gas interface has been proposed and then half of the water molecules of the surface layer are removed and replaced by fatty alcohol molecules to produce a condensed monolayer. He has considered that the water molecules can form two types hexamer rings; polyboat and polychair conformations. The upper most surface layer of water exhibits a polychair or polyboat structure depending on the surface pressure of the monolayer. At the transition point from liquid condensed to solid phase, the monolayer is represented by saturated polychair network whereas at collapse point it is saturated polyboat network. When the film pressure is about 1 dyne/cm, the monolayer is represented by saturated polyshell network. Below 1 dyne/cm network is unsaturated. The author has shown that the pure water surface can be represented by polyshell network. From the proposed model the area per molecule and film pressure can be predicted; he has shown good agreement between the

predicted values and experimental data from literature. The main difference among polyboat, polychair and polyshell is that in the saturated polyshell each oxygen atom from the first oxygen plane of fatty alcohol molecules is hydrogen bonded to two vicinal water molecules whereas in saturated polyboat or polychair network each oxygen from first oxygen plane is bonded to three vicinal water molecules. Therefore the polyshell structures are not as strong as either polyboat or polychair.

The earlier work on mixed monolayers comes from Collet, Adam, Schulman, Harkins, Rideal, Goddard, Ries, Dervichian, Cadenhead, Joos and many others [120-139].

Barnes and LaMer [140] have studied the evaporation resistance of mixed monolayers of n-long chain alcohols of very high purity and showed that if mixtures form ideal solution at all pressures, it obeys equation:

$$\ln r_{12} = x_1 \ln r_1 + x_2 \ln r_2 \qquad (1.19)$$

where r_1, r_2 and r_{12} are the specific evaporation resistances of pure components 1, 2 and the mixture respectively.

Costin and Barnes [141] have reported π-A isotherms of monolayers of octadecanol and docosyl sulphate and their mixtures on 0.1M KCl at 25°C. The molecular area of the

mixtures are found to be less than the average area obtained by additivity rule. Using Goodrich's method, they have calculated excess free energy of mixing and showed that the system behaves nonideally. The results have been discussed in terms of energy barrier theory and relationship between excess free energy of activation and excess free energy of mixing has been established.

Shah and Shiao [142] have shown that the average area per molecule in mixed monolayers of alkyl alcohols depends on chain length compatibility of the surfactant molecule. They have shown that as the difference between the chain length of two film forming components goes on increasing, the excess area per molecule also increases.

Roberts et al. [143] have studied the interactions in mixed monolayers of myristic acid and cetyl alcohol determining π-A isotherms. Close packed monolayers were observed due to strong intermolecular interactions.

Recently Matuo et al. [144-146] have studied mixed monolayers of long normal chain fatty acids with long normal chain esters using π-A isotherms. They have obtained two dimensional phase diagrams and their partial molar enthalpy changes from the thermodynamic treatment of multi-component surface films. It has been found that chain length of the acid plays an important role in thermodynamic stability of mixed monolayer.

Rakshit and Zografi [147] have studied the thermodynamics of mixing of fatty acid monolayers. The authors have studied the thermodynamic properties of mixed fatty acids in the region of surface vapour pressure. From the deviation of expected ideal behaviour the authors have estimated the activity coefficients. From the measurement of surface heat of vapourization, the solubility parameters of each fatty acid have been determined. By measuring the activity coefficients, the excess free energy of mixing and partial molar enthalpy of mixing, it is possible to explain qualitatively the extent of non-ideality of the mixed monolayers.

Matuo et al. [148] have studied mixed monolayers of two bipolar/bipolar systems and compared them with monopolar/monopolar systems. The phase diagrams of these systems are comparable with monopolar/monopolar system. However, apparent molar energy in bipolar/bipolar systems are higher than those of monopolar/monopolar systems.

Verger and Pattus [149] have recently studied lipid-protein interactions by monolayer technique. The authors say, that the experiments with monolayers have the unique advantage of the arrangement and packing of the molecules can be easily measured and controlled. The monolayer technique is ideally suited for the study of mode of action of lipolytic enzymes at interfaces using controlled mixtures of lipids.

Gaines [150] has integrated the thermodynamic equation of state for mixed insoluble monolayers to evaluate free energy of mixing in terms of activity coefficients of the subphase in the surface layer. According to the author, the resulting expression will permit prediction of free energies of mixing when molecular models which account for the interactions between surfactants and the subphase are developed. He has developed the treatment using Goodrich theory.

In our laboratory, Katti and his coworkers have studied π-A, ΔV-π and μ - π of various mixed monolayers at air-water interface [66, 151-152]. They have observed that when a mixed monolayer consists of the different polar groups but of the same chain-length, the system forms an ideal mixture. If the polar groups and chain lengths are different, the system shows non-ideal behaviour with strong molecular interactions.

In any mixed monolayer system it is important to understand whether the mixtures form miscible or immiscible films. The miscibility depends upon the intermolecular interactions between the two film forming compounds. The various derived properties obtained from π-A and μ-π curves give the extent of miscibility in any mixed monolayer. The various derived properties are as follows:

The deviation from ideality in the following plots will indicate the miscibility.

a) Surface fluidity - mole fraction ($\phi - x_1$)

b) Area per molecule (at a constant pressure) - mole fraction ($A - x_1$)

c) Compression modulus - mole fraction ($K_s - x_1$)

d) Excess free energy of mixing - mole fraction ($\Delta G^E - x_1$)

e) Collapse pressure - mole fraction ($\pi_c - x_1$)

f) Phase diagrams.

The importance and limitation of each individual property is discussed in Chapter III.

<u>The collapse pressure of the monolayers</u>

The measurement of collapse pressure during the compression of monolayer gives valuable information. Smith and Berg [153] have given a short but excellent review on collapse of the monolayers. According to them the films of solid surfactants appear to be subject to two distinct types of collapse: (i) nucleation and growth of bulk solid fragments; (ii) the fracture of the film. The latter generally occurs only when compression is rapid and carried to surface pressures much higher than required for nucleation. The film fracture is the only type of collapse which is generally noticeable in a π-A isotherms; usually as a spike or plateau of maximum π. However, it is reported that the

fracture pressures have got poor reproducibility because they are highly dependent on rate of compression [154]. Smith and Berg [153] have reported that fewer studies have been done on films held at constant area, but all reveal instability at surface pressures considerably below the fracture pressures. According to Brooks and Alexander [155] an increasing loss of monolayer area held at constant pressure indicates collapse. Following the above definition of the collapse pressure, we have measured collapse pressures as increasing loss of surface pressure of a monolayer held at constant area.

In the mixed monolayers, the collapse pressures give the criterion for the non-ideality of the mixed monolayer. Joos [156] has developed an equation to predict the collapse pressure of a miscible monolayer from the collapse pressures of the two pure components. This will be discussed in detail in Chapter III.

From the surveyed literature, it is clear that the chain-chain van der Waals interactions play an important role in miscibility in a mixed monolayer, rather than the polar group. Therefore it was thought worthwhile to undertake an exhaustive study of various mixed monolayers of n-long chain compounds where the polar groups are the same but a wide difference in the chain length. The

following three systems have been chosen for the study.

1) Hexadecanol ($C_{16}H_{33}OH$) with Docosanol ($C_{22}H_{45}OH$)

2) Hexadecoxy ethanol ($C_{16}H_{33}OC_2H_4OH$) with Docosanoxy ethanol ($C_{22}H_{45}OC_2H_4OH$)

3) Hexadecoxy propanol ($C_{16}H_{33}OC_3H_6OH$) with Docosanoxy propanol ($C_{22}H_{45}OC_3H_6OH$).

The above systems have been undertaken for the measurement of film pressure - area (π-A), surface viscosity - film pressure ($\mu - \pi$) isotherms and the collapse pressures (π_c) at 25°C. The details of experimental set-up and the procedure have been given in Chapter II.

Mixed monolayers of polymers with long chain compounds have also been studied. The details of the literature has been presented in Chapter IV.

REFERENCES

1. Cited e.g. ref. [14] p.1
2. C.H. Giles, Chem.Ind.(London) (1969) 1616.
3. A. Pockels, Nature (London) 43 (1891) 437.
4. A. Pockels, Nature (London) 48 (1893) 152.
5. G.L. Gaines Jr, Thin Solid Films 99 (1983) ix.
6. Cited e.g. ref. [14] p.2.
7. W.B. Hardy, Proc.Roy.Soc.(London) A86 (1912) 610.
8. I. Langmuir, J.Am.Chem.Soc. 39 (1917) 1848.
9. W.D. Harkins, J.Am.Chem.Soc. 39 (1917) 541.
10. C.H. Giles and S.D. Forrester, Chem.Ind.(London) (1970) 80.
11. C.H. Giles and S.D. Forrester, Chem.Ind.(London) (1971) 42.
12. S.D. Forrester and C.H. Giles, Chem.Ind.(London) (1979) 469.
13. V.K. Agarwal, Thin Solid Films 50 (1978) 3.
14. G.L. Gaines Jr. Insoluble Monolayers at Liquid-Gas Interface, Interscience Publishers (1966).
15. B. Kanner and J.E. Glass, Ind.Eng.Chem. 61(5) (1969) 31.
16. J.G. Hawke and A.E. Alexander, J.Colloid Sci. 11 (1956) 419.
17. The Encyclopedia of Chemistry eds. C.A. Hampel and G.G. Hawley (1973), Van Nostrand Reinhold Co., New York, p.696.
18. O. Levine and W.A. Zisman, J.Phys.Chem. 61 (1957) 1068 and 1188.
19. A. Hughes and E.K. Rideal, Proc.Roy.Soc.(London) A137 (1932) 62.
20. I. Langmuir, Science 87 (1938) 493.
21. G. Hedestrand, J.Phys.Chem. 28 (1924) 1244.
22. N.K. Adam, J.Phys.Chem. 29 (1925) 610.

23. E.K. Rideal, J.Phys.Chem. 29 (1925) 1585.

24. Chem.Eng.News 61(8) (1983) 23.

25. P. Day, Chem.Br. 19 (1983) 306.

26. Chem.Br. 18 (1982) 334.

27. E.E. Uzgiris and R.D. Kornberg, Nature (London) 301 (1983) 125.

28. A.D. Bangham and R.M.C. Dawson, Biochem.J. 75 (1960) 133.

29. R.M.C. Dawson, J.Am.Oil.Chem.Soc. 59 (1982) 401.

30. Chem.Eng.News 61(21) (1983) 26.

31. R.N. Shukla, S.B. Kulkarni, M.K. Gharpurey and A.B. Biswas, Indian J.Tech. 1 (1963) 141.

32. S.S. Katti, M.V. Natekar, S.D. Sansare, S. Pathak and S.D. Pradhan, Indian J.Tech. 7 (1969) 93.

33. Cited e.g. ref. [37] p.2

34. Cited e.g. ref. [37] p.2

35. Cited e.g. ref. [37] p.2

36. Cited e.g. ref. [37] p.2

37. M. Joly, Recent Prog.Surf.Sci. 1 (1964) 1.

38. W.J. Moore Jr. and H. Eyring, J.Chem.Phys. 6 (1938) 391.

39. R.J. Myers and W.D. Harkins, J.Chem.Phys. 5 (1937) 601.

40. I. Langmuir and V.J. Schaefer, J.Am.Chem.Soc., 59 (1937) 2400.

41. M. Joly, Proc. 2nd Int.Congr.Rheology (ed. V.G.W. Harrison), Butterworths, London (1953) p.365.

42. M. Joly, J.Phys.Radium 7 (1946) 83 and 112.

43. M. Joly, J.Colloid Sci. 5 (1950) 49.

44. M. Joly, Kolloid Z. 126 (1952) 35.

45. M. Joly, Surface Phenomena in Chemistry and Biology, eds. J.F. Danielli, K.G.A. Pankhurst and A.C. Riddiford, Pergamon Press, New York (1958) p.88.

46. M. Joly, J.Colloid Sci. 11 (1956) 519.

47. M. Joly, Surface and Colloid Sci. 5 (1972) 1 and 79, ed. E. Matijevic, Wiley-Interscience.

48. D.G. Dervichian and M. Joly, Compt.Rend. 204 (1937) 1318.

49. M. Joly, J.Phys.Radium 8 (1937) 471.

50. E. Boyd and W.D. Harkins, J.Am.Chem.Soc. 61 (1939) 1188.

51. A.A. Trapeznikov, Acta Physicochim URSS 9 (1938) 273.

52. L. Fourt, J.Phys.Chem. 43 (1939) 887.

53. G.C. Nutting and W.D. Harkins, J.Am.Chem.Soc. 62 (1940) 3155.

54. A.E. Alexander, Trans.Faraday Soc. 37 (1941) 117.

55. L.E. Copeland, W.D. Harkins and G.E. Boyd, J.Chem.Phys. 10 (1942) 357.

56. A.A. Trapeznikov, Akad.Nauk SSSR, 2 (1944) 54.

57. A.K. Mukharjee, J.Indian Chem.Soc. 30 (1953) 680.

58. J.T. Davis, Biochim.Biophys.Acta. 11 (1953) 165.

59. N.L. Jarvis, J.Phys.Chem. 69 (1965) 1789.

60. S.S. Katti, S.B. Kulkarni, M.K. Gharpurey and A.B. Biswas, J.Colloid Interface Sci. 22 (1966) 207.

61. G.S. Patil, S.S. Katti and A.B. Biswas, J.Colloid Interface Sci. 25 (1967) 462.

62. S.S. Katti and G.S. Patil, J.Colloid Interface Sci. 28 (1968) 227.

63. G.S. Patil and S.S. Katti, J.Colloid Interface Sci. 30 (1969) 219.

64. A.G. Gaonkar and S.S. Katti, J.Colloid Interface Sci. 65 (1978) 232.

65. A.G. Gaonkar and S.S. Katti, J.Colloid Interface Sci. 68 (1979) 144.

66. A.G. Gaonkar and S.S. Katti, J.Colloid Interface Sci. 69 (1979) 549.

67. A.G. Gaonkar and S.S. Katti, J.Colloid Interface Sci. 73 (1980) 381.

68. D.W. Deamer and D.G. Cornwell, Biochim.Biophys.Acta. 116 (1966) 555.

69. G.E. Boyd and F. Vaslow, J.Colloid Sci. 13 (1958) 275.

70. R.P. Enever and N. Pilpel, Trans.Faraday Soc. 63 (1967) 781 and 1559.

71. N. Pilpel and R.P. Enever, Trans.Faraday Sco. 64 (1968) 231.

72. F. Vilallonga, Biochim.Biophys.Acta. 163 (1968) 290.

73. A.A. Trapeznikov and L.A. Zaozerskoya, Kolloid Z. 34 (1972) 579.

74. M. Hayashi, T. Muramatsu and I. Hara, Biochim.Biophys.Acta 255 (1972) 98.

75. M. Hayashi, T. Muramatsu and I. Hara, Biochim.Biophys.Acta 291 (1973) 335.

76. M. Hayashi, T. Muramatsu, I. Hara and T. Seimiya, Chem.Phys.Lipids, 15 (1975) 209.

77. F.C. Goodrich, L.H. Allen and A. Poskanzer, J.Colloid Interface Sci. 52 (1975) 201.

78. A. Poskanzer and F.C. Goodrich, J. Colloid Interface Sci. 52 (1975) 213.

79. F.C. Goodrich and D.W. Goupil, J.Colloid Interface Sci. 75 (1980) 590.

80. R.D. Neuman, J.Colloid Interface Sci. 53 (1975) 161.

81. S. Hard and H. Löfgren, J.Colloid Interface Sci. 60 (1977) 529.

82. P. Joos, Rheol.Acta 10 (1971) 138.

83. G. Colacicco, A.R. Buckelew Jr. and E.M. Scarpelli, J.Colloid Interface Sci. 46 (1974) 147.

84. P. Chatelain, F. Defrise-Quertain and J.M. Ruysschaert, J.Colloid Interface Sci. 72 (1979) 287.

85. D. Langevin, J.Colloid Interface Sci. 80 (1981) 412.

86. J.F. Crilly and J.C. Earnshaw, Biomedical Applications of Laser Light Scattering, ed. D.B. Sattelle, W.I. Lee and B.R. Ware; Elsevier Biomedical Press (1982) p.123.

87. K. Miyano, B.M. Abraham, J.B. Ketterson and S.Q. Xu, J.Chem.Phys. 78 (1983) 4776.

88. B.M. Abraham, K. Miyano, S.Q. Xu and J.B. Ketterson, Phys.Rev.Lett. 49 (1982) 1643.

89. F.C. Goodrich, Proc.Roy.Soc.(London), A310 (1969) 359.

90. F.C. Goodrich and A.K. Chatterjee, J.Colloid Interface Sci. 34 (1970) 36.

and

91. F.C. Goodrich, L.H. Allen, A.K. Chatterjee Proc.Roy.Soc.(London) A320 (1971) 537.

92. F.C. Goodrich and L.H. Allen, J.Colloid Interface Sci. 37 (1971) 68.

93. F.C. Goodrich and L.H. Allen, J.Colloid Interface Sci. 40 (1972) 329.

94. F.C. Goodrich, Prog.Surf.Membrane Sci. 7 (1973) 151.
ed. J.F. Danielli, M.D. Rosenberg and D.A. Cadenhead,
95. Academic Press, New York.

95. F.C. Goodrich, Solution Chemistry of Surfactants 2 (1979) 733, ed. K.L. Mittal, Plenum Publishing Co.

96. W.D. Harkins, The Physical Chemistry of Surface Films, Reinhold Publishing Co., New York (1952) p.106.

97. Ref. [14] p.156.

98. M. Lundquist, Prog.Chem.Fat other Lipids 16 (1978) 101.

99. Ref. [96] p. 111

100. Ref. [96] p. 115

101. N.K. Adam, The Physics and Chemistry of Surfaces, Oxford University Press, London (1941).

102. D.G. Dervichian, J.Chem.Phys. 7 (1939) 931.

103. W.D. Harkins and L.E. Copeland, J.Chem.Phys. 10 (1942) 272.

104. S.S. Stenhagen and E. Stenhagen, Nature (London), 156 (1945) 239.

105. A.E. Alexander, Proc.Roy.Soc.(London), A179 (1942) 470 and 486.

106. J.H. Schulman and A.H. Hughes, Proc.Roy.Soc.(London) A138 (1932) 430.

107. N.K. Adam and J.W.W. Dyer, Proc.Roy.Soc.(London) A106 (1924) 694.

108. M.K. Barnett and W.A. Zisman, J.Phys.Chem. 67 (1963) 1534.

109. J.A. Spink, J.Colloid Sci. 18 (1963) 512.

110. T.W. Healy and J. Ralston, Nature (London) 220 (1968) 1026.

111. A.V. Deo, S.B. Kulkarni, M.K. Gharpurey and A.B. Biswas, Indian J.Chem. 2 (1964) 43.

112. R.N. Shukla, M.K. Gharpurey and A.B. Biswas, J.Colloid Interface Sci. 23 (1967) 1.

113. Eng-Si Lo and Meng-Kun Lu, Hua Hsuch 4 (1975) 98.

114. H.L. Rosano and V.K. La Mer, J.Phys.Chem. 60 (1956) 348.

115. R.J. Archer and V.K. La Mer, J.Phys.Chem. 59 (1955) 200.

116. I.S. Costin and G.T. Barnes, Chem.Phys.Chem.Awendungstechnik Grenzflaechenaktiven Stoffe Ber. Int.Kongr.6th 1972 (Pub: 1973), 2 Teil, 441.

117. B.M.J. Kellner, J.Colloid Interface Sci. 74 (1980) 308.

118. F.J. Garfias, J.Phys.Chem. 83 (1979) 3126.

119. F.J. Garfias, J.Phys.Chem. 84 (1980) 2297.

120. P. Collet, J.Phys.Radium 3 (1922) 128.

121. N.K. Adam, and G. Jessop, Proc.Roy.Soc.(London) A120 (1928) 473.

122. W.D. Harkins and R.T. Florence, J.Chem.Phys. 6 (1938) 847 and 856.

123. J.H. Schulman and A.H. Hughes, Biochem J. 29 (1938) 1243.

124. J.H. Schulman and E.K. Rideal, Proc.Roy.Soc.(London) B122 (1937) 29.

125. J. Marseden and J.H. Schulman, Trans.Faraday Soc. 34 (1938) 748.

126. J.H. Schulman and E.G. Cockbain, Trans.Faraday Soc. 36 (1940) 651.

127. H.E. Ries Jr. and H.D. Cook, J.Colloid Sci. 9 (1954) 535.

128. D.G. Dervichian, Surface Phenomena in Chemistry and Biology, eds. J.F. Danielli, K.G.A. Pankhurst and A.C. Riddiford, Pergamon Press, New York (1958) p.70.

129. D.O. Shah and J.H. Schulman, Adv.Chem.Ser. 84 (1968) 189.

130. D.A. Cadenhead and M.C. Phillips, Adv.Chem.Ser. 84 (1968) 131.

131. D.O. Shah and J.H. Schulman, J. Lipid Res. 8 (1967) 215.

132. F. Villallonga, R. Altschul and M.S. Fernandez, Biochim.Biophys.Acta. 135 (1967) 406.

133. D. Chapman, F. Owens, M.C. Phillips and D.A. Walker, Biochim.Biophys.Acta. 183 (1969) 458.

134. D.A. Cadenhead,and R.A. Demchak, J.Colloid Interface Sci. 35 (1971) 154.

135. J.M. Trillo, S.G. Fernandez and P.S. Pedrero, J.Colloid Interface Sci. 26 (1968) 518.

136. E.D. Goddard and J.H. Schulman, J.Colloid Sci. 8 (1953) 329.

137. P. Joos and R. Ruyssen, Bull.Soc.Chim.Belges 76 (1967) 308.

138. P. Joos, Bull.Soc.Chim.Belges, 76 (1967) 591.

139. P. Joos, R. Vochten and R. Ruyssen, Bull-Soc.Chim.Belges 76 (1967) 601.

140. G.T. Barnes and V.K. La Mer, Retardation of Evaporation by Monolayers: Transport Process, ed. V.K. La Mer, Academic Press, New York (1962) p.9.

141. I.S. Costin and G.T. Barnes, J.Colloid Interface Sci. 51 (1975) 106 and 122.

142. D.O. Shah and S.Y. Shiao, Adv.Chem.Ser. 144 (1975) 153.

143. K. Roberts, R. Osterlund and C. Axberg, J.Colloid Interface Sci. 55 (1976) 563.

144. H. Matuo, N. Yosida, K. Motomura and R. Matuura, Bull.Chem.Soc.Jpn. 52 (1979) 667.

145. H. Matuo, K. Motomura and R. Matuura, Bull.Chem.Soc.Jpn. 52 (1979) 673.

146. H. Matuo, K. Motomura and R. Matuura, Bull.Chem.Soc.Jpn. 54 (1981) 2205.

147. A.K. Rakshit and G. Zografi, J.Colloid Interface Sci. 80 (1981) 474.

148. H. Matuo, D.K. Rice, D.M. Balthasar and D.A. Cadenhead, Chem.Phys.Lipids, 30 (1982) 367.

149. R. Verger and F. Pattus, Chem.Phys.Lipids 30 (1982) 189.

150. G.L. Gaines Jr., J.Colloid Interface Sci. 85 (1982) 16.

151. G.V. Patil, A.B. Biswas and R.N. Shukla, J.Indian Chem.Soc. 49 (1972) 1349.

152. Y.K. Kuchhal, S.S. Katti and A.B. Biswas, J.Colloid Interface Sci. 49 (1974) 48.

153. R.D. Smith and J.C. Berg, J. Colloid Interface Sci. 74 (1980) 273.

154. W. Robinowitch, F.R. Robertson and S.G. Mason, Canad.J.Chem. 38 (1960) 1881.

155. J.H. Brooks and A.E. Alexander, Retardation of Evaporation by Monolayers: Transport Process, ed. V.K. La Mer, Academic Press, New York (1962) p. 245.

156. P. Joos, Bull.Soc.Chim.Belges. 78 (1969) 207.

C H A P T E R - II

EXPERIMENTAL

EXPERIMENTAL

Introduction

The origin of the film balance can be traced back to Pockels [1]. She first introduced the use of trough and barriers for the measurement of surface pressure. Langmuir [2] made improvements in the balance and developed a horizontal float method for direct measurement of surface pressure. Later on Adam and Jessop [3] developed end loop system for attaching to sides of trough while maintaining the necessary float mobility. Harkins and Anderson [4] have modified the Wilhemy method [5] to get surface pressures directly. In this method major disadvantage is the contact angle of the liquid on the plate. Once the monolayer forming molecules are present at the interface the contact angle increases as the plate moves up with increase in film pressure. However, in the Langmuir type horizontal film pressure balance, the contact angle problem does not appear at all. This is the greatest advantage in Langmuir type balances.

In spite of certain advantages and disadvantages, both the methods are commonly used for the film pressure measurements. The choice of the type of the balance is often dictated by the type of the interface and the suitability of experimental set-up.

In the present investigation a completely indigenous manually operated Langmuir type horizontal film pressure balance, constructed in our laboratory, has been used. The details of the apparatus will be discussed in the following:

Langmuir trough

The trough in which the substrate liquid is contained warrants special attention. Not only the material used for constructing the trough is important but also the size and the shape. The trough must hold a large volume of liquid with a large exposed area for the manipulation and at the same time it should not contaminate the substrate liquid. The trough edges must be smooth, sharp and non-wettable to prevent spilling over the substrate. Therefore the trough must be constructed either of a hydrophobic material or the edges should be made hydrophobic by coating of suitable material. Most of the early work has been done with metal troughs coated with paraffin wax. However, Langmuir and Schaefer [6] have reported the contamination of the subphase from brass, aluminium, gold and rhodium plated troughs. The glass (or silica) troughs have an advantage of purity but the fragility of the material and poor adhesion of the paraffin wax to the smooth glass edges are the disadvantages. In recent times

the use of plastic materials for the troughs has become popular. The troughs of teflon, perspex, nylon and polyethylene are in practice. In such troughs it is essential to varify that low molecular weight fragments, plasticizer or mold-releasing agents do not contaminate the substrate liquid.

In the present investigation a rectangular perspex trough was constructed in the laboratory. The inner dimensions of the trough were 71 cm x 15.8 cm x 2 cm. This trough was mounted in a wooden case having meter scales on the either side of the longitudinal axis.

The trough was cleaned with running tap water, followed by 50% acetone-water mixture. Then again with tap water and followed by distilled water. The trough was filled with distilled water and kept for 24 hrs to make it sure that it is free from water soluble organic contaminants.

The edges of the trough were very sharp. This is necessary to confine the film in desired area; otherwise the slipage of the film through the contact between the barrier and trough is inevitable. The trough edges were made hydrophobic by applying a very thin layer of solution of paraffin in xylene.

The barriers

The use of the metal strips (now called as barriers) to vary the surface area was first suggested by Pockels [1]. The substrate liquid (which is usually water, therefore it will be referred as 'substrate water') is filled upto the brim of the trough; therefore when the barrier is kept on the edges of the trough across the width, its entire lower surface touches to substrate water; thus makes the compartments in the trough.

The material of which the trough is made up of should be preferably used for making the barriers. The barriers are the square rectangular strips; the size is left to the choice of the investigator but usually it is 1 cm x 1 cm and extends beyond at least by 2-3 cms of both sides of the trough. The edges of the barriers are also necessarily sharp and hydrophobic to avoid the slipage of the film.

In the present investigation the rectangular strips of perspex of the size 22 cm x 1 cm x 0.5 cm were used as barrier. A brass rod of the same size was fixed to these barriers by synthetic adhesive to get the rigidity. The working edge of the barriers (perspex side) was made hydrophobic in the same way as the trough edges.

Temperature control

All monolayer properties are extremely sensitive to the temperature. Therefore one is compelled to control and maintain the temperature of the substrate water to make the measurements meaningful. This is done by circulating thermostated water through a serpentine coil which is immersed in the substrate water. The temperature of the substrate water, in the present investigation, was successfully maintained with an accuracy of $\pm$ 0.1^{o}C and temperature was displayed by a temperature indicator.

Water level indicator

Change in the water level may introduce error in measurement of surface pressure. The level of water in the trough was maintained constant with help of water level indicator. It consists of a small funnel type apparatus having a glass pointer at the stem. The funnel is so adjusted to the trough that the pointer just touches the water surface. The evaporation of the water causes the level to drop; the water can be added through the funnel (so that the film above the water surface is not disturbed) till the original level is attained.

The horizontal film pressure balance

The principle of the operation of the horizontal film balance is illustrated in Fig. 2.1. The balance consisted

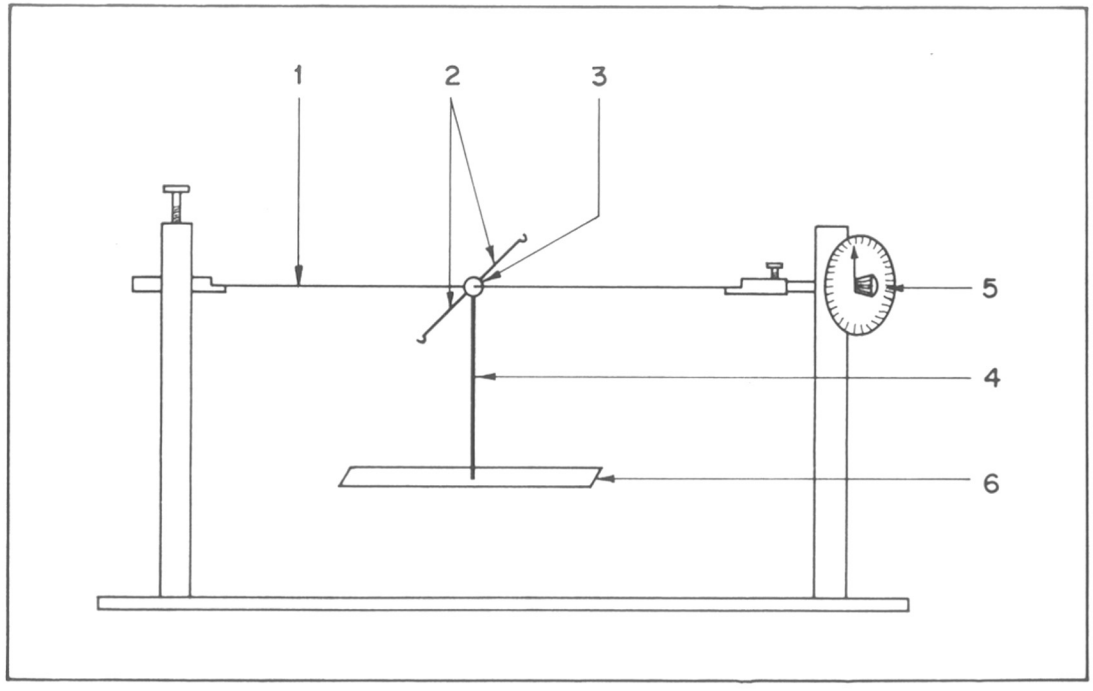

FIG. 2·1 : HORIZONTAL LANGMUIR FILM PRESSURE BALANCE.

1 : TORSION WIRE , 2 : SIDE ARMS OF BRASS ,

3 : REFLECTING MIRROR , 4 : VERTICAL BRASS ROD ,

5 : PROTRACTOR , 6 : MICA FLOAT.

of a thin paraffinned mica float of the size 13.5 x 1.3 x 0.2 cm. A thin brass rod was wax soldered at the centre of the float. The other end of the brass rod is screwed to a small brass disc which was clamped tightly at the centre of a torsion wire. A small reflecting plane mirror was fixed on the upper face of the disc. Two horizontal calibration arms (perpendicular to the torsion wire) were screwed to the disc carrying mirror. The torsion wire in the present investigation was 37 s.w.g. stainless steel wire of suitable length. The angle of twist of the torsion wire was measured by protractor (0.5° smallest division) which was fixed at one end of the torsion wire.

The gap between the trough edges and the float must be properly sealed. Langmuir [2] used air jets for this purpose. Adam and Jessop [3] introduced the technique of blocking the gaps with thin flexible, paraffinned ribbon of gold or platinum foil, half immersed in the water. Guastalla [7] used vaselined threads. Allan and Alexander [8] found that very fine nylon monofilaments were most suitable for low pressure measurements. In the present work, teflon ribbons were used as suggested by Mann and Hansen [9]. This proved to be very satisfactory.

The float separates the aqueous surface and film covered surface. As the surface pressure of the film

increases, the float laterally moves towards the clean water surface. This is detected on the lamp and scale arrangement. The float can be brought back to its original position by twisting torsion wire and thus knowing the angle of twist. The surface pressure (film pressure) in dynes/cm can be obtained by multiplying the angle of twist with the calibration constant.

Calibration of the film pressure balance

Before doing any monolayer experiments, one has to calibrate the film pressure balance. The calibration has to be checked from time to time and has to be recalibrated whenever the torsion wire is changed. The calibration is done as follows:

Small metal rings of known weight (w gm) were placed in the hook of the calibration arm. This produces a torque in the torsion wire which is indicated by the deflection on the lamp and scale arrangement. By twisting the torsion wire the float was brought back to original position. The angle of twist θ was noted. Then the sensitivity 's' of the torsion wire is given by:

$$S_{(\text{dynes/cm/degree rotation})} = \frac{W.g.l.}{\theta.L.L'} \qquad (2.1)$$

g = gravitational constant

l = perpendicular distance of the ring from torsion wire

L = length of the brass rod connecting the float,

L' = effective length of the float i.e. length of the float plus half the width of the gaps at each end.

For various w values, corresponding θ values were noted. The plot of w vs θ gives a straight line passing through the origin. From the slope of the graph, the average value of the calibration constant S was calculated; in the present investigation one degree rotation of torsion head corresponds to 0.1542 dynes/cm surface pressure. This calibration was checked from time to time and was found to be constant.

Substrate

The use of well defined substrate is the necessity in the monolayer work. The substrate in most of the cases (and in the present investigation also) is water. Water can be purified in many ways. The use of ion exchange resins to prepare the substrate water should be avoided because the resins are likely to introduce organic contaminants. The use of complexing agents (e.g. EDTA) to remove heavy metal ions should be strictly avoided because the complexing agents seriously affect the properties of insoluble film [10]. Purification of

substrate water by activated charcoal or other adsorbents has reported to be satisfactory in some studies [11,12] but Pak and Gershfeld [10] proved it ineffective.

In the present case double distilled water was used as the substrate. The second distillation was done in all glass apparatus with alkaline potassium permanganate. The pH of this water varied from 6 to 6.5 whereas the conductivity varied from 2-3 x 10^{-6} mhos.

Spreading solvent

Some materials spread spontaneously from pure bulk phase on the substrate surface. Since many substances do not spread well by themselves, it is common practice to use 'spreading solvent' to assist the spreading. In the former method of spreading, it is difficult to know precisely the amount of material spread secondly, the useful study of a mixed monolayer is not possible by the separate spreading of the two components from their bulk phases. Therefore, second method of spreading (i.e. through spreading solvent) was adopted in the present study.

A good spreading solvent should be non-reactive volatile, insoluble in the substrate and free from surface active contaminants.

Some of the common organic solvents are n-hexane, cyclohexane, benzene, chloroform and ethyl ether.

Chloroform is highly volatile and dissolves in water [13]. Harkins and Nutting [14] found petroleum ether (60-80°C) to better spreading solvent than benzene. Walker and Ries [15] have shown that the isotherms of stearic acid in n-hexane and in benzene were identical except a small change in collapse pressure. Robbins and La Mer [16] have made very interesting observations on the effect of solvent on the monolayer. They have studied effects produced by benzene or hexane as spreading solvents upon the π-A isotherms of stearic acid and octadecanol. The authors have given a π-A isotherm produced when large amount (6.16 ml) of pure benzene is allowed to evaporate on water surface, this may be due to non-volatile impurities in the benzene. According to the authors, not only the specific solvent, but the amount of solvent per molecule of monolayer, contribute to the measured properties. It is interesting to note the tremendous expansion of octadecanol π-A isotherm as the concentration of spreading solution goes on changing.

In the present investigation, twice distilled BDH Analar grade petroleum ether boiling in the range 60-65°C was used as spreading solvent for n-long chain component mixtures whereas the twice distilled BDH Analar grade benzene was used for polymer mixture systems. The concentration of the spreading solution prepared was about

0.7 to 1 mg/ml and of this, 0.06 - 0.08 ml was spread in about 500 sq.cm area.

Surface Viscosity

Several methods are available in the literature for the measurement of surface viscosity. Methods of measuring surface viscosity are more or less directly derived from those used in the bulk rheology. Joly [17,18] has published two excellent reviews on the surface viscosity in which he has discussed various methods for the measurement of surface viscosity. There are four principal methods used for the surface viscosity measurements:

1) Motion of a floating object
2) Damped oscillations of a torsion pendulum
3) Flow through a surface canal
4) Rotation method

Motion of a floating object: By following the pointer of a torsion balance whose head is subjected to a constant rotational velocity, a small disc undergoes uniform circular motion in a circular canal bounding the film. The resistance to the motion of the disc is determined from the torsion of the balance wire and from velocity V of the disc relative to canal border. The surface viscosity is given by

$$\mu = \frac{F_1 - F_o}{KV} \qquad (2.2)$$

F_1 and F_o are the resisting forces in the presence and absence of the film.

K is a calibration constant.

Damped oscillation of a torsion pendulum: The measurement of surface viscosity by determining the damping of a torsion pendulum oscillating in the film is one of the oldest methods of surface rheology [17,18]. Two types of apparatus have been used a) an oscillating vane or needle, b) an oscillating ring, disc or bob. For an oscillating needle, the mechanical conditions are not the same everywhere in the film and are often poorly defined. Therefore, the viscosities determined in this way are approximate and indicate no more than an order of magnitude. If a ring of mica, instead of a needle, is used, the rheological parameters are much better defined and the sensitivity of the method is notably increased [18]. This method is easy for knowing whether a given system exhibits Newtonian or non-Newtonian viscosity. In case of a Newtonian system, the plot of logarithm of amplitude against number of swings shows a straight line, if the straight line is not obtained, the system is non-Newtonian.

Flow along a surface canal: The idea of surface canal viscometer is based on the capillary viscometers of Poiseuille or Ostwald for bulk viscosity. Two techniques

are in practice depending upon either the flow generated by establishment of constant surface pressure difference at the two ends of the canal or it is generated by motion of the substrate. The first method may be applied only to insoluble monolayers whereas the second may be applied to adsorbed films.

In automatic recording film balances Trurnit and Lauer [19] have introduced a slit viscometer consisting of a compression bar with a horizontal slit at the level of water surface. The slit has opening and closing arrangements. Slit is closed till a certain pressure is obtained and then it is opened so that film flows through the slit on to the clean water surface behind the slit-bar. The film pressure tends to decrease, but the constant pressure device maintains it constant by moving the slit bar. The bar motion is recorded as a function of time; which gives a straight line, the slope of which is a function of film viscosity.

Rotation method: This method is used for the study of non-Newtonian surface viscosity. It is, therefore, advantageous to adopt the Couette viscometer. Here the essential requirement is a pair of concentric rings of which one turns about its axis with a constant rotational velocity and the other is suspended by means of a torsion

wire . The resistance of a film present in the annular space opposes this motion. The deflection of suspended ring is a function of viscosity of the film. The torque exerted by the stationary ring measures the surface viscosity.

De Bernard [20] has constructed a most sensitive rotational surface viscometer. Both the rings were made-up of glass filament and were paraffined. The outer ring was suspended with the help of a phosphor bronze wire and the ring was so adjusted that it was just touching the water surface. The inner ring was connected to a motor system so as to rotate with a constant speed. The outer ring had a small opening so as to allow the film to enter the annular space between the two rings. The deflection of the outer ring due to the viscous drag of the film is a means of surface viscosity. In addition to these rings, there is a damping device. This is required to reduce the motion of the water under floating rings. This consists of a mica ring, coated with wax which floats and maintains a plate (disc) of non-waxed mica just below the surface of the water. With this brake system complete immobility of the monolayer present outside the outer ring is obtained. It has been observed that the monolayer viscosity is independent of the distance at which the unwaxed mica plate (disc) is placed below the water surface.

Surface viscometer used in the present study

The parts of the rotational viscometer constructed in the laboratory are shown in Fig. 2.2. This consisted of two concentric rings (b and d) of mica coated with paraffin wax and floating on the surface of the water (i.e. just touching the water level). The inner ring (b) having outer diameter R_1 = 3.15 cm was wax soldered to three brass rods (b') connected to a brass disc (K) having screwing arrangement. This disc was connected to a coaxial stainless steel tube (F) of diameter 3.5 cm; the other end of the stainless steel tube was connected to a synchronous motor through gear system. Thus the inner ring could be rotated about its vertical axis at a desirable speed. This enables to take measurements at different shear rates (g).

$$g = \frac{2\pi.R_1}{(R_2-R_1).t} \qquad (2.3)$$

R_1 = outer radius of inner ring

R_2 = inner radius of outer ring

t = period of rotation of inner ring.

The outer ring (d) having inner radius R_2 = 5.18 cm was fixed on a brass support with the help of wax. The support carries a small reflecting mirror and the arrangement for

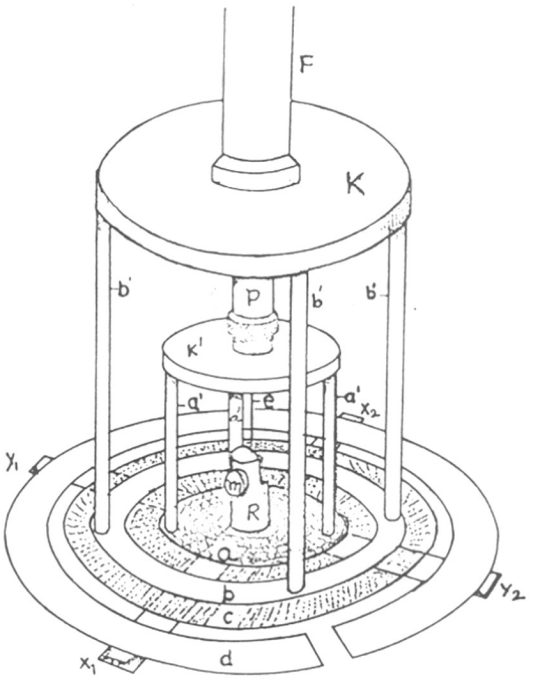

a) INNER DISC FLOATING ON WATER SURFACE
b) INNER RING WHICH IS ROTATING WITH CONSTANT SPEED
c) MICA DISC IMMERSED IN WATER
d) OUTER RING WHICH IS SUSPENDED BY PHOSPHOR BRONZE WIRE (e)
f) STAINLESS STEEL TUBE CONNECTED TO INNER RING
g) STAINLESS STEEL TUBE CONNECTED TO INNER DISC

FIG. 2·2 : SURFACE VISCOMETER.

clamping the torsion wire. The phosphor-bronze wire of suitable gauge (37 s.w.g.) and length (67 cm) was used as torsion wire in our experiments. A brass disc of known moment of innertia (I), was suspended at its centre by the phosphor bronze wire. The period of oscillation (T_o) for the disc was found out. The torque constant (C) of the wire is given by

$$C = \frac{4\pi^2 I}{T_o^2} \quad ; \quad I = \frac{MR^2}{2} \qquad (2.4)$$

where M = weight of the brass disc

R = radius of the disc.

It should be confirmed before fixing the wire (along with the outer ring) to the viscometer that the wire is completely free from wrinkles and after fixing it should not touch the inner walls of the stainless steel tube through which it passes. The upper end of the wire is fixed to a brass holder which has arrangements to move up-down.

A damping arrangement as suggested by De Bernard [20] has been introduced. This consisted of a waxed mica disc (a) floating on the water surface and a non-waxed mica disc (c) just below the water surface. The two discs are connected to three thin brass rods (a') which are connected to coaxial

stainless steel tube (p) of 1.5 cm diameter. This tube (p) passes through the tube (F) without touching it. The end of the tube is connected to levelling arrangement for, adjusting the level of two mica discs. The deflection of the outer ring due to viscous drag of monolayer was notified by a lamp-scale arrangement.

If θ is the angle of rotation of the outer ring; the moment M is given by

$$M = C\theta = \frac{CD}{2L} \qquad (2.5)$$

where C = torque constant of the wire

D = difference in the deflection between film covered water surface and pure water surface with same period of rotation

L = distance between mirror and scale.

The torque of the monolayer for the same moment M is given by

$$M = \frac{8\pi^2\mu}{t} \times \frac{(R_1^2 \times R_2^2)}{(R_2^2 - R_1^2)} \qquad (2.6)$$

Equating the equations (2.5) and (2.6)and rearranging we get

$$\mu = \frac{C}{16\pi^2 L} \times \left(\frac{1}{R_1^2} - \frac{1}{R_2^2}\right) . D.t. \qquad (2.7)$$

R_1, R_2 and t are as defined earlier. The eqn.(2.7) has been used in the present investigation to calculate surface viscosity.

Experimental procedure

General precautions

The complete experimental set-up* along with the surface viscometer has been shown in Fig. 2.3.

The monomolecular films are extremely sensitive to slightest amount of impurities such as air-borne greasy materials and dust particles. Enough precautions have to be taken to avoid such contamination. The apparatus was placed in a constant temperature, constant humidity and dust free room. The Langmuir film balance, along with the trough and the viscometer was covered by a glass case having sliding door. The glass case and the apparatus were mounted on two different angle-iron stands to avoid vibrations. Both the angle iron stands were made free from vibrations by putting proper packing material at the bottom. Thus the Langmuir balance and trough were guarded from vibrations as far as possible.

The substrate water comes in direct contact with the trough, barriers, float, teflon ribbon, viscometer rings, the serpentine coil, temperature sensor and water

---

* Details of the dimensions are given in Appendix II.

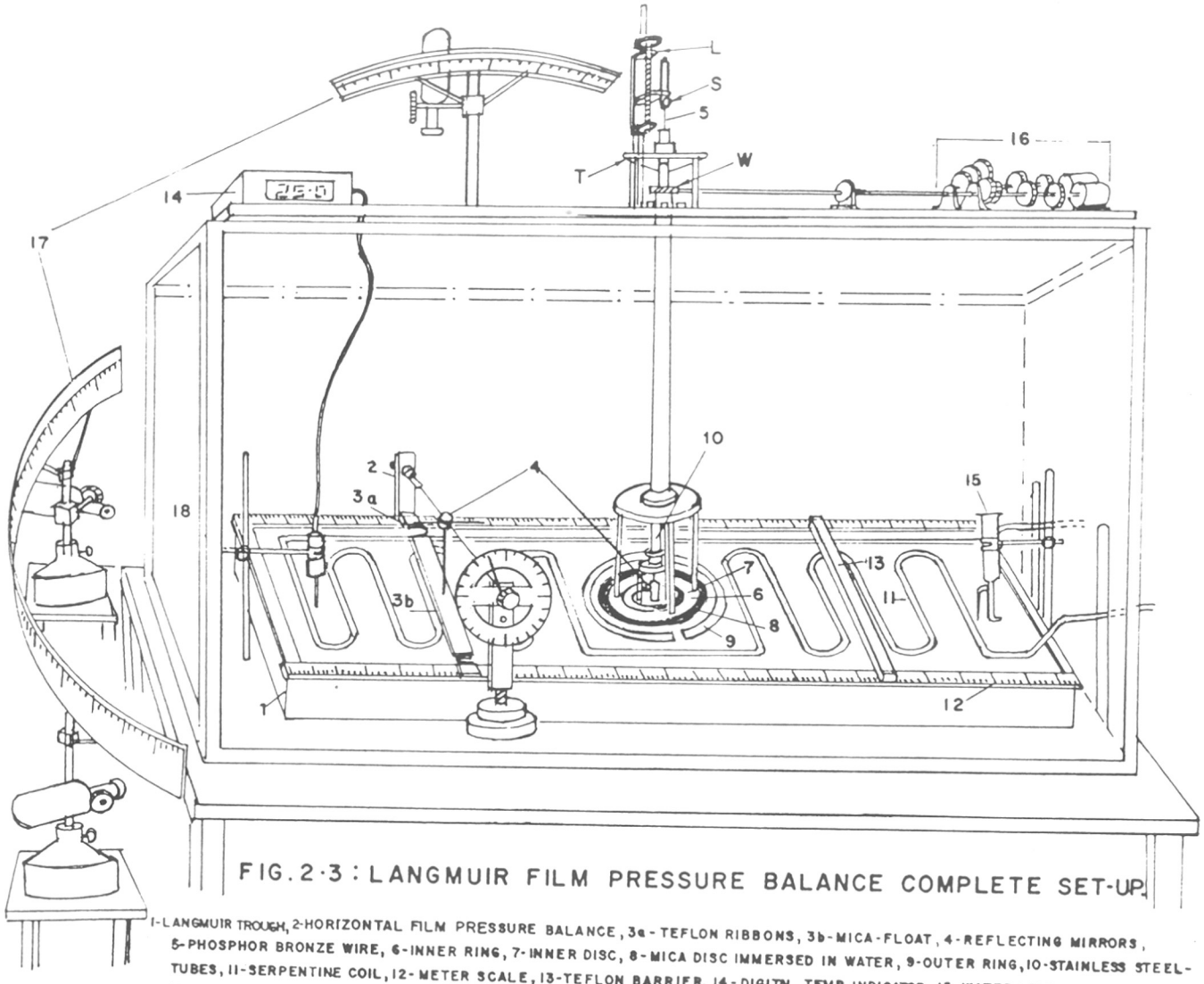

FIG. 2·3 : LANGMUIR FILM PRESSURE BALANCE COMPLETE SET-UP.

1-LANGMUIR TROUGH, 2-HORIZONTAL FILM PRESSURE BALANCE, 3a-TEFLON RIBBONS, 3b-MICA-FLOAT, 4-REFLECTING MIRRORS, 5-PHOSPHOR BRONZE WIRE, 6-INNER RING, 7-INNER DISC, 8-MICA DISC IMMERSED IN WATER, 9-OUTER RING, 10-STAINLESS STEEL-TUBES, 11-SERPENTINE COIL, 12-METER SCALE, 13-TEFLON BARRIER, 14-DIGITAL TEMP. INDICATOR, 15-WATER LEVAL INDICATOR, 16-SYNCHRONOUS MOTORS WITH GEAR SYSTEM, 17-LAMP & SCALE ARRANGEMENT, 18-GLASS CASE.

level indicator. Therefore, these parts should be extremely clean, free from greasy materials.

Before starting any experiments all the precautions mentioned above have been taken care of.

Set up to be made ready before starting the experiment

The cleaned trough was mounted perfectly horizontal on the table with help of three levelling screws. The cleaned serpentine coil was placed in the trough; the ends of the coil were attached to proper rubber tubes for the circulation of thermostated water.

The paraffined mica float was properly fixed to the centre of the torsion wire of the horizontal film pressure balance. The height of the trough was so adjusted that the float comes just above (0.5 mm) the edges of the trough. The gaps between the float and the trough edges were sealed with wax by teflon ribbon, keeping the movement of the float free. The trough was then filled with double distilled water (substrate) till the water level comes just above (0.5 to 1 mm) the edge of the trough. The water level indicator was fixed so that its glass pointer just touches the water surface. The circulation of thermostated water through the serpentine coil was started to get the desired temperature. Barriers were placed on the trough; two on working side of float and one on other side of the float.

Approximately one hour is required to obtain the desired temperature of the substrate water. During this time some impurities spread on the water surface. The floating particles sometimes can be seen with naked eye. Such particles were removed by sucking them with help of a glass tube drawn into capillary which is attached to a water suction pump. During this sucking process the barriers were brought near to float (i.e. compressing). The water on both sides of the float was cleaned. During this process water level goes down, which is maintained by adding fresh substrate water through the water level indicator. The surface cleaning is accomplished when no film pressure is developed even when the surface area is reduced to 1% of its original value by moving the barrier. It is necessary to confirm this just before spreading the film.

Preparation of the spreading solution

Following compounds have been used in the present study:

1) Hexadecanol; $C_{16}H_{33}OH$
2) Eicosanol; $C_{20}H_{41}OH$
3) Docosanol; $C_{22}H_{45}OH$
4) Hexadecoxy ethanol; $C_{16}H_{33}OC_2H_4OH$
5) Octadecoxy ethanol; $C_{18}H_{37}OC_2H_4OH$

6) Docosanoxy ethanol; $C_{22}H_{45}OC_2H_4OH$

7) Hexadecoxy propanol; $C_{16}H_{33}OC_3H_6OH$

8) Docosanoxy propanol; $C_{22}H_{45}OC_3H_6OH$

9) Poly(vinyl stearate); (PVS)

10) Poly(vinyl acetate) ; (PVAc)

All the long chain compounds were prepared and purified in the laboratory. The details are given in Appendix I. The purity of all the long chain compounds was checked on a gas chromatogram (Varian 3700). All the compounds were found to be more than 99% pure. The extrapure samples of PVS and PVAc were obtained from Polysciences; Warrington USA. The molecular weight of PVS is 5000 and that of PVAc is 435000. These samples were used as supplied. All the long chain compounds were evacuated in a vacuum desiccator for three hours to remove traces of moisture and were always preserved in a desiccator.

Petroleum ether and benzene were used as spreading solvents in our study. The purification of these solvents was done as described earlier.

The mixtures were prepared by weighing calculated amounts of two components (to get required mole fraction) in a 5 ml, A grade, volumetric flask. The mixture was

dissolved in the appropriate spreading solvent (approximately 1 ml) and then the flask was filled upto the mark with the spreading solvent. This spreading solution is now ready for the experiment.

The desired amount of spreading solution was administered through Agla micrometer syringe (manufactured by Burroughs Wellcome Co. London) with accuracy of 0.0002 ml at different places over the desired area of the clean water surface. Before spreading the solution the initial position of the reflected spot of light from Langmuir balance was noted.

Experimental procedure for π-A isotherms

The calibration of the film balance and the preparations of spreading solution has been described earlier.

The position of the reflected spot of light on the scale from the film pressure balance was noted. The working barrier was placed at such a distance from float so that the area between the barrier and the float was approximately 500 sq.cm. The general precautions mentioned earlier were observed and it was also confirmed that the water surface is clean. Approximately 0.06 to 0.10 ml of spreading solution was delivered through Agla

micrometer syringe at different places in the working area. Fifteen minutes were allowed to evaporate the solvent. (In case of polymer mixtures, where benzene was used as spreading solvent, thirty minutes were allowed to evaporate the solvent).

If any pressure is developed, it is indicated by the deflection of the spot of light on the scale. In that case spot was brought back to its initial position and the angle of twist was noted. In the pilot experiment the area was varied with approximately 0.50 $\AA^2$ /molecule with 2-3 minutes interval after every compression. This gives a rough idea about the nature of π-A isotherm. Subsequent experiments were done more carefully. In these experiments the area was reduced initially by 0.50 $\AA^2$ /molecule (upto 4 dynes/cm) and afterwards the decrement was reduced to 0.25 to 0.05 $\AA^2$ / molecule depending on the pressure. However, the 2 minutes interval was kept constant between each compression. Finally the collapse is indicated by a decrease in film pressure at constant area within two to three minutes.

Repeated experiments were done with fresh spreading solutions and with different initial concentrations to ensure the reproducibility. The reported curves in the present work are average of minimum triplicate experiments within the experimental error.

The reproducibility of film pressure was ± 0.20/dynes/cm whereas area was ± 0.20 $\mathring{A}^2$/molecule.

Experimental procedure of μ-π curves

The viscosity attachment was placed in the appropriate position as shown in Fig. 2.3.

The other arrangements such as levelling of the trough attaching the float, filling the trough with double distilled water, sweeping the working surface of the water etc. and the precautions about the cleanliness of the various parts remains the same as described earlier.

The position of the spot on the scale reflected from outer ring was recorded. The inner ring was then rotated with a constant speed with the help of synchronous motor and the deflection was noted. In the present study for the pure water surface no deflection was observed for all shear rates.

After assuring this, the monolayer was spread as usual. The synchronous motor was started and the deflection of the outer ring was measured as a function of film pressure. From the deflection, the surface viscosity was calculated using the equation (2.7). The same procedure was repeated for other shear rates (six shear rates were studied for each film).

Minimum triplicate experiments were carried out using fresh spreading solutions with different initial concentrations. The average curve was calculated from the replicate experiments which were within the experimental error.

The rotational viscometer used in the present investigation has been criticized because of the finite thickness of the rings which is several times higher than the thickness of monomolecular film. The finite thickness of the rings produce motion in the bulk substrate. Goodrich and Allan [21,22] pointed out that the sensitivity of surface viscometer measuring low surface viscosities is much less than that of an ideal viscometer with the rings of zero thickness. Secondly, in such viscometers, it is very difficult, but not impossible, to generate interfacial flow of constant shear rate in the annular space of the rings [23]. Goodrich [23] has tried to apply hydrodynamic analysis for non-Newtonian monolayer system. In these cases the application of hydrodynamic theory is much more complicated and found unsatisfactory; equations are very complex and no exact solution can be found. However, the viscometer used by us works well with range of moderate to high viscosities (1 to 10^{-3} surface poise) [24]. The viscosity of various monolayers studied by us lies in this range.

REFERENCES

1. A. Pockels, Nature (London), 43 (1891) 437.
2. I. Langmuir, J.Am.Chem.Soc. 39 (1917) 1848.
3. N.K. Adam and G. Jessop, Proc.Roy.Soc.(London), A110 (1926) 423.
4. W.D. Harkins and T.F. Anderson, J.Am.Chem.Soc. 59 (1937) 2189.
5. L. Wilhelmy, Ann.Physik, 119 (1863) 117.
6. I. Langmuir and V.J. Schaefer, J.Am.Chem.Soc. 59 (1937) 2400.
7. J. Guastalla, Compt.Rend. 189 (1929) 241.
8. A.J.G. Allan and A.E. Alexander, Trans.Faraday Soc. 50 (1954) 863.
9. J.A. Mann Jr. and R.S. Hansen, Rev.Sci.Instr. 34 (1963) 702.
10. C.Y.C. Pak and N.L. Gershfeld, J.Colloid Sci. 19 (1964) 831.
11. H. Bull, J.Am.Chem.Soc. 67 (1945) 4.
12. F.C. Goodrich, Proc. 2nd Int.Congr. of Surf.Activity, 1 (1957) 85.
13. H.D. Cook and H.E. Ries Jr., J.Phys.Chem. 60 (1956) 1533.
14. W.D. Harkins and G.C. Nutting, J.Am.Chem.Soc. 61 (1939) 1702.
15. D.C. Walker and H.E. Ries Jr. Nature (London), 203 (1964) 292.
16. M.L. Robbins and V.K. La Mer, J.Colloid Sci. 15 (1960) 123.
17. M. Joly, Recent Progress in Surface Science, 1 (1964) 1.
18. M. Joly, Surface and Colloid Science, 5 (1972) 1.

19. H.J. Trurnit and W.E. Lauer, Rev.Sci.Instr. 30 (1959) 975.

20. L. De Bernard, Proc. 2nd Int.Congr.Surf.Activity, London, 1 (1957) 7.

21. F.C. Goodrich and L.H. Allen, J.Colloid Interface Sci. 37 (1971) 68.

22. F.C. Goodrich and L.H. Allen, J.Colloid Interface Sci. 40 (1972) 329.

23. F.C. Goodrich, Prog.Surf.Membrane Sci. 7 (1973) 151.

24. G.T. Barnes, Colloid Sci. Specialist Periodical Reports, 3 (1979) 150.

C H A P T E R - III

MIXED MONOLAYERS OF n-LONG CHAIN COMPOUNDS

INTRODUCTION

In our laboratory considerable amount of work has been carried out on the physical properties of monolayers of n-long chain alcohols, alkoxy ethanols, propanols, butanols and some of their mixtures in connection with water evaporation control project. The success in controlling the evaporation depends on efficacy and stability of the insoluble monolayer spread on the water surface. There are many factors in nature affecting the stability of the monolayer e.g. wind, dust and other external impurities.

Instead of a single component monolayer, if two component (mixed) monolayer is formed and if the two components show strong intermolecular interactions, the mixed monolayer should be better evaporation retardant than the pure components. With this view, some of the mixed monolayers have been studied in our laboratory. From the literature survey (Chapter I) it is clear that the mixed monolayers in which both components have same chain length but different polar groups show little interactions between two components. This means that the polar group plays an insignificant role in nonideal behaviour of mixed monolayer, whereas mixed monolayers having the same polar group but different chain length give nonideal behaviour.

Therefore, it was thought worthwhile to study the mixed monolayers having the same polar groups but a wide

chain length difference. For such a study, alcohol + alcohol, alkoxy ethanol + alkoxy ethanol and propanol + propanol systems were chosen.

The literature survey reveals that Patil et al. [1] have studied mixed monolayers of alcohol + alcohol and alkoxy ethanol + alkoxy ethanol by studying π-A isotherms at three mole fractions only. Similarly, Kuchhal et al. [2] have studied the above type of mixtures only at 1:1 molar ratio by measuring surface potential and π-A isotherms. Taking into account these facts, a systematic study of the following three systems was undertaken by measuring surface viscosity, surface pressure, area per molecule and collapse pressure with a view to get more insight into the nonideal and miscible behaviour.

System I : Hexadecanol ($C_{16}H_{33}OH$) with Docosanol ($C_{22}H_{45}OH$) (abbreviated as C_{16}-OH + C_{22}-OH).

System II : Hexadecoxy ethanol ($C_{16}H_{33}OC_2H_4OH$) with Docosanoxy ethanol ($C_{22}H_{45}OC_2H_4OH$) (abbreviated as C_{16}-OC_2H_4OH + C_{22}-OC_2H_4OH)

System III: Hexadecoxy propanol ($C_{16}H_{33}OC_3H_6OH$) with Docosanoxy propanol ($C_{22}H_{45}OC_3H_6OH$) (abbreviated as C_{16}-OC_3H_6OH + C_{22}-OC_3H_6OH).

The above three systems have been studied at air-water interface at five different mole fractions (viz. mole fraction of C_{16}-component → 0.20, 0.33, 0.50, 0.66 and 0.80) and at 25°C. The complete experimental details have been described in Chapter II.

Surface viscosity - film pressure curves (μ-π)

Surface viscosity (μ) was measured as a function of film pressure (π) on a rotational type viscometer as described in Chapter II. The surface viscosity for all the mixtures was found to be non-Newtonian. The μ-π curves for various mixtures at different shear rates have been given in Figs. 3.1 to 3.15. The variation of surface viscosity with the film pressure in the Figs. 3.1 to 3.15 may be explained by visualising the molecular arrangements in different phases. Surface viscosity is low at low film pressures since the film molecules are randomly oriented and are bound to water molecules through hydrogen bonding. As the film is compressed the molecules are brought together, the chain-chain interaction starts operating and surface viscosity increases. It is predominent at Lc → I transition. As the film is further compressed, the molecules rearrange themselves almost vertical to the water surface. During this process, the surface viscosity increases rapidly with film pressure. The further compression of the film makes

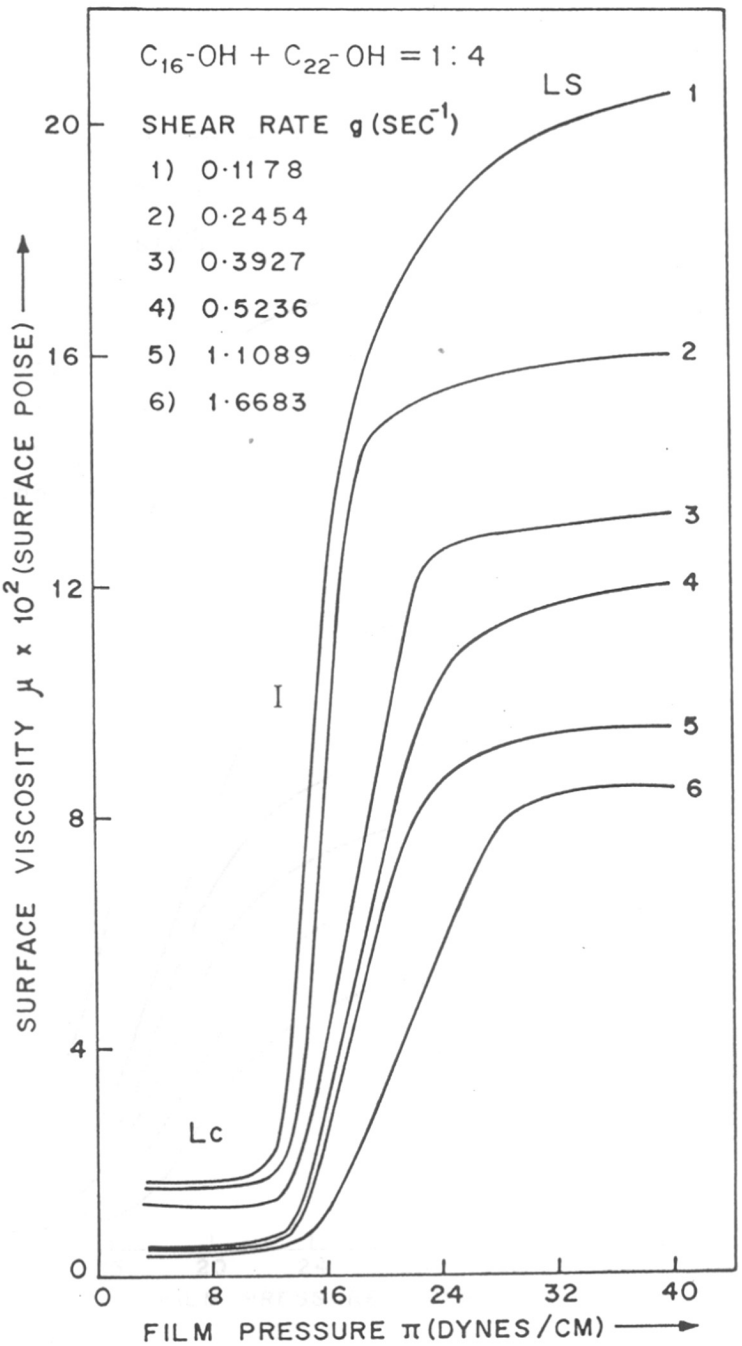

FIG. 3·1 : SURFACE VISCOSITY (μ) AGAINST FILM PRESSURE (π) FOR VARIOUS SHEAR RATES.

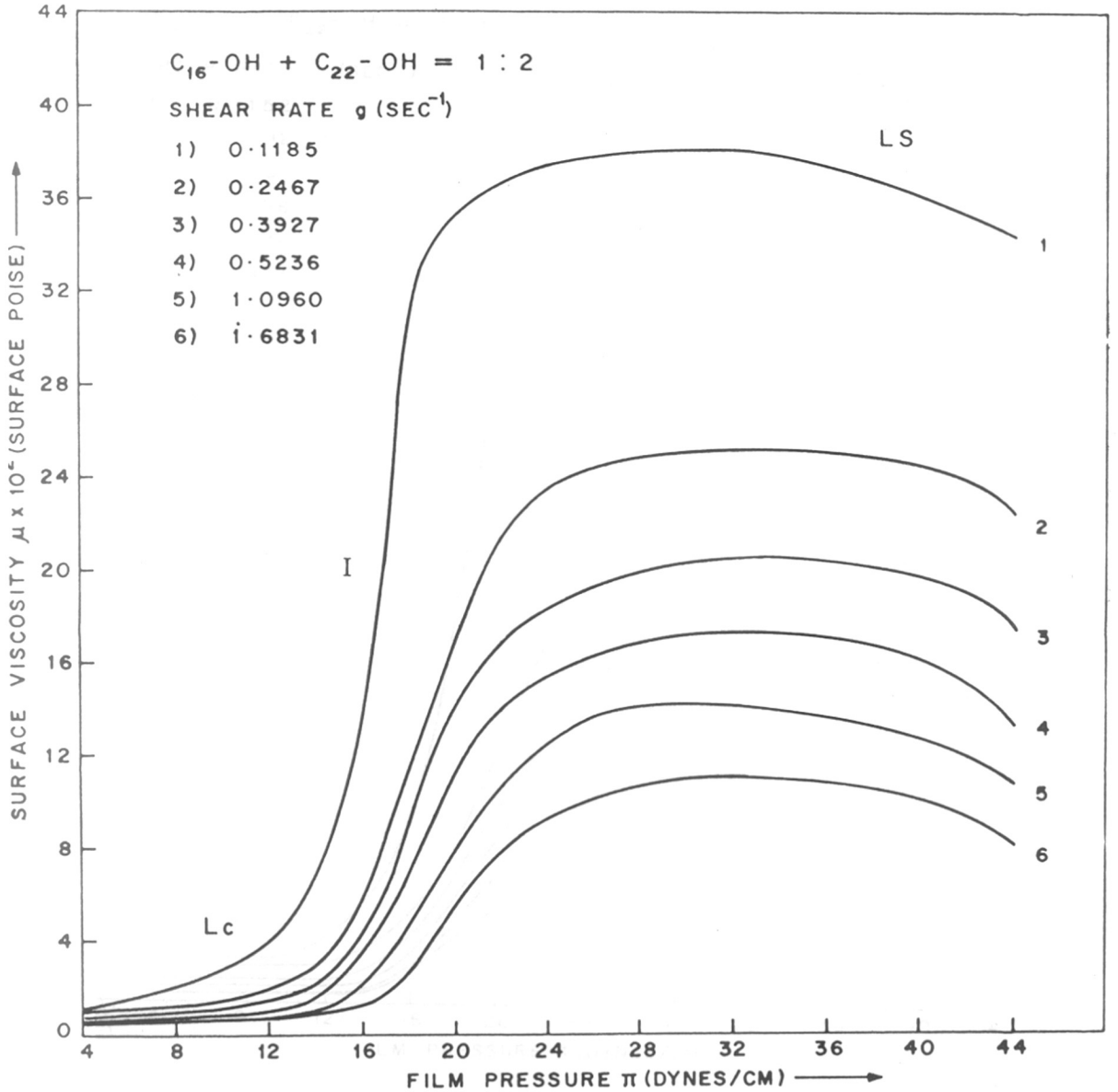

FIG. 3·2 : SURFACE VISCOSITY (μ) AGAINST FILM PRESSURE (π) FOR VARIOUS SHEAR RATES.

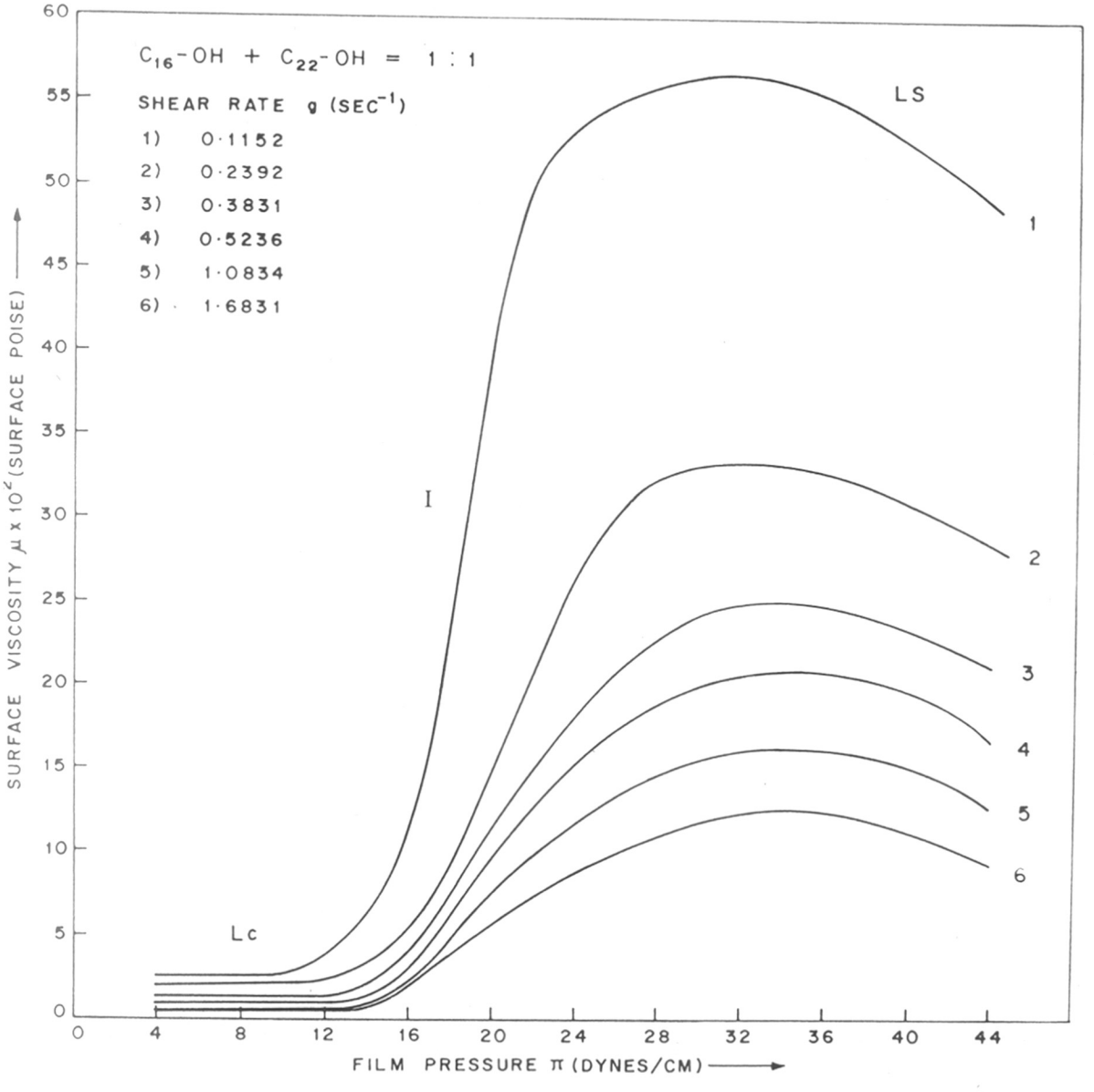

FIG. 3·3 : SURFACE VISCOSITY (μ) AGAINST FILM PRESSURE (π) FOR VARIOUS SHEAR RATES.

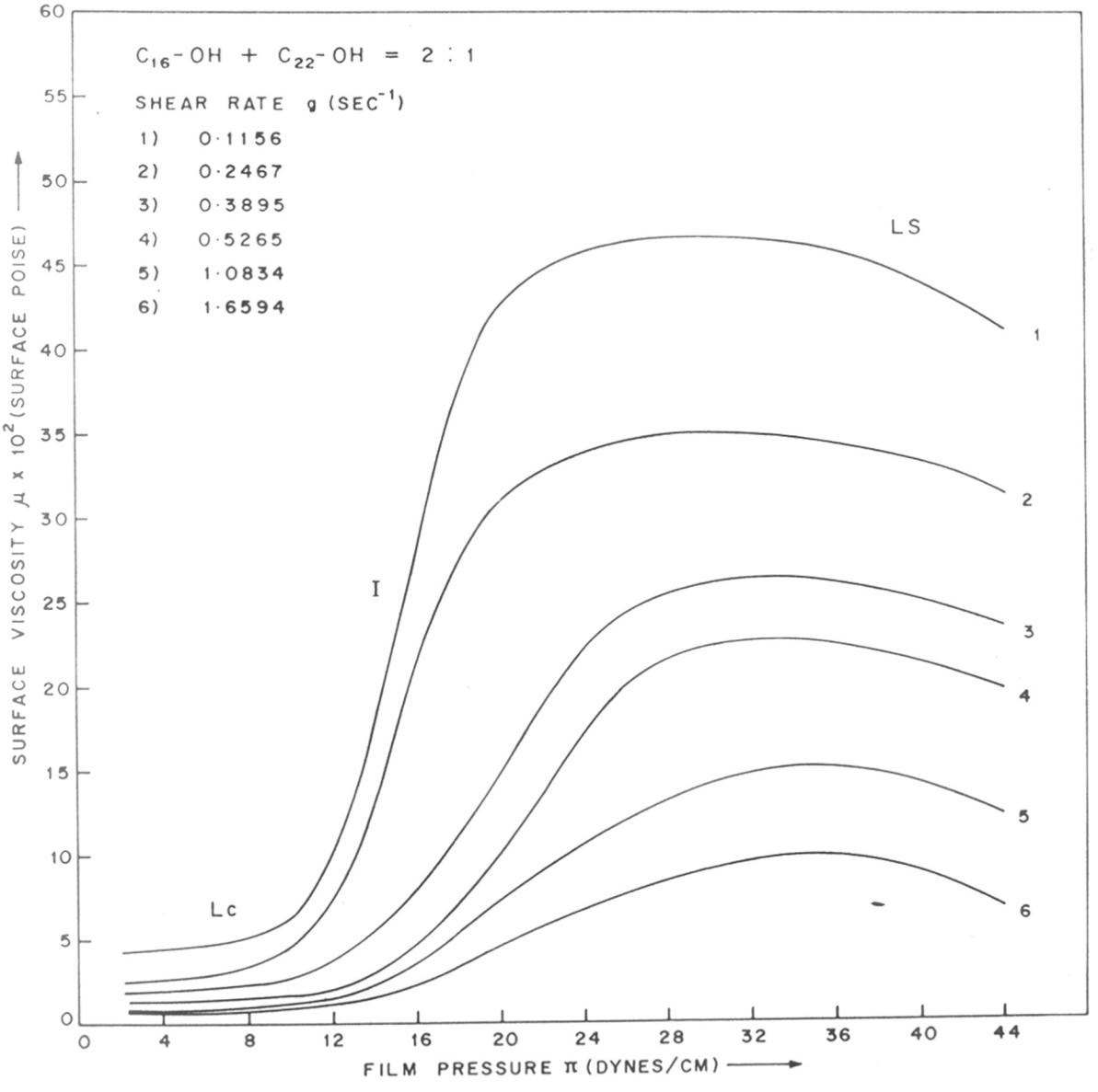

FIG. 3·4 : SURFACE VISCOSITY (μ) AGAINST FILM PRESSURE (π) FOR VARIOUS SHEAR RATES.

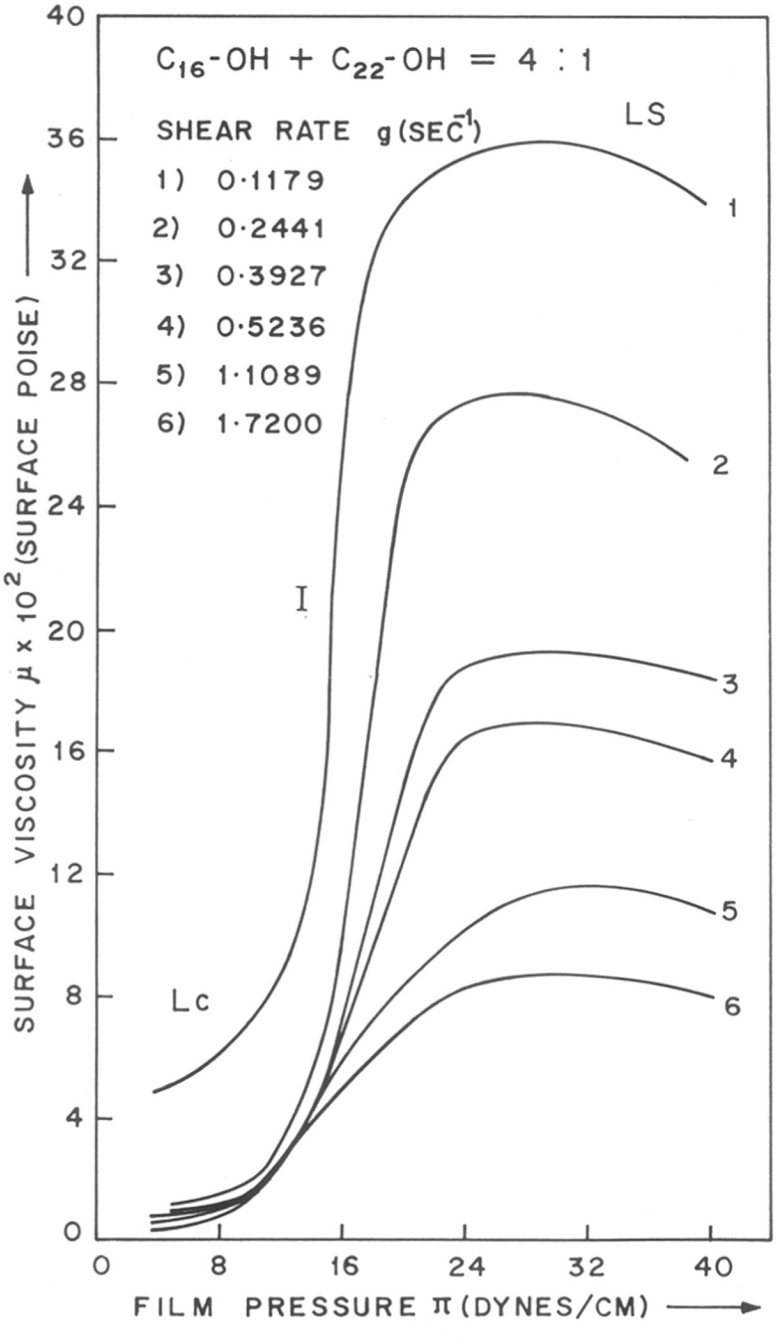

FIG. 3·5 : SURFACE VISCOSITY (μ) AGAINST FILM PRESSURE (π) FOR VARIOUS SHEAR RATES.

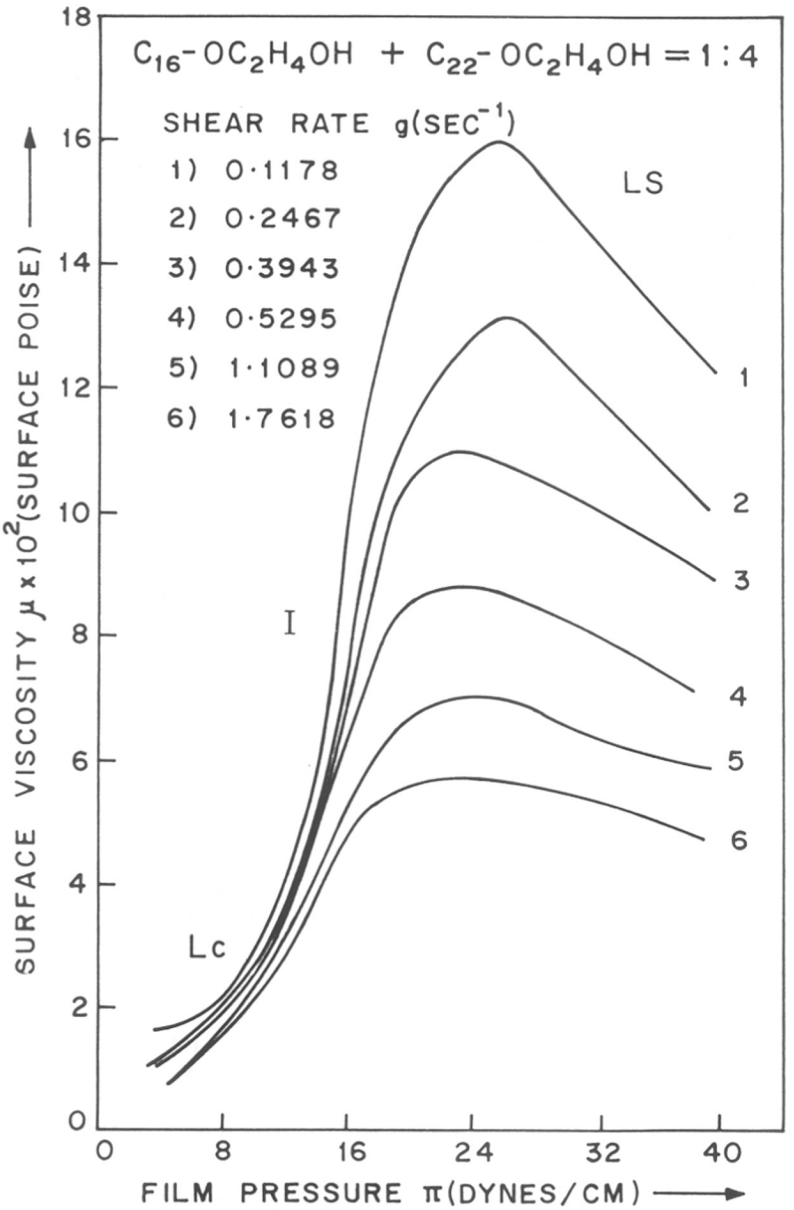

FIG. 3·6 : SURFACE VISCOSITY (μ) AGAINST FILM PRESSURE (π) FOR VARIOUS SHEAR RATES.

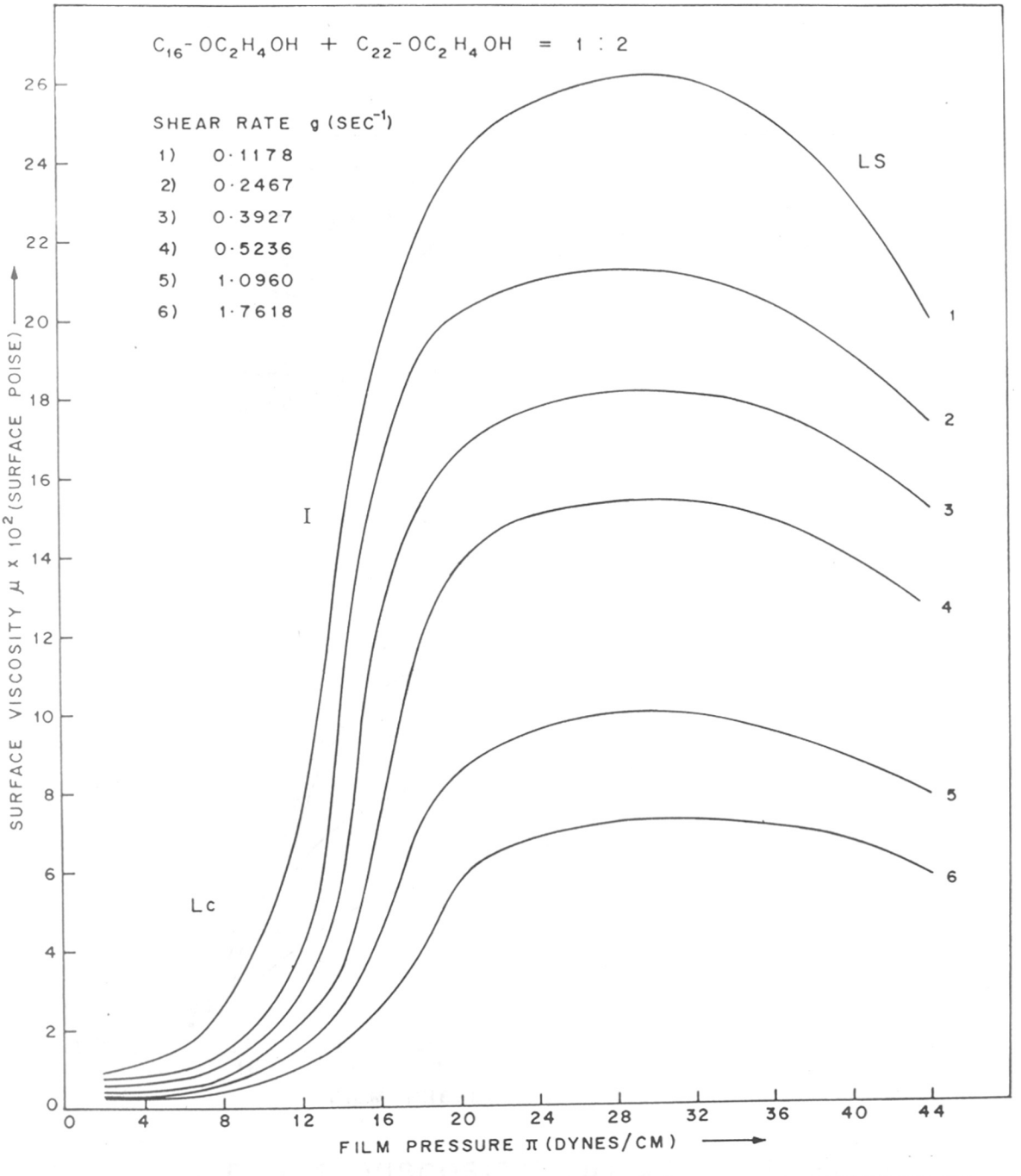

FIG. 3·7 : SURFACE VISCOSITY (μ) AGAINST FILM PRESSURE (π) FOR VARIOUS SHEAR RATES.

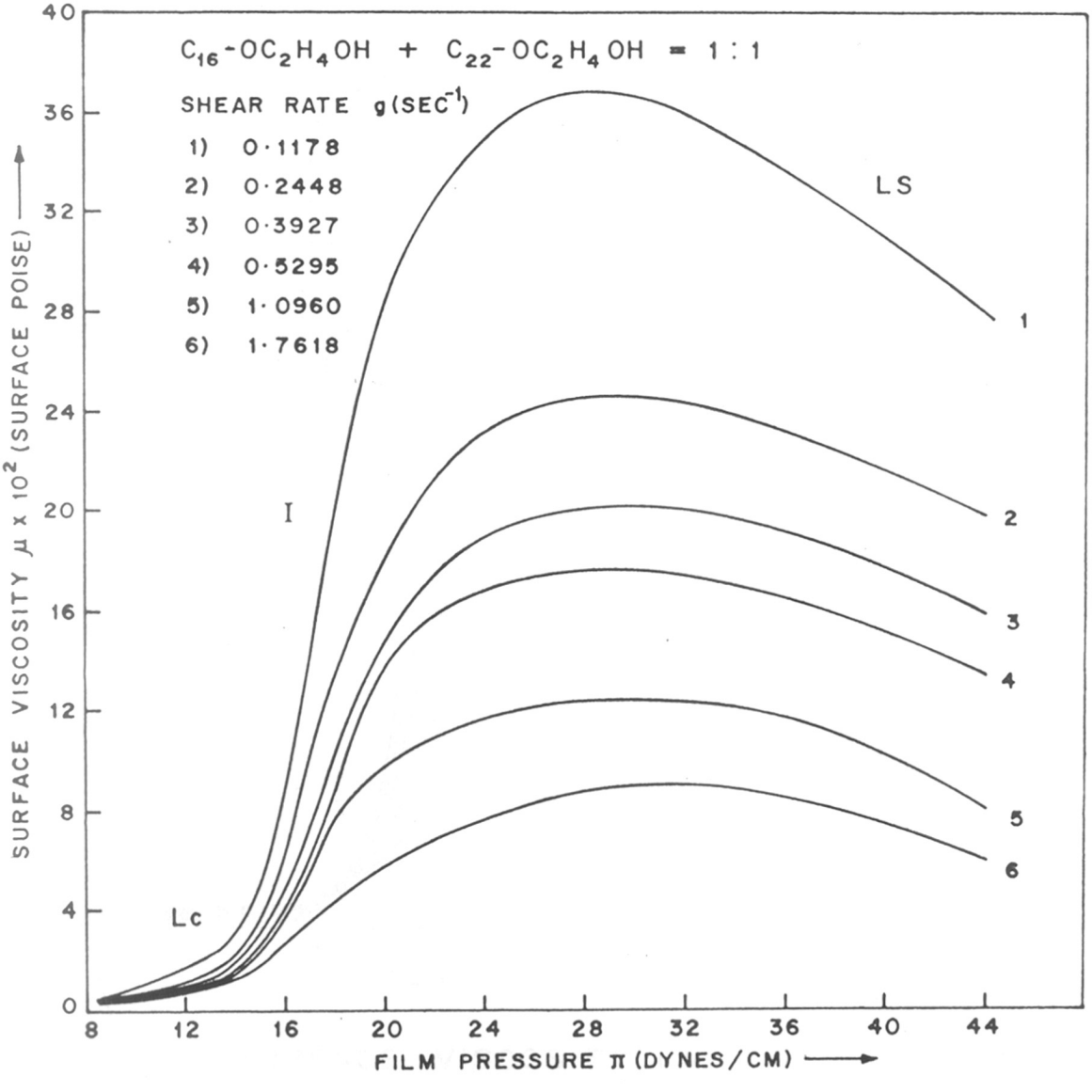

FIG. 3·8 : SURFACE VISCOSITY (μ) AGAINST FILM PRESSURE (π) FOR VARIOUS SHEAR RATES.

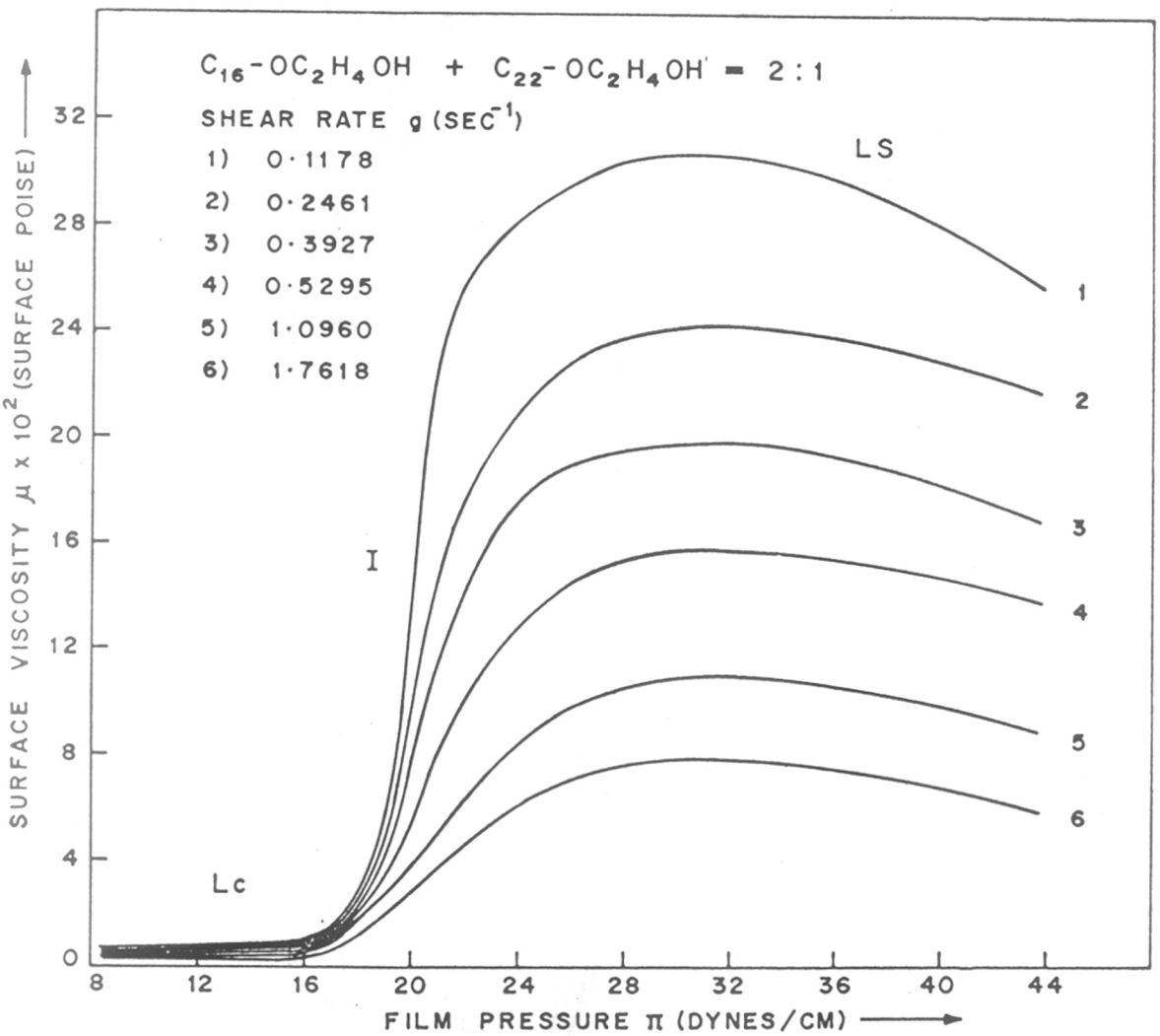

FIG. 3·9 : SURFACE VISCOSITY (μ) AGAINST FILM PRESSURE (π) FOR VARIOUS SHEAR RATES.

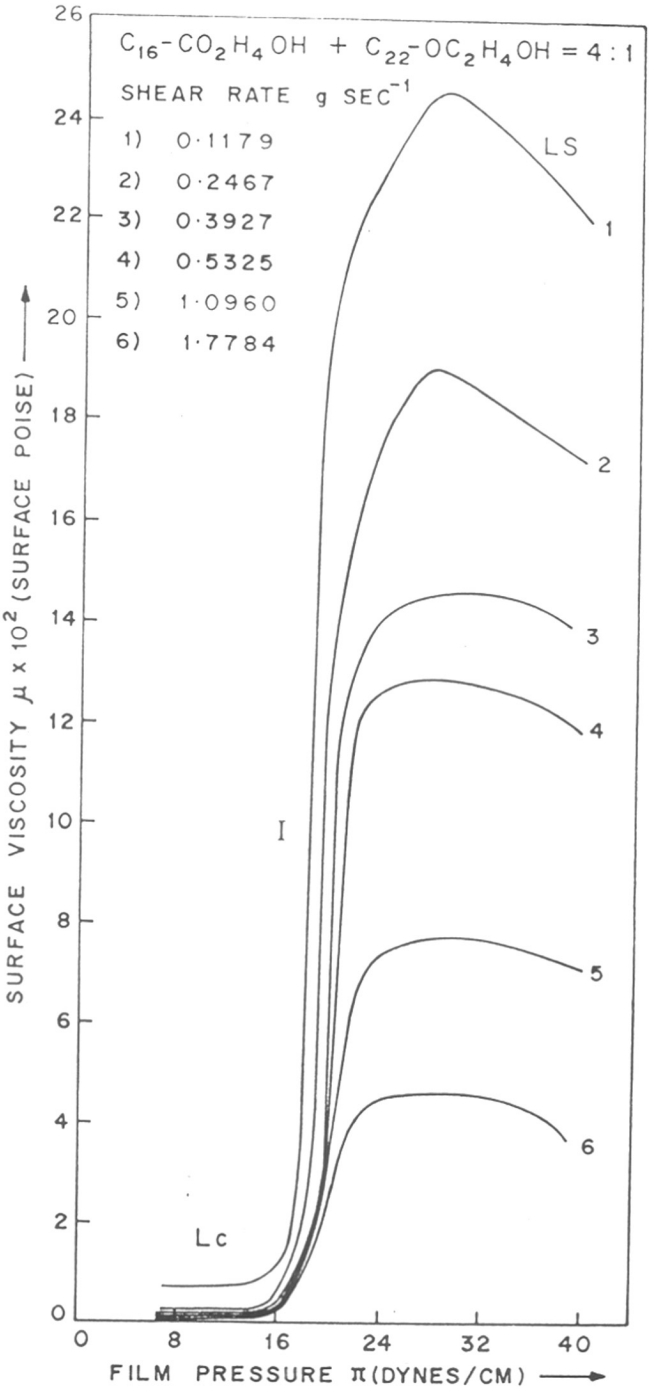

FIG. 3·10 : SURFACE VISCOSITY (μ) AGAINST FILM PRESSURE (π) FOR VARIOUS SHEAR RATES.

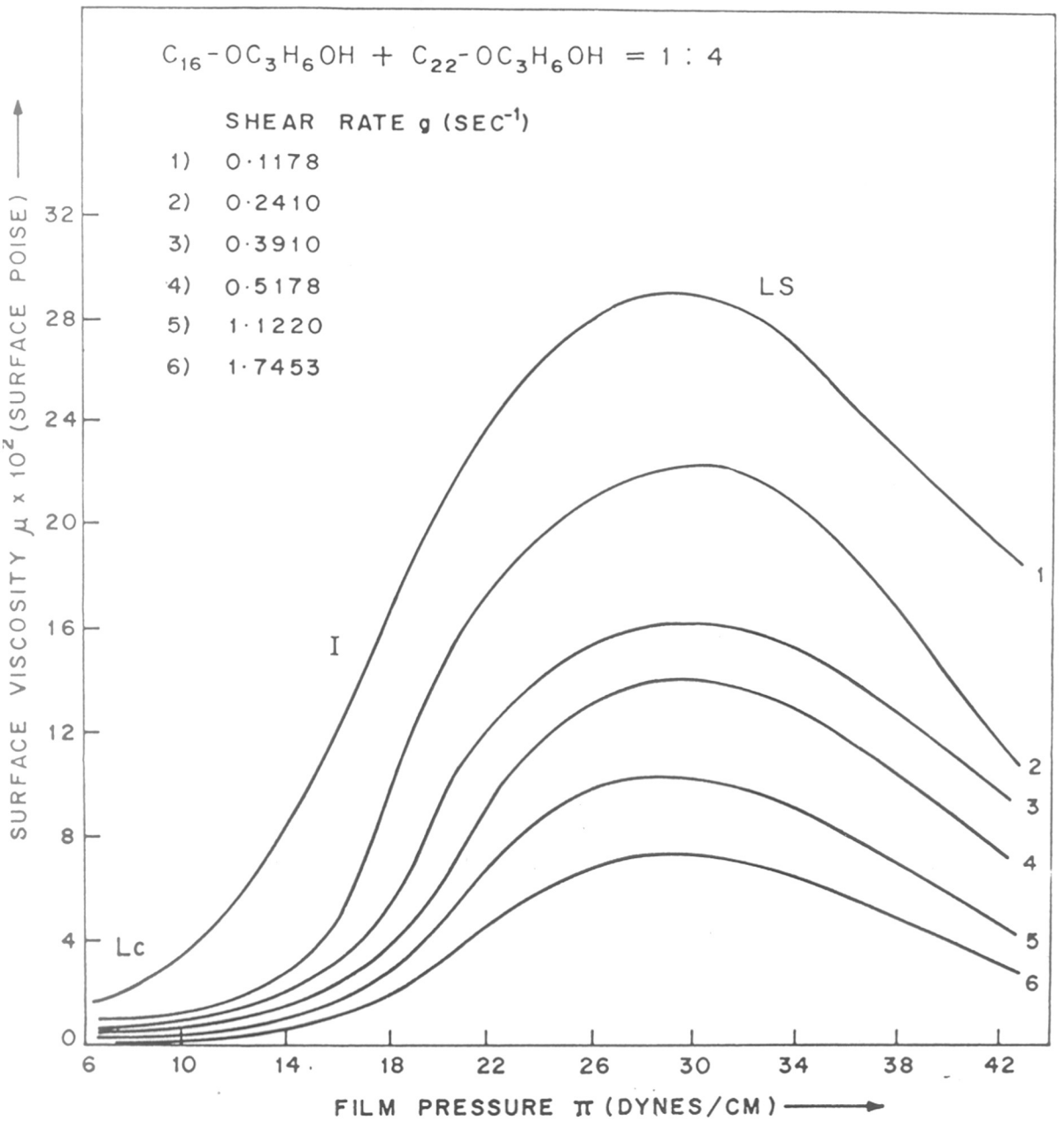

FIG. 3·11 : SURFACE VISCOSITY (μ) AGAINST FILM PRESSURE (π) FOR VARIOUS SHEAR RATES.

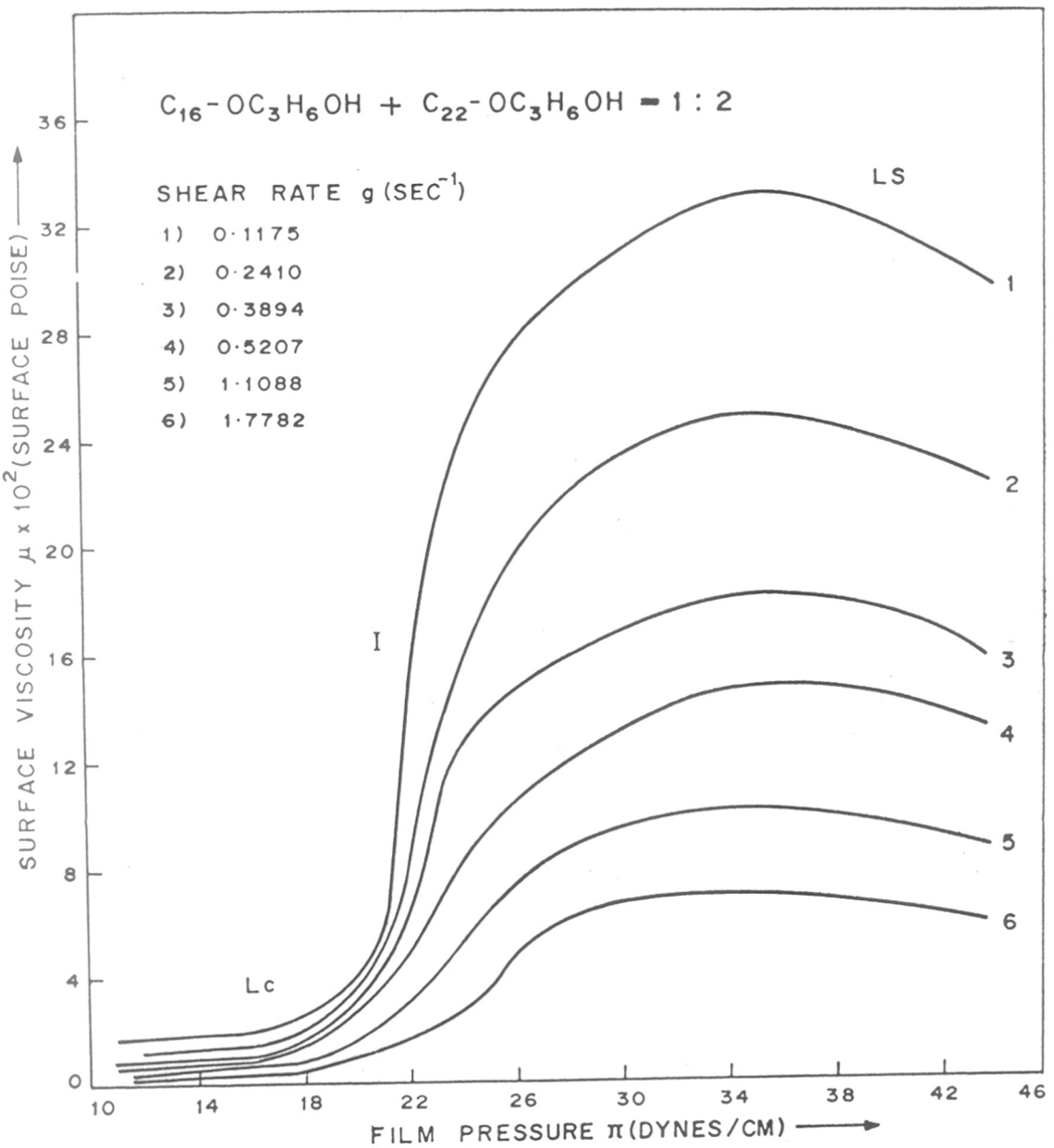

FIG. 3·12 : SURFACE VISCOSITY (μ) AGAINST FILM PRESSURE (π) FOR VARIOUS SHEAR RATES.

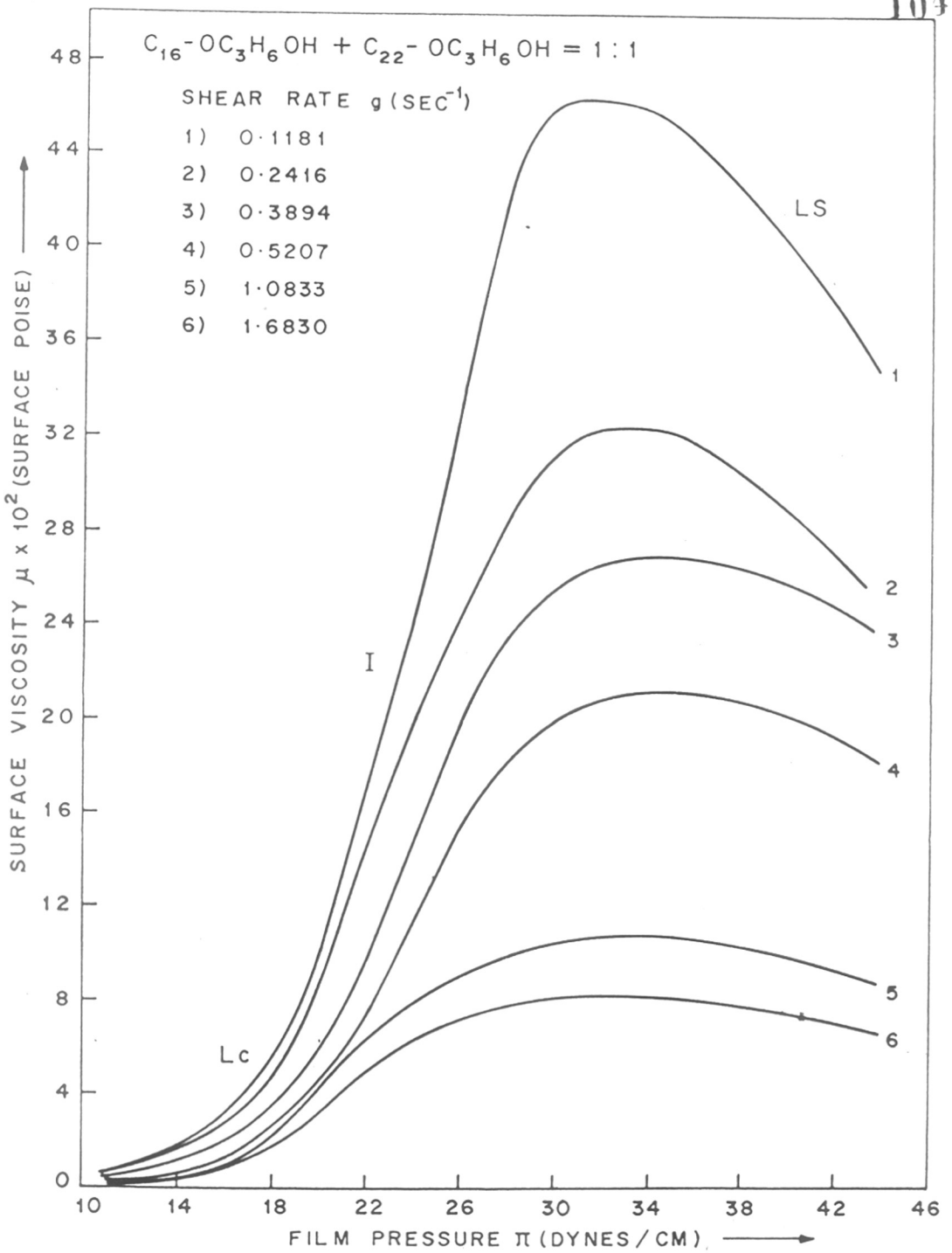

FIG. 3·13 : SURFACE VISCOSITY (μ) AGAINST FILM PRESSURE (π) FOR VARIOUS SHEAR RATES.

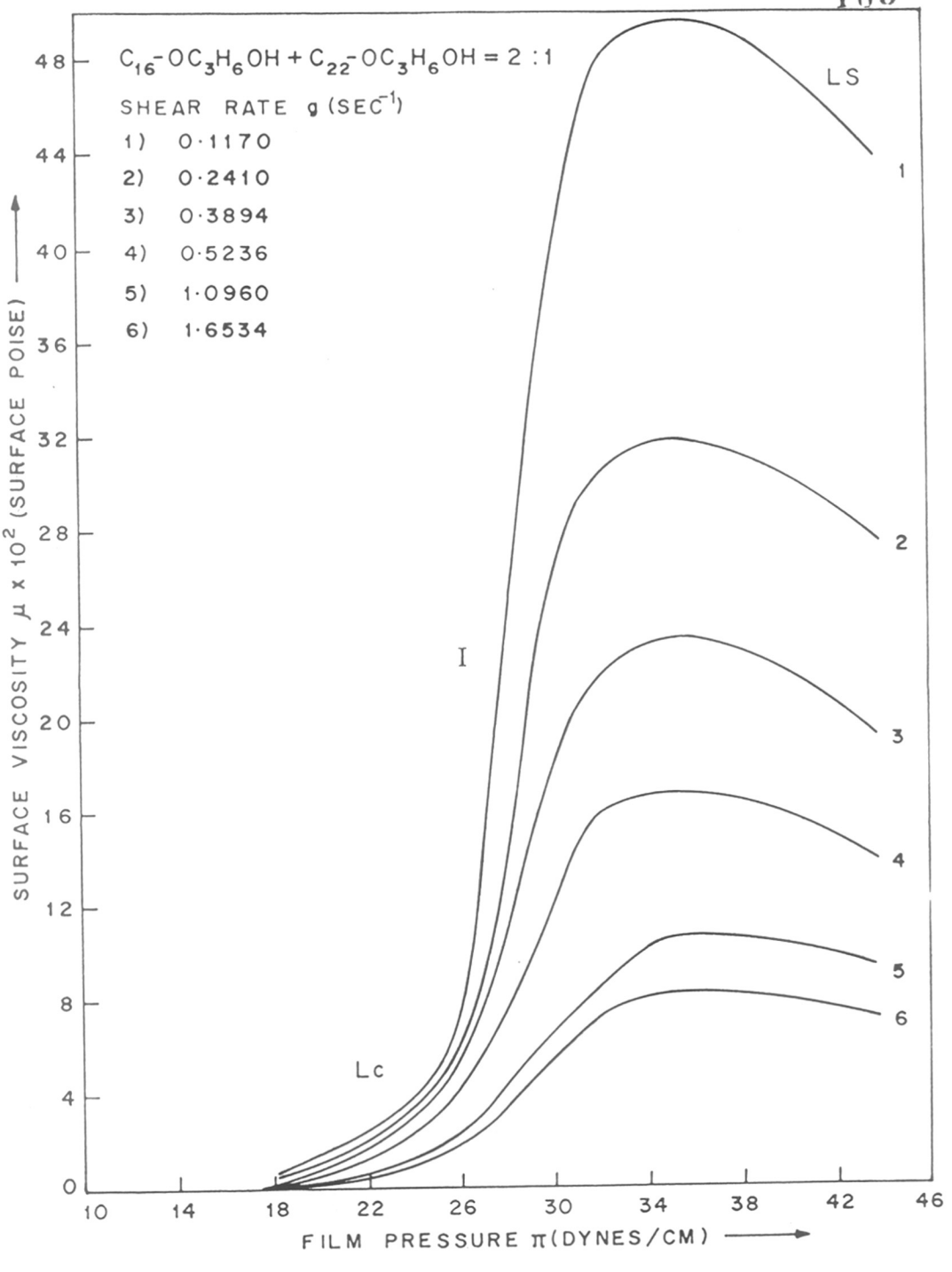

FIG. 3·14 : SURFACE VISCOSITY (μ) AGAINST FILM PRESSURE (π) FOR VARIOUS SHEAR RATES.

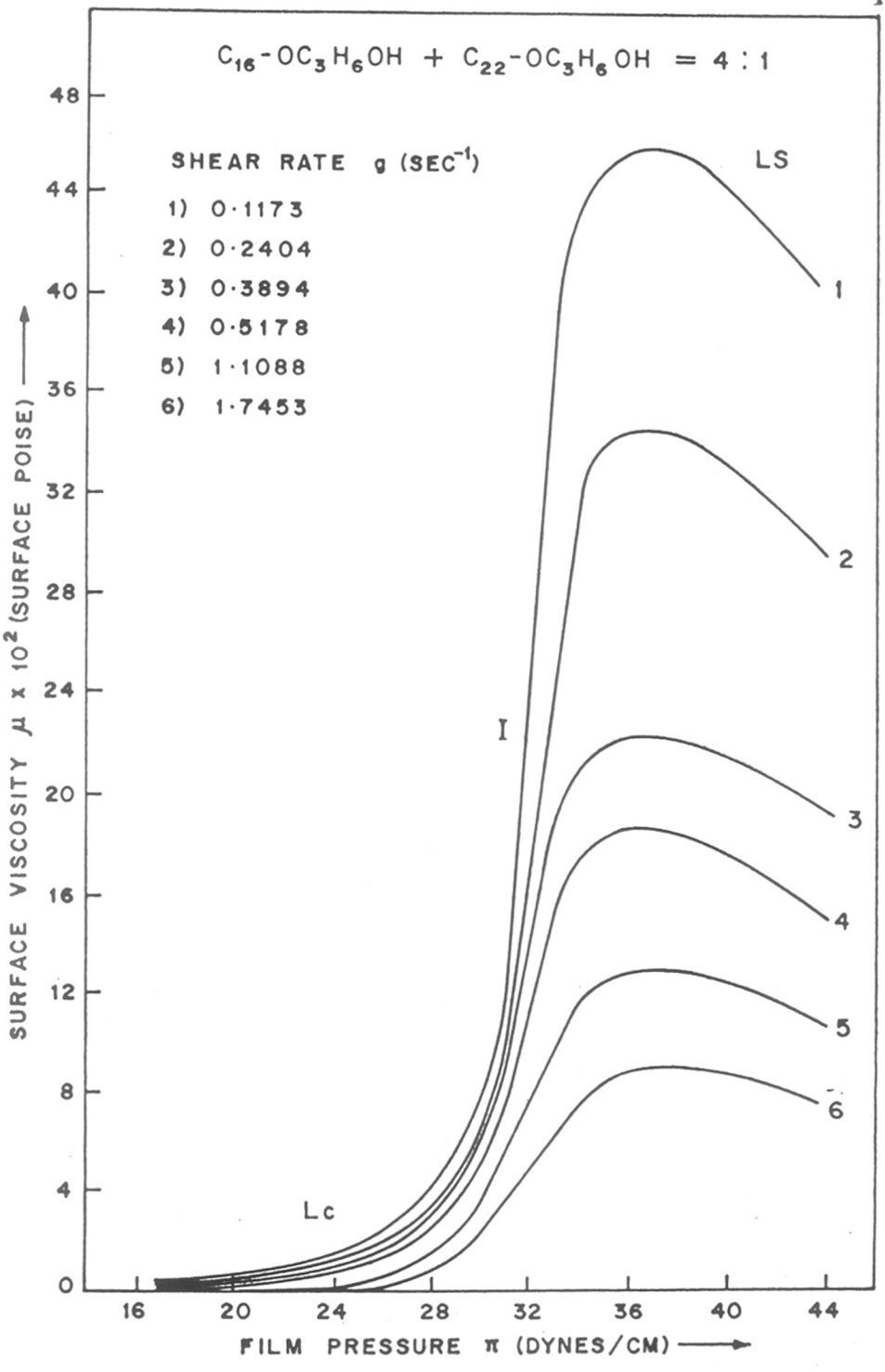

FIG.3·15 : SURFACE VISCOSITY (μ) AGAINST FILM PRESSURE (π) FOR VARIOUS SHEAR RATES.

the hydrogen bond between the film molecules and the water sub-phase weak because of the unfavourable angle between -OH...O or $-OC_2H_4OH$ ... O or $-OC_3H_6OH$ ... O and the dipole dipole repulsive forces become dominent. The overall force of association of the film molecule becomes weak and consequently the surface viscosity either decrease or remains constant in the high pressure region where LS phase is observed. From these curves it can be observed that the surface viscosity is lowest for mixtures of 1:4 (C_{16}:C_{22}) in all the three systems. This indicates that intermolecular interactions for this particular mole fraction is weak compared to other mole fractions. (This is observed in Fig. 3.17 by maximum ϕ_o at this mole fraction). The same conclusion can also be drawn from π-A isotherms.

In mixed monolayers it is important to understand whether the two components have formed a miscible and homogeneous mixtures. The surface viscosity technique has also been used successfully to find out the miscibility. Before going into the details of this; let us first understand the method to calculate surface viscosity at zero and at infinite shear rate.

Surface viscosity at zero and at infinite shear rates can be calculated using Joly's [3] equations described in detail in Chapter I.

$$P_{i(g)} = \frac{\ln (\mu o/\mu g)}{\ln (\mu o/\mu_\infty)} \qquad (3.1)$$

$$P_{i(g)} = \exp [-1/g.\ \tau_i] \qquad (3.2)$$

μo, μ_∞ and τ_i can be obtained simultaneously from Eqns. (3.1) and (3.2). First, a curve of μ against shear rate g is plotted. Extrapolating this curve to various zero and infinite shear rates, τ_i can be calculated till a constant value of τ_i is obtained within the range of $\pm$ 0.25. Assuming the average of these τ_i values to be correct and using corresponding μ_o and μ_∞, μ values were back calculated for various shear rates. A new curve of μ against g for calculated values was plotted. If the experimental μ values fit correctly on this calculated curve, the values of μo, μ_∞ and τ_i were considered to be correct. A fairly good fit has been obtained for all the three systems studied. μ against g plots ("i" state) have been shown in Fig. 3.16 as a typical example.

Boyd and Vaslow [4] have also studied the surface viscosity of mixed monolayers. According to the authors, if the components are immiscible, the fluidity ($\phi = 1/\mu$) of the heterogeneous film will be given by

$$\phi_{12} = x_1 \cdot \phi_1 + x_2 \phi_2 \qquad (3.3)$$

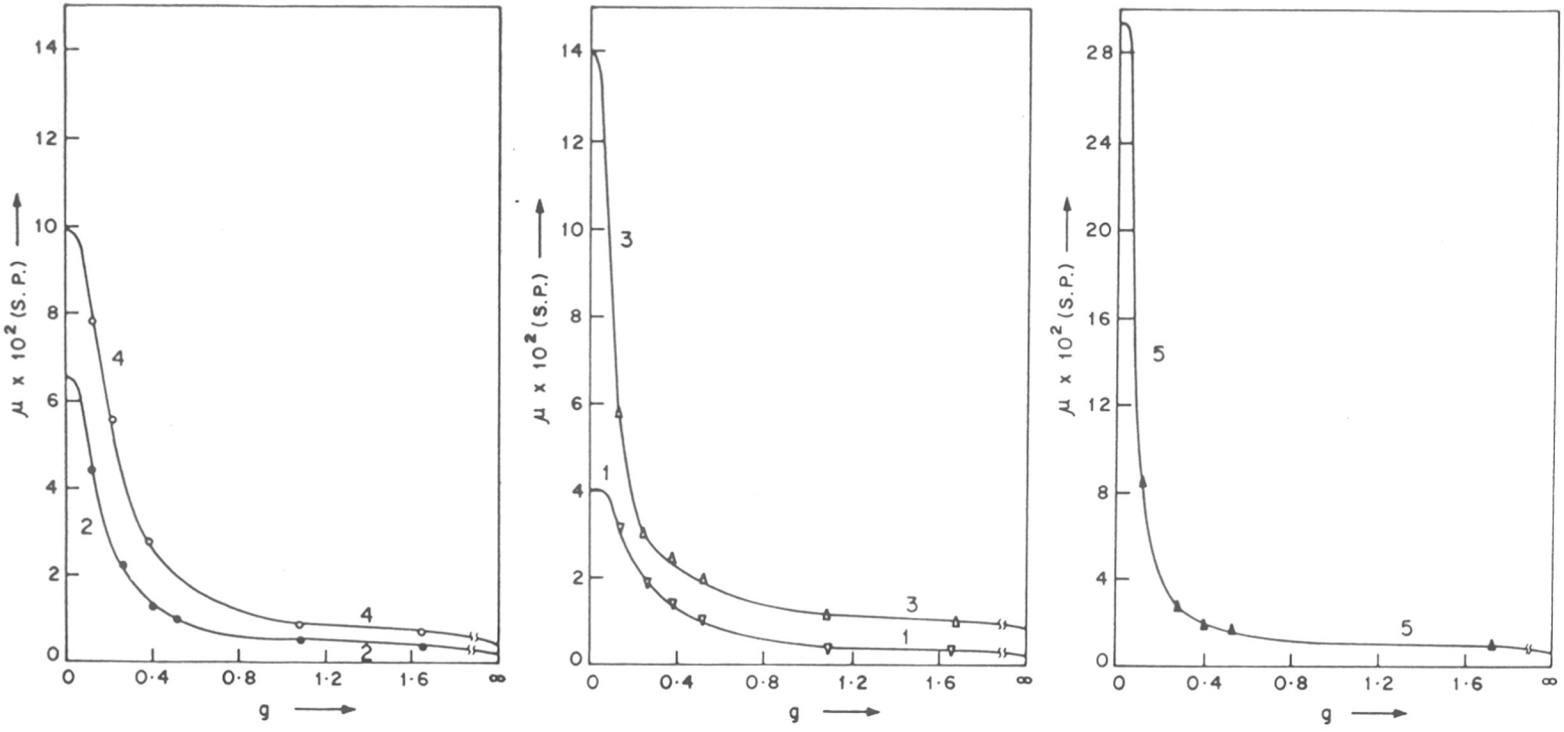

FIG.3·16 : SURFACE VISCOSITY (μ) AGAINST SHEAR RATE (g) FOR THE SYSTEM C_{16}-OH + C_{22}-OH . CURVE (MOLE FRACTION OF C_{16}-OH) 1 - 0·20 ; 2 - 0·33 ; 3 - 0·50 ; 4 - 0·66 ; 5 - 0·80. THE SMOOTH CURVES ARE DRAWN FROM THE COMPUTED VALUES OF μ AND THE POINTS DENOTE THE EXPERIMENTAL VALUES.

Any deviation from the Eqn.(3.3) will indicate the miscibility and non-ideality of the system.

The Fig. 3.17 shows the plots of fluidities at zero and at infinite shear rate ($\phi_o = 1/\mu o$; $\phi_\infty = 1/\mu_\infty$) against mole fraction for the three systems. All the three systems show deviation from the ideal behaviour. This indicates strong intermolecular interactions in all the three systems studied.

Determination of various flow parameters

July [3] has developed the theory for surface viscosity. He has assumed quasi-hexagonal network of monolayer molecules at the water surface. Considering that in a mixed monolayer, the two components loose their separate identity and act as one unit, we can apply the same theory to mixed monolayers. This theory has already been discussed in detail in Chapter I.

The transition Lc → I was assigned 'state i' and I → LS as state 'i-1'. The values of μo, μ_∞ were calculated as described earlier for both the states.

$$\Delta F_i = kT. \ln \left(\frac{\mu_o A}{h}\right) \qquad (3.4)$$

$$(\Delta F_i - \Delta F_i') = kT. \ln \left(\frac{\mu o}{\mu_\infty}\right) \qquad (3.5)$$

$$W_{i-k(0.94\ r_i)} = kT.\ln \left[\left(\sqrt{kT/2\pi.M}\right) x \left(\tau_i/0.94\ r_i\right)\right] \qquad (3.6)$$

All the parameters have been defined already in Chapter I.

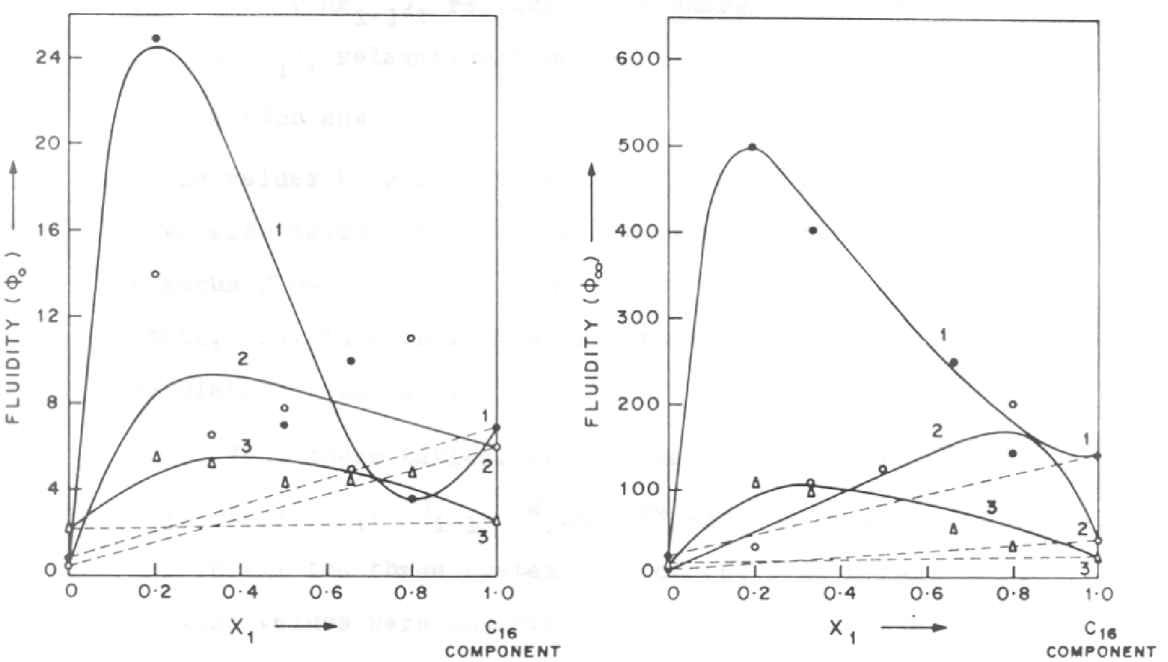

FIG. 3·17 : FLUIDITY AT ZERO SHEAR RATE (Φ_0) AND AT INFINITE SHEAR RATE (Φ_∞) AGAINST MOLE FRACTION FOR THREE SYSTEMS. CURVE 1 - C_{16}-OH + C_{22}-OH ; 2 - C_{16}-OC_2H_4OH + C_{22}-OC_2H_4OH ; 3 - C_{16}-OC_3H_6OH + C_{22}-OC_3H_6OH.

Using the above equations we have calculated the values of free energy of activation for viscous flow, ΔF_i (ΔF_{i-1}), residual free energy of activation $\Delta F'_i$ ($\Delta F'_{i-1}$), relaxation time τ_i (τ_{i-1}) and intermolecular interaction energy W_{i-k} $(0.94\ r_i)$ $(W_{i-k-1}(0.94\ r_{i-1}))$. These values have been tabulated in Table I to III. We have also calculated the free energy of activation for viscous flow when all the molecules are not in the same state, i.e. in between the two states i and i-1 and are tabulated in Table IV.

From these tables, it is clear that the values of ΔF_i, ΔF_{i-1}, τ_i, τ_{i-1}, $W_{i-k}(0.94\ r_i)$ and $W_{i-k-1}(0.94\ r_{i-1})$ and in all the three systems are of the same order. Similar values were observed for one component system also. This leads us to conclude that the phenomenon of viscosity is similar in all the cases, which is independent of the mixture, and the nature of the compounds. Even the values of $\Delta F_{(g)}$ are also of the same order of magnitude. Therefore the viscosity phenomenon seems to be the same even if all the molecules are not in the same state.

The fact that the values of various flow parameters for mixed monolayers are of the same order as that of the corresponding pure components indicate that the quasi-

TABLE I

Surface viscosity and related data for the mixed monolayers of C_{16}-OH + C_{22}-OH in state "i" and "i-1"

STATE 'i'								STATE "i-1"						
Mole fraction of C_{16}-OH, x_1	μ_o (g/sec.)	μ_∞ (g/sec.)	τ_i (sec.)	$\Delta F_i \times 10^{13}$ (ergs/cm^2)	$\Delta F_i' \times 10^{13}$ (ergs/cm^2)	$(\Delta F_i - \Delta F_i') \times 10^{13}$ (ergs/cm^2)	$[W_{i-k}(0.94\, r_i)] \times 10^{13}$ (ergs/cm^2)	μ_o (g/sec.)	μ_∞ (g/sec.)	τ_{i-1} (sec.)	$\Delta F_{i-1} \times 10^{13}$ (ergs/cm^2)	$\Delta F_{i-1}' \times 10^{13}$ (ergs/cm^2)	$(\Delta F_{i-1} - \Delta F_{i-1}') \times 10^{13}$ (ergs/cm^2)	$[W_{i-1-1}(0.94\, r_{i-1}) \times 10^{13}$ (ergs/cm^2)
0.00 (a)	1.150	0.125	4.5	10.85	9.95	0.90	10.86	-	-	-	-	-	-	-
0.20	0.040	0.002	2.7	9.54	8.31	1.23	10.73	0.199	0.071	3.03	10.20	9.78	0.42	10.78
0.33	0.065	0.0025	3.56	9.76	8.42	1.34	10.85	0.407	0.081	2.80	10.51	9.85	0.66	10.75
0.50	0.139	0.008	6.16	10.06	8.88	1.17	11.09	0.595	0.095	3.05	10.65	9.90	0.75	10.80
0.66	0.099	0.004	2.82	9.92	8.60	1.32	10.78	0.480	0.080	2.23	10.56	9.82	0.74	10.67
0.80	0.293	0.007	7.68	10.35	8.82	1.53	11.20	0.391	0.059	2.45	10.47	9.69	0.78	10.74
1.00 (a)	0.140	0.007	5.23	10.00	8.77	1.23	10.99	-	-	-	-	-	-	-

(a) : From Ref. G.S. Patil, S.S. Katti and A.B. Biswas, J.Colloid Interface Sci. 25 (1967) 462.

TABLE II

Surface viscosity and related data for the mixed monolayers of C_{16}-OC_2H_4OH + C_{22}-OC_2H_4OH in state "i" and "i-1"

STATE "i"								STATE "i-1"						
Mole fraction of C_{16}-OC_2H_4OH; x_1	μ_o (g/sec.)	μ_∞ (g/sec.)	τ_i (sec.)	$\Delta F_i \times 10^{13}$ (ergs/cm^2)	$\Delta F_i' \times 10^{13}$ (ergs/cm^2)	$(\Delta F_i - \Delta F_i') \times 10^{13}$ (ergs/cm^2)	$[W_{i-k}(0.94\, r_i)]\times 10^{13}$ (ergs/cm^2)	μ_o (g/sec.)	μ_∞ (g/sec.)	τ_{i-1} (sec.)	$\Delta F_{i-1} \times 10^{13}$ (ergs/cm^2)	$\Delta F'_{i-1} \times 10^{13}$ (ergs/cm^2)	$(\Delta F_{i-1} - \Delta F'_{i-1}) \times 10^{13}$ (ergs/cm^2)	$[W_{i-k-1}(0.94\, r_{i-1})] \times 10^{13}$ (ergs/cm^2)
0.00 (a)	4.200	0.50	4.61	11.40	10.53	0.87	10.84	-	-	-	-	-	-	-
0.20	0.070	0.028	4.50	9.77	9.39	0.38	10.92	0.17	0.035	2.33	10.12	9.47	0.65	10.65
0.33	0.150	0.009	5.78	10.08	8.93	1.15	11.02	0.28	0.067	2.50	10.34	9.76	0.58	10.69
0.50	0.125	0.008	5.01	10.01	8.88	1.13	10.97	0.405	0.082	3.00	10.49	9.84	0.65	10.77
0.66	0.195	0.015	6.90	10.20	9.15	1.05	11.11	0.33	0.069	2.48	10.42	9.78	0.64	10.70
0.80	0.090	0.005	3.79	9.89	8.71	1.18	10.87	0.25	0.035	1.83	10.31	9.51	0.80	10.60
1.00 (a)	0.160	0.025	5.15	10.09	9.33	0.76	10.94	-	-	-	-	-	-	-

(a) From Ref. S.S. Katti and G.S. Patil, J.Colloid Interface Sci. 28 (1968) 227.

TABLE III

Surface viscosity and related data for the mixed monolayers of C_{16}-OC_3H_6OH + C_{22}-OC_3H_6OH in state "i" and "i-1"

STATE "i"								STATE "i-1"						
Mole fraction of C_{16}-OC_3H_6OH; x_1	μ_o (g/sec.)	μ_∞ (g/sec.)	T_i (sec.)	$\Delta F_i \times 10^{13}$ (ergs/cm^2)	$\Delta F_i' \times 10^{13}$ (ergs/cm^2)	$(\Delta F_i - \Delta F_i') \times 10^{13}$ (ergs/cm^2)	$[W_{i-k}(0.94 r_i)] \times 10^{13}$ (ergs/cm^2)	μ_o (g/sec.)	μ_∞ (g/sec.)	T_{i-1} (sec.)	$\Delta F_{i-1} \times 10^{13}$ (ergs/cm^2)	$\Delta F_{i-1}' \times 10^{13}$ (ergs/cm^2)	$(\Delta F_{i-1} - \Delta F_{i-1}') \times 10^{13}$ (ergs/cm^2)	$[W_{i-k-1}(0.94 r_{i-1})] \times 10^{13}$ (ergs/cm^2)
0.00 (a)	0.52	0.065	3.60	10.69	9.84	0.85	10.78	-	-	-	-	-	-	-
0.20	0.180	0.009	3.25	10.23	9.00	1.23	10.70	0.310	0.064	2.70	10.46	9.81	0.65	10.66
0.33	0.190	0.010	2.70	10.24	9.03	1.21	10.64	0.350	0.067	2.75	10.50	9.82	0.68	10.68
0.50	0.235	0.045	2.60	10.31	9.63	0.68	10.65	0.473	0.061	2.00	10.60	9.76	0.84	10.58
0.66	0.230	0.018	2.82	10.31	9.26	1.05	10.65	0.550	0.059	2.90	10.67	9.75	0.92	10.74
1.00 (a)	0.400	0.035	4.40	10.53	9.52	1.01	10.92	-	-	-	-	-	-	-

(a) From Ref: A.G. Gaonkar and S.S. Katti, J.Colloid Interface Sci. 65 (1978) 232.

TABLE IV

Various values of $\Delta F_{(g)}$ at different shear rates for $C_{16}\text{-}OC_3H_6OH + C_{22}\text{-}OC_3H_6OH \simeq 1:1$ system.

Shear Rate (g) $sec.^{-1}$	$\Delta F_{(g)} \times 10^{13}$ ergs/cm^2 (AT A = 21.1 $\AA^2$)	$\Delta F_{(g)} \times 10^{13}$ ergs/cm^2 (AT A = 20.45 $\AA^2$)
0.05	10.43	10.56
0.10	10.42	10.55
0.30	10.26	10.40
0.50	10.12	10.25
1.00	9.95	10.06

hexagonal network theory suggested by Joly [3] is also applicable to mixed monolayers and the mixed monolayers studied by us form a homogeneous mixture for all the mole fractions. The variation of $\Delta F_{(g)}$ with the shear rate confirms the non-Newtonian behaviour in the mixed monolayers.

Film pressure area per molecule (π-A) isotherms

The π-A isotherms for the three systems have been given in Figs. 3.18 - 3.20. It is clearly seen from these isotherms that the initial area per molecule goes on increasing as the size of polar group increases. The isotherms at 0.20 mole fraction (of C_{16}-component) of system I and II show the LS phase. C_{22}-OC_3H_6OH exhibits throughout liquid condensed phase. Rest all the mixtures along with pure components show liquid condensed to solid phase change. The values of area per molecule extrapolated to zero film pressure in solid phase (A_o), transition pressures (π^{eq}), collapse pressures (π_c), compressibilities (C_s) and compression moduli (K_s) are tabulated in Table V for ready reference.

As stated earlier in Chapter I, the miscibility can be understood by various ways from π-A isotherms. These will be discussed in the following.

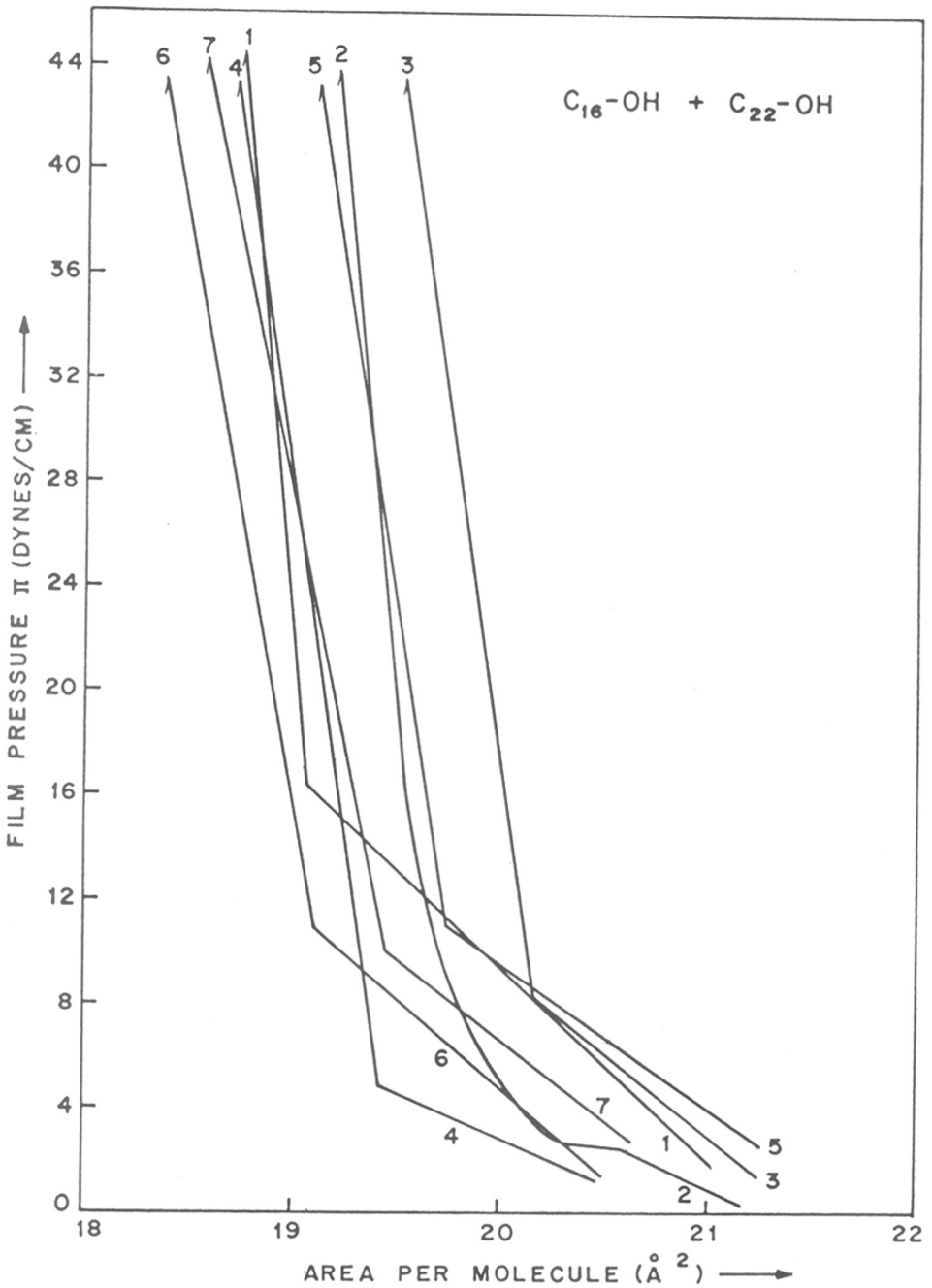

FIG. 3·18 : π – A ISOTHERMS OF C_{16}-OH, C_{22}-OH AND THEIR MIXTURES AT 25°C MOLE FRACTION OF C_{16}-OH : CURVE 1–0·0(C_{22}-OH); 2–0·20; 3–0·33; 4–0·50; 5–0·66; 6–0·80; 7–1·0(C_{16}-OH).

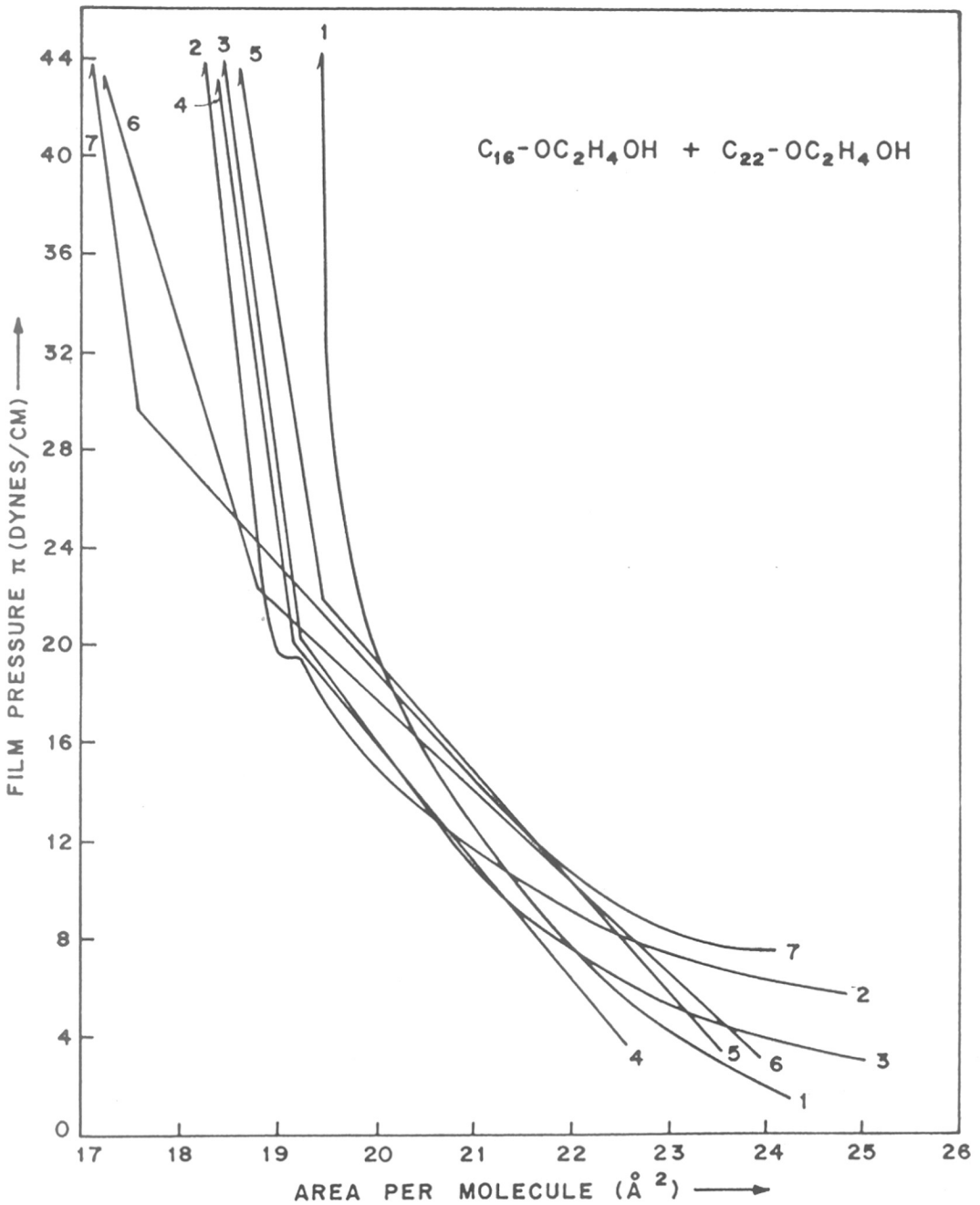

FIG. 3·19 : π – A ISOTHERMS OF C_{16}-OC_2H_4OH, C_{22}-OC_2H_4OH AND THEIR MIXTURES AT 25°C MOLE FRACTION OF C_{16}-OC_2H_4OH : CURVE 1–0·0 (C_{22}-OC_2H_4OH); 2–0·20; 3–0·33; 4–0·50; 5–0·66; 6–0·80; 7–1·0 (C_{16}-OC_2H_4OH).

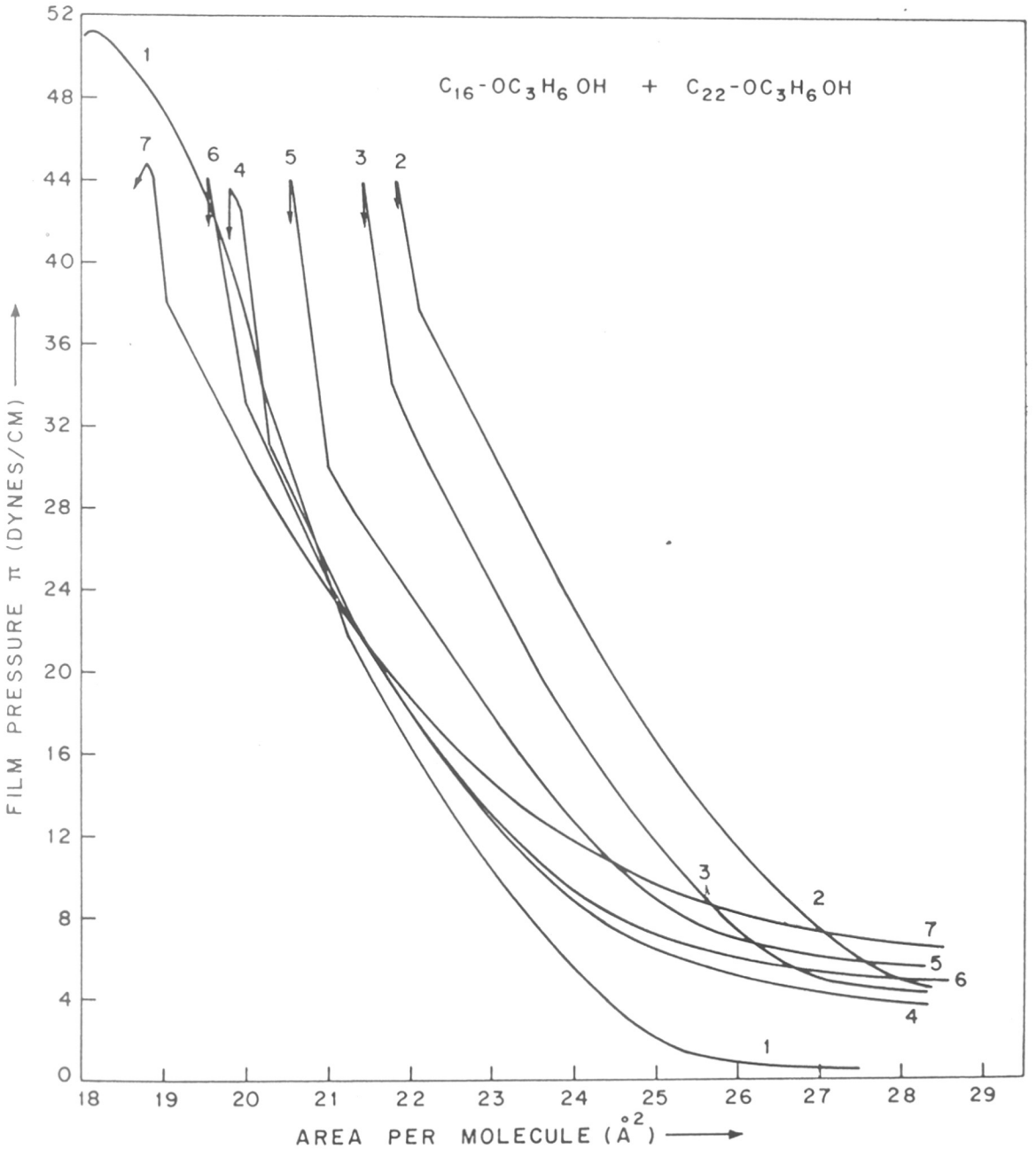

FIG. 3·20 : π – A ISOTHERMS OF C_{16}-OC_3H_6OH , C_{22}-OC_3H_6OH AND THEIR MIXTURES AT 25°C. MOLE FRACTION OF C_{16}-OC_3H_6OH : CURVE 1 – 0·0 (C_{22}-OC_3H_6OH) ; 2 – 0·20 ; 3 – 0·33 ; 4 – 0·50 ; 5 – 0·66 ; 6 – 0·80 ; 7 – 1·0 (C_{16}-OC_3H_6OH).

TABLE V

Area per molecule (A_o), Transition Pressure (π^{eq}), Collapse Pressure (π_c) Compression Modulus (K_s) and compressibility for the three systems.

System	Mole fraction of C_{16} component x_1	A_o ($Å^2$)	Transition Pressures π^{eq}			π_c (dynes/cm)	Compression modulus K_s (dynes/cm)		Compressibility C_s (cm/dyne)	
			Lc → LS	Lc → S	LS → S		Lc	S	Lc; C_s x 10^3	S; C_s x 10^4
C_{16}-OH + C_{22}-OH	0.00 (C_{22})	19.26	-	16.6	-	44.5	154	1725	6.49	5.79
	0.20	19.75	2.8	-	8.0	43.9	80	1250	12.50	8.00
	0.33	20.32	-	8.2	-	43.5	120	1200	8.33	8.33
	0.50	19.52	-	4.9	-	43.1	62	1100	16.10	9.09
	0.66	19.77	-	11.0	-	43.35	110	925	9.09	10.8
	0.80	19.35	-	10.9	-	43.6	122	825	8.19	12.1
	1.00 (C_{16})	19.72	-	10.2	-	44.0	132	1125	7.57	8.88
C_{16}-OC_2H_4OH + C_{22}-OC_2H_4OH	0.00 (C_{22})	19.65	-	33.2	-	44.3	188	4600	5.32	2.17
	0.20	19.50	19.4	-	22.0	43.8	70	630	14.2	15.8
	0.33	19.72	-	20.9	-	43.5	78	610	12.8	16.3
	0.50	19.75	-	20.2	-	43.0	95	600	10.5	16.6
	0.66	20.25	-	22.0	-	43.1	97	500	10.3	20.0

TABLE V (contd.)

C_{16}-OC_3H_6OH + C_{22}-OC_3H_6OH	0.80	20.55	-	22.3	-	43.3	82	230	12.2	43.4
	1.00(C_{16})	18.75	-	29.4	-	43.8	75	475	13.3	21.0
	0.00(C_{22})	-	-	-	-	51.1	200	225	5.0	44.4
	0.20	23.5	-	37.0	-	43.9	155	525	6.45	19.0
	0.33	22.85	-	34.6	-	43.8	146	750	6.85	13.3
	0.50	21.55	-	31.0	-	43.5	134	680	7.46	14.7
	0.66	22.00	-	30.2	-	43.7	120	640	8.33	15.6
	0.80	21.50	-	33.0	-	41.1	128	480	7.81	20.8
	1.00(C_{16})	20.10	-	38.2	-	44.8	125	675	8.00	14.8

Area per molecule against mole fraction curves ($A-x_1$)

In any study on mixed monolayers it is important to establish the number of phases present in the monolayer. But this is usually very difficult task.

An approach usually used is to plot monolayer areas for a given surface pressure against monolayer composition [5-7]. A linear plot indicates that the areas are additive i.e. obey the following equation.

$$A_{12} = x_1A_1 + x_2A_2 \qquad (3.7)$$

If a mixed monolayer behaves according to the above equation, it indicates either complete immiscibility or miscibility with ideal mixing. Any deviations from the above equation indicates miscibility and non-ideality [6-8]. According to Phillips and Joos [9] a linear region in the area - composition plot can occur when the system is only partially miscible. Thus in the above equation of additivity rule a two component monolayer is treated as a two dimensional binary solution, ignoring the water which supports the monolayer. The advantage in such a treatment is that much of thermodynamic theory of three dimensional binary systems can be adapted to the two dimensional cases; and a knowledge of the amount of water in the surface is not required [7].

In Fig. 3.21 A-x_1 plots have been shown for the three systems at three different surface pressures. In these plots positive and negative deviations are observed. The extent of deviation goes on decreasing as the film pressure increases. This indicates the non-ideality and miscibility is observed in all the three systems, however it can be best judged at low pressures.

The non-ideality obtained in Fig. 3.21 can be explained on the lines of Cadenhead and Muller-Landau [10] model. The model distinguishes between contributions made by mere geometric accommodation or "space filling" and that related to changed intermolecular hydrophobic interactions. The space filling will always be accompanied by altered molecular interactions. The area per molecule will always decrease if space filling takes place. In most of the instances geometric accommodation will result in enhanced dispersive interaction such that further condensation takes place. When one of the components is miscible in the other, but cannot accommodate itself, disturbs the packing of the second component such that the average area per molecule of the mixture is increased; the positive deviation from ideality is observed. The dispersive interactions are decreased in case of positive deviations. The schematic representation of the above consideration has been shown in Fig. 3.22. Such types of A - x_1 plots have been used by

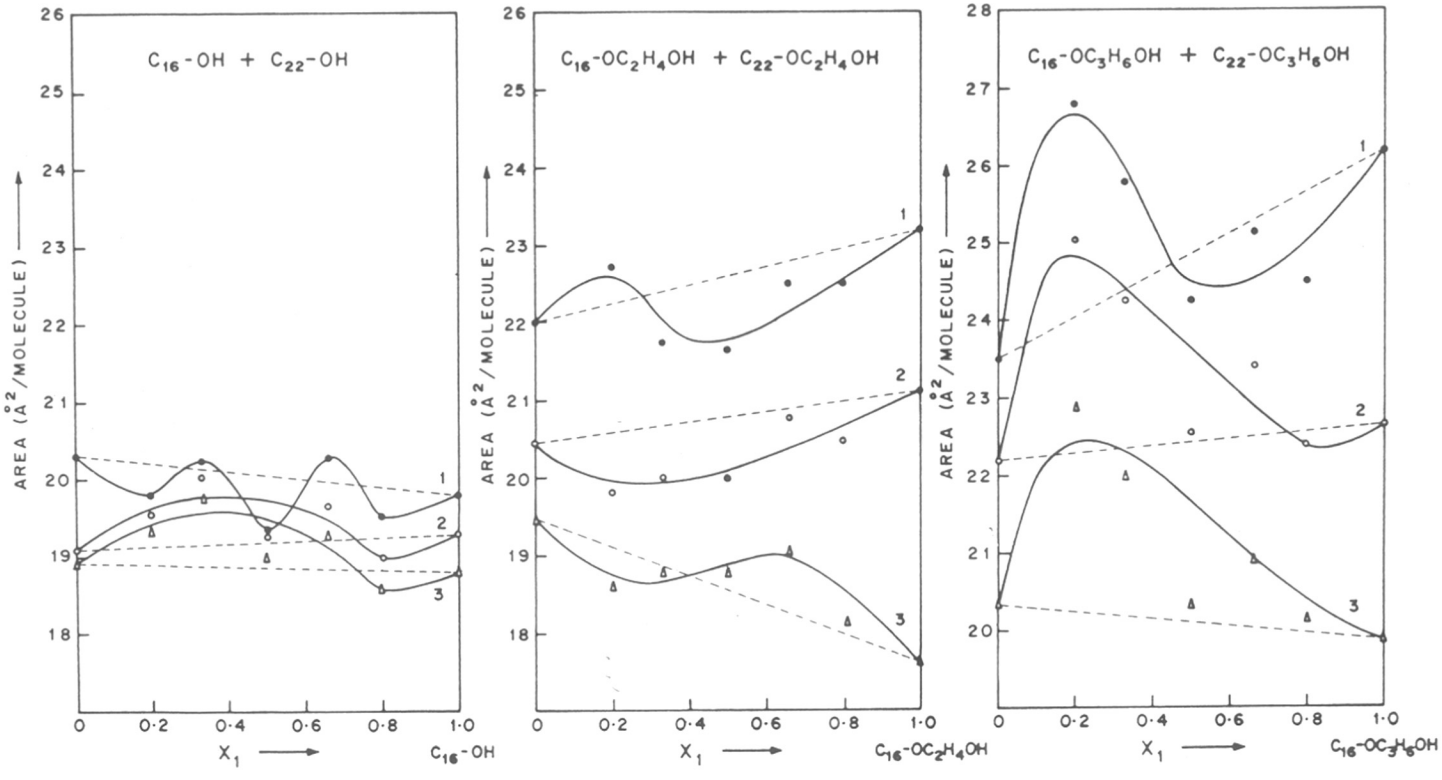

FIG. 3·21 : AREA AGAINST MOLE FRACTION FOR THREE SYSTEMS. CURVE NO. 1 - 8 DYNES/CM ; 2 - 16 DYNES/CM ; 3 - 32 DYNES/CM.

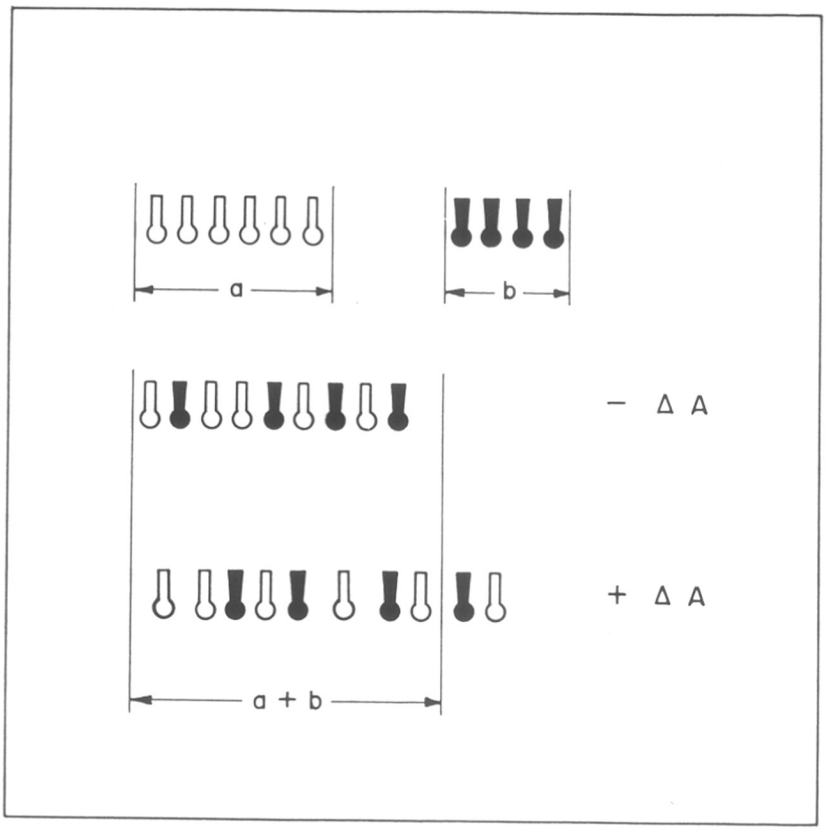

FIG. 3·22 : SCHEMATIC MODEL FOR MIXED MONOLAYER INTERACTIONS.

TOP : SEPARATE COMPONENTS.

CENTER : GEOMETRIC ACCOMODATION WITH CONDENSATION.

BOTTOM : MISCIBILITY WITH DISTURBED PACKING.

many authors to illustrate miscibility in mixed monolayer systems [1, 6-9, 11, 12]. However, some attempts to interpret ΔA ($\Delta A = A_{12} - x_1 . A_1 + x_2 A_2$) values in terms of intermolecular interactions involved in condensed films are sometimes found to be misleading [13,14].

Surface compression modulus against mole fraction curves ($K_s - x_1$).

To support the miscibility observed in $A-x_1$ plots many times surface compression modulus is plotted against the mole fraction. In Fig. 3.23 the variation of compression moduli as a function of mole fraction has been plotted for all the three systems. The compression modulus has been calculated in two states i.e. in liquid condensed (Lc) and solid (S). The values of K_s are much lower in liquid condensed state as compared to those in solid state. The compression modulus was calculated at four places in each state for each mole fraction using following formula from ref. [15].

$$K_s = A_o . f_1 / (A_o - A_1) \qquad (3.8)$$

where A_o is extrapolated area at zero pressure and A_1 is a smaller area (than A_o) at film pressure f_1. The points shown in Fig. 3.23 are the average of four K_s values in the particular state. The dotted line joining two pure

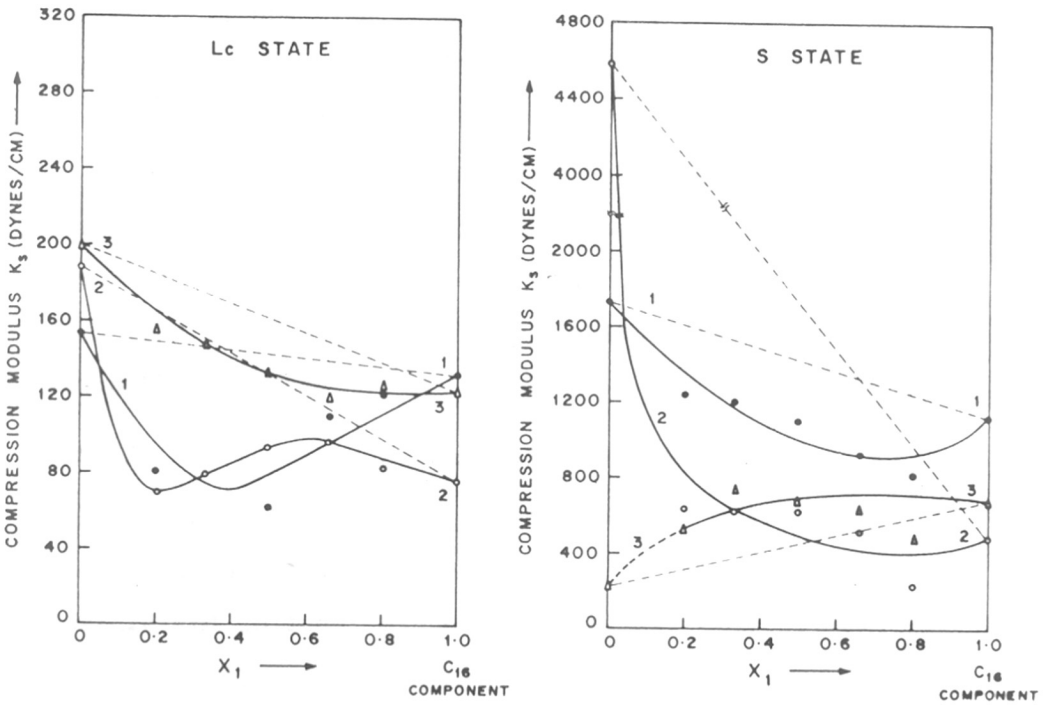

FIG. 3·23 : COMPRESSION MODULUS (Ks) AGAINST MOLE FRACTION FOR THREE SYSTEMS IN LIQUID CONDENSED (Lc) AND SOLID (S) STATE. 1 - C_{16}-OH + C_{22}-OH ; 2 - C_{16}-OC_2H_4OH + C_{22}-OC_2H_4OH ; 3 - C_{16}-OC_3H_6OH + C_{22}-OC_3H_6OH.

components indicate the ideal behaviour (additivity rule).

All the mixtures in both states show non-ideality and miscibility. The negative deviation from ideal behaviour is observed in all the cases, except for system III in 'S state'. The observed negative deviation is complementary to positive deviation in $A - x_1$ plots. In case of system III in 'S' state apparent positive deviation is observed. This is because 'S' state is not observed for C_{22}-OC_3H_6OH component. The point shown in Fig. 3.23 for C_{22}-OC_3H_6OH is the average of four K_s values above 40 dynes/cm.

Excess thermodynamic properties of mixing

An excess thermodynamic function is defined as the difference between the value of function in a given mixture and in ideal mixture of the same composition. Goodrich [16] considered mixed monolayers as two dimensional solutions and showed that excess free energy of mixing (ΔG^E) can be calculated from the π-A isotherms of the two pure components and the mixed monolayer.

The excess Gibbs free energy for the mixing of two insoluble film components 1 and 2 may be written as

$$\Delta G^E = N \left[\int_{\pi^*}^{\pi} (A_{12} - x_1 A_1 - x_2 A_2) \, d\pi \right] \qquad (3.9)$$

where N is Avogadro's number and π^* is the surface pressure below which the binary monolayer can be assumed to be ideally mixing. It is assumed that the surface pressure of condensed monolayer in equilibrium with its vapour is zero. This assumption is valid if the excess free energy of mixing of the monolayer vapour is negligible in comparison with that of the condensed monolayer and Goodrich has conveniently put $\pi^* = 0$. This is justified in most of the cases because the surface vapour pressures are extremely low.

The above Eqn.(3.9) can be divided into three parts.

$$I_{12} = \int_0^{\pi} A_{12}\, d\pi \; ; \quad I_1 = \int_0^{\pi} A_1 . d\pi \; ; \quad I_2 = \int_0^{\pi} A_2 . d\pi \qquad (3.10).$$

These integrals can be separately evaluated graphically by determining the area under the curve of corresponding π-A isotherms at a particular pressure. The π-A isotherm is extrapolated to zero pressure while integrating the isotherm.

In Fig. 3.24 the values of ΔG^E have been plotted against mole fraction at different surface pressures for the three systems. The curves show positive and negative deviations. Large negative deviations are observed at

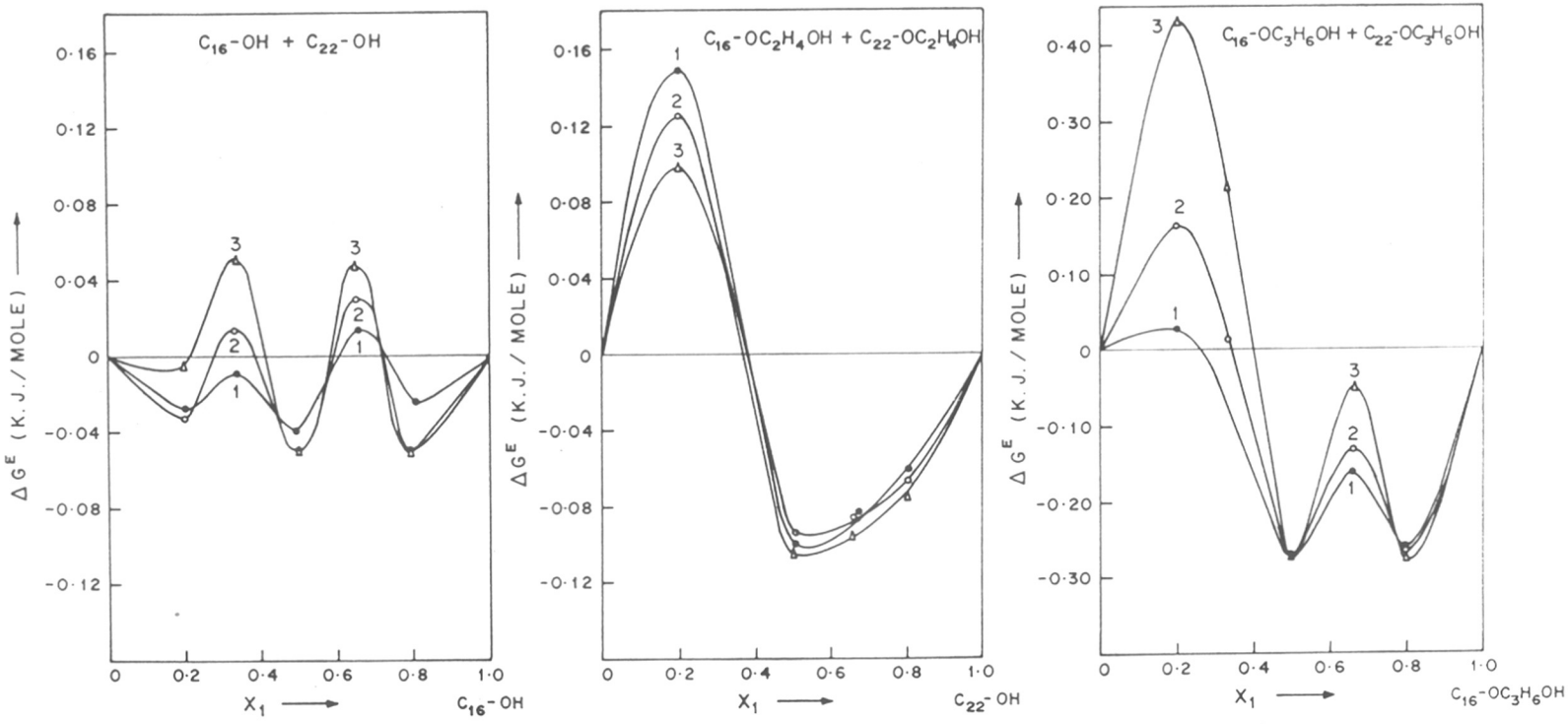

FIG.3·24 : EXCESS FREE ENERGY OF MIXING VERSUS MOLE FRACTION FOR THE SYSTEMS.
CURVE 1 - 8 DYNES/CM ; 2 - 16 DYNES/CM ; 3 - 32 DYNES/CM .

0.50 and 0.80 mole fractions for all the systems. This is indicative of a strong intermolecular interaction between the two film forming molecules at these mole fractions. The mixed monolayer of these mole fractions must be more stable than both pure components. Large negative deviation also indicates compact packing of molecules forming monolayer. The positive deviation indicates the loose packing of the molecules and the intermolecular interactions may be repulsive in nature. This is also confirmed from high fluidity for all the three systems (see Fig. 3.17).

However, this particular method of calculating ΔG^E by integrating π-A isotherm has got its own limitations [6]. Gershfeld [17] has pointed out the error involved in extrapolating the π-A isotherm to zero pressure. Therefore, it is extremely necessary to have the experimental measurements of surface pressures at very large area per molecule. Gershfeld [18] has shown the differences in the ΔG^E values in gaseous region and in condensed states. According to Lucassen-Reynders [19] the Goodrich's treatment includes not only terms arising from excess interactions between the monolayer components but also terms coming from changes in water content of the surface.

Inspite of these limitations, the method has been normally used to judge the non-ideality of the systems. This type of treatment has been used by many other investigators [1,7,8,11,20,21].

Barnes [7] has related the excess free energy of mixing (ΔG^E) value to the excess free energy of activation (ΔG^{*E}) for a molecule to evaporate from the water surface into the atmosphere through the following relation.

$$\Delta G^{*E} = -K.\Delta G^E \qquad (3.11)$$

where K is a constant. The large negative values of ΔG^E implies that large positive value for ΔG^{*E}. This means that a mixed monolayer showing large negative ΔG^E should have large specific resistance to evaporation. In the case of three systems studied in the present investigation, the mixed monolayers at 0.50 and 0.80 mole fractions should be good water evaporation retardants compared to other mole fractions which in fact has been confirmed directly from semi-field experiments.

Collapse pressure

Collapse pressure data can also be used to test the miscibility [6]. Using the chemical potential of each component in the surface and bulk phases an equation has been deduced by Joos [22] which allows to predict the

collapse pressures of a mixed insoluble monolayer with miscible components from the collapse pressures of each component separately. The equation is given as follows:

$$1 = \frac{\gamma_{1,m}}{f_{1,m}} \cdot x^{s}_{1,c} \cdot \exp\left[\frac{(\pi_{c,m}-\pi_{c,1})\omega_1}{kT}\right] + \frac{\gamma_{2,m}}{f_{2,m}} \cdot x^{s}_{2,c} \cdot \exp.\left[\frac{(\pi_{c,m}-\pi_{c,2})\omega_2}{kT}\right] \qquad (3.12)$$

ω_1 and ω_2 are cross-sectional area of component 1 and 2.

$\gamma_{1,m}$ and $\gamma_{2,m}$ are the surface activity coefficients of component 1 and 2 in monolayer $f_{1,m}$ and $f_{2,m}$ are the bulk activity coefficient of component 1 and 2 in monolayer. $x^{s}_{1,c}$ and $x^{s}_{2,c}$ are the mole fractions of components 1 and 2 at the collapse point ($x^{s}_{1,c} + x^{s}_{2,c} = 1$)

$\pi_{c,1}$ and $\pi_{c,2}$ are the collapse pressures of component 1 and 2.

$\pi_{c,m}$ is collapse pressure of mixed monolayer.

For an ideal mixed monolayer there is no interaction between component 1 and 2 and $\gamma_{1,m} = \gamma_{2,m} = 1$; $f_{1,m} = f_{2,m} = 1$. Therefore one can calculate using the above Eqn.(3.12), the collapse pressure of a mixed monolayer ($\pi_{c,m}$) for ideal behaviour at various mole fractions.

In Fig. 3.25 the collapse pressures have been plotted against mole fractions for the three systems. The dotted curve joining the two pure components indicate the ideal

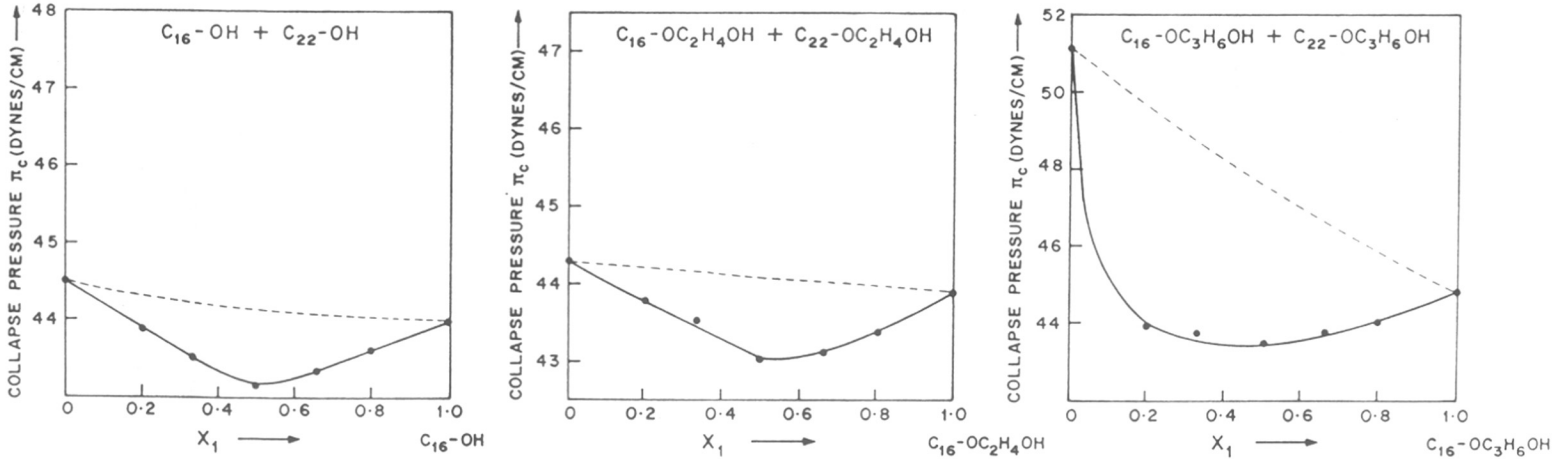

FIG.3·25 : COLLAPSE PRESSURE (π_c) AGAINST MOLE FRACTION FOR THREE SYSTEMS. THE DOTTED CURVE SHOWS IDEAL BEHAVIOUR FOR THE SYSTEMS ACCORDING TO JOOS THEORY.

behaviour of the system; which is calculated using the Eqn.(3.12). A clear negative deviation is observed from the ideal behaviour in all the three systems, indicating the non-ideal behaviour for the systems studied. Joos's treatment has been used by some other investigators also [9,22-25].

The limitations of the above treatment are that the collapse pressures must represent an equilibrium between the monolayer and the collapsed bulk phase. If the collapse pressures are determined by kinetic effects, the thermodynamic treatments are not applicable [6].

Phase diagrams

The miscibility or otherwise can also be detected in mixed monolayers by studying the surface phase rule. Defay [26] and Crisp [27] have extended the phase rule of Gibbs to include surface explicity. For variable surface tension (surface pressure), temperature and external pressure, the phase rule is given as:

$$F = C^B + C^S - P^B - P^S + S \qquad (3.13)$$

F = the number of degree of freedom

C^B = number of components in bulk which are in equilibrium.

C^S = number of components restricted to surface

P^B = number of bulk phases

P^S = number of surface phases

S = types of surfaces

To test whether two surface components at air-water interface are mutually miscible, mixing of two components is done at the surface concentration where each component is in equilibrium with its own surface vapour i.e. transition region of the isotherm. In this case $C^B = 2$ (air and water), $C^S = 2$ (components A and B), $P^B = 2$ (air and water) S = 3 (air/water; monolayer/water; monolayer/air). The phase rule is then written as

$$F = 2 + 2 - 2 + 3 - P^S$$

$$F = 5 - P^S \qquad (3.14)$$

If the two components A and B are miscible, $P^S = 2$ (condensed AB and vapour AB) then

$$F = 3$$

For constant temperature and external pressure, the transition pressure will vary with the composition. If A and B are immiscible $P^S = 3$ (two condensed phases of A and B, plus the surface vapour); for constant temperature and pressure, F = 0, the transition pressure will be independent of composition.

Exact thermodynamic equations of multi-component mixed monolayers have been derived recently by Motomura et al. [28-31] to describe phase transition in two component monolayers. When the π-A isotherm of a monolayer shows a phase change from α to β (α is expanded phase and β is condensed phase) the mole fraction of the second component in condensed state is given as follows [31]:

$$x_2^{\pi,\beta} = x_2^{\pi,\alpha} + \left\{(a^\beta - a^\alpha)\left(\partial \pi^{eq} / \partial x_2^{\pi,\alpha}\right)_{T,P}\right\} \Big/ \left\{(RT/x_1^{\pi,\alpha}.x_2^{\pi,\alpha}) + \left(\partial a^\alpha / \partial x_2^{\pi,\alpha}\right)_{T,P,\pi}\right. \quad (3.15)$$

$$\left. \cdot \left(\partial \pi^{eq} / \partial x_2^{\pi,\alpha}\right)_{T,P} + \int_0^\pi \left[\partial^2 a^\alpha / \left(\partial x_2^{\pi,\alpha}\right)^2\right]_{T,P,\pi} d\pi \right\}$$

Super-scripts α,β designate the corresponding phases, π^{eq} is the equilibrium surface pressure (which corresponds to surface pressure at the break point on the π-A curve), a^α and a^β correspond to partial molar area in respective phases.

If the π-A isotherms are of similar nature irrespective of composition the above Eqn.(3.15) reduces in terms of mean area per molecule A to [29,31]:

$$x_2^{\pi,\beta} = x_2^{\pi,\alpha} + \left[(A^\beta - A^\alpha).x_1^{\pi,\alpha} \cdot x_2^{\pi,\alpha} / kT\right] \left(\partial \pi^{eq} / \partial x_2^{\pi,\alpha}\right)_{T,P} \quad (3.16)$$

In numerical calculations the values of A^{β} and A^{α} can be approximated to two pure components at corresponding surface pressure. Using the Eqn. (3.16), the $x_2^{\pi,\beta}$ can be calculated.

Now, it is possible to obtain two curves; one is the experimental π^{eq} - $x_2^{\pi,\alpha}$ and the other theoretical π^{eq} - $x_2^{\pi,\beta}$. The points on the two curves corresponding to the same surface pressure, gives the composition of expanded and condensed phase which are in equilibrium with each other. Therefore, the two curves give the two dimensional phase diagram of the system.

Motomura and his co-workers [32-42] have determined the two dimensional phase diagrams for various mixed monolayer systems. They have calculated the mole fraction in the condensed phase where a mixed monolayer undergoes a phase change from liquid expanded to liquid condensed.

In the present system, studied by us, a phase change from liquid condensed (Lc) to solid (S) is observed. This means that the two phases Lc and S are coexisting at Lc → S transition. Therefore, using Eqn. (3.16), we have determined the phase diagrams for a phase change from Lc to S. The phase diagrams, for all the three systems, have been shown in Fig. 3.26.

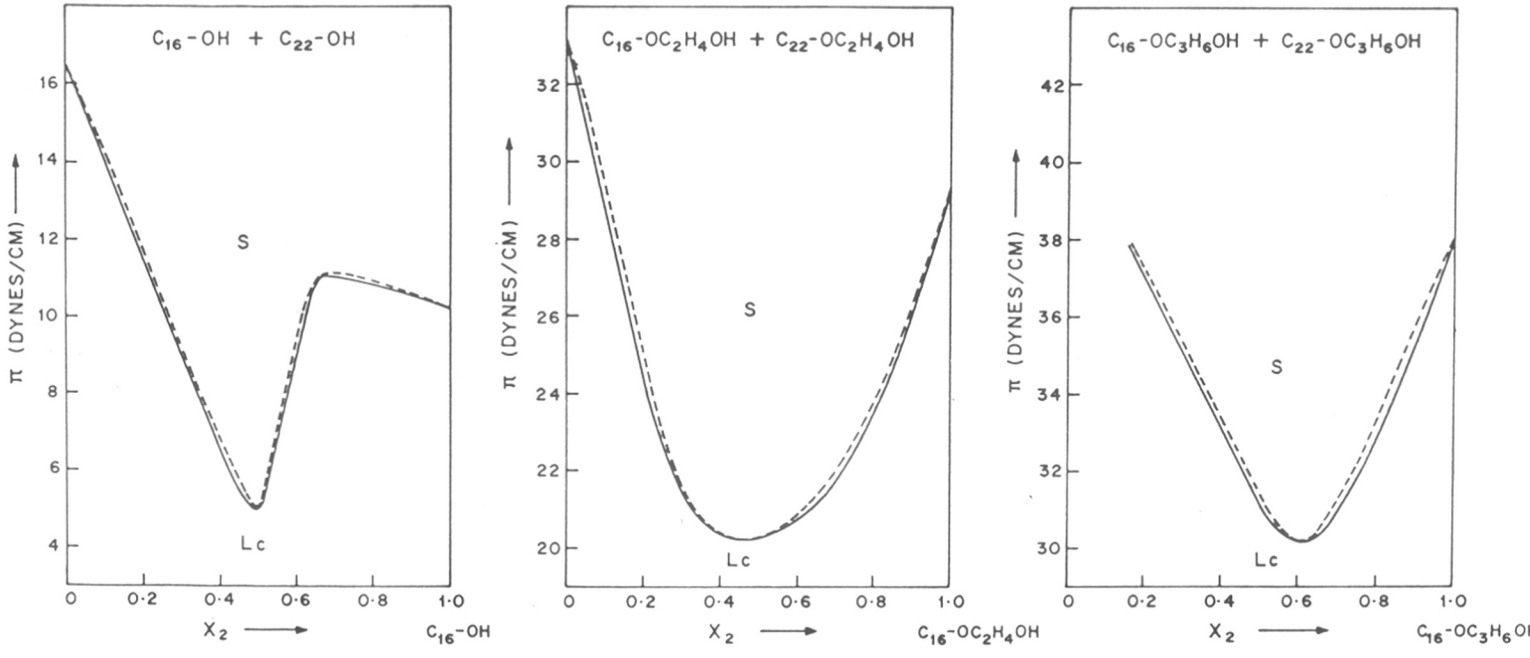

FIG. 3·26 : PHASE DIAGRAMS FOR THE THREE SYSTEMS.

A minimum is observed in the phase diagrams of all the systems. Such type of phase diagrams have been called as negative azeotropic type [33, 40,43]. At this minimum point, the composition of the liquid condensed and solid phases are equal, therefore this point corresponds to a azeotropic point, which is well known in three dimensional phase diagrams.

This indicates that the two components are miscible in both liquid condensed as well as solid states. The fact that negative azeotrope is observed in the phase diagram, indicates that the mutual interactions between the two components in the mixed monolayer are stronger than the interactions between pure component molecules themselves.

Conclusions

1) The miscibility and non-ideality is observed in all the systems which has been confirmed by various derived properties such as A-x_1, K_s - x_1, ΔG^E - x_1, $\pi_c \rightarrow x$, ϕ - x_1 and phase diagrams.

2) The study indicates that mutual interactions between the two components in mixed monolayer are stronger than the interactions between the pure component molecules themselves.

3) The mixed monolayers of 0.50 and 0.80 mole fractions (of C_{16}- component) exhibit large negative excess free energy of mixing which in turn suggest that these mixed monolayers should be better evaporation retardants than other mole fractions. This has also been confirmed on the semi-field experiments.

4) The various flow parameters have been calculated from the surface viscosity measurements using Joly's theory. The values of flow parameters indicate that the quasi-hexagonal network structure suggested by Joly is also applicable to the mixed monolayers studied in the present investigation. The application of Joly's theory also suggest that the mixed monolayers are miscible and homogeneous.

REFERENCES

1. G.V. Patil, A.B. Biswas and R.N. Shukla, J.Indian Chem.Soc. 49 (1972) 1349.

2. Y.K. Kuchhal, S.S. Katti and A.B. Biswas, J.Colloid Interface Sci. 49 (1974) 48.

3. M. Joly, Kolloid Z. 126 (1952) 35.

4. G.E. Boyd and F. Vaslow, J.Colloid Sci. 13 (1958) 275.

5. D.G. Dervichian, Surface Phenomena in Chemistry and Biology, eds.J.F. Danielli, K.G.A. Pankhurst and A.C. Riddiford, Pergamon Press, New York, 1958 p.70.

6. G.T. Barnes, Colloid Sci. 2 (1975) 173; A Specialist Periodical Report.

7. I.S. Costin and G.T. Barnes, J.Colloid Interface Sci. 51 (1975) 106.

8. D.A. Cadenhead and M.C. Phillips, Adv.Chem.Ser. 84 (1968) 131.

9. M.C. Phillips and P. Joos, Kolloid Z. 238 (1970) 499.

10. D.A. Cadenhead and F. Muller-Landau, J.Colloid Interface Sci. 78 (1980) 269.

11. A.G. Gaonkar and S.S. Katti, J.Colloid Interface Sci. 69 (1979) 549.

12. D.A. Cadenhead, Structure of Biological Membranes (1976), eds. S. Anrahamsson and I. Pascher, Plenum Pub.Co., New York, p.63.

13. K. Tajima and N.L. Gershfeld, Biophys.J. 22 (1978) 489.

14. N. Funasaki, J. Colloid Interface Sci. 90 (1982) 551.

15. H.E. Ries Jr., J.Colloid Interface Sci. 88 (1982) 298.

16. F.C. Goodrich, Proc. 2nd.Int.Congr. on Surf.Activity 2 (1957) 85.

17. N.L. Gershfeld, Techniques of Surface and Colloid Chemistry and Physics, 1 (1972) 1; eds. R.J. Good, R.R. Stromberg and R.L. Patrick; Marcel Dekker Inc., New York.

18. N.L. Gershfeld, Methods in Membrane Biology, 1 (1974) 86 ed. E.D. Korn, Plenum Press, New York.

19. E.H. Lucassen-Reynders, J.Colloid Interface Sci. 42 (1973) 554.

20. D.O. Shah and J.H. Schulman, J.Lipid Res. 8 (1967) 215.

21. G. Gabrielli, M. Puggelli and R. Faccioli, J.Colloid Interface Sci. 41 (1972) 63.

22. P. Joos, Bull.Soc.Chim.Belges 78 (1969) 207.

23. P. Joos and R.A. Damel, Biochim.Biophys.Acta. 183 (1969) 447.

24. M. Puggelli and G. Gabrielli, J.Colloid Interface Sci. 61 (1977) 420.

25. P. Joos, R. Ruyssen, J.M. Trillo, S.G. Fernandez and P.S. Pedrero, J.Chim.Phys. 66 (1969) 1665.

26. R. Defay, I. Pregogine, A. Bellemans and D.H. Everett, Surface Tension and Adsorption , Wiley, New York (1966) pp. 74-78.

27. D.J. Crisp, Surface Chemistry, Suppl. Research London, (1949) p. 17 and 23.

28. K. Motomura, J.Colloid Interface Sci. 48 (1974) 307.

29. K. Motomura, K. Sekita and R. Matuura, J.Colloid Interface Sci. 48 (1974) 319.

30. K. Motomura, T. Yano, M. Ikematsu, H. Matuo and R. Matuura, J.Colloid Interface Sci. 69 (1979) 209.

31. K. Motomura, Adv.Colloid Interface Sci. 12 (1980) 1.

32. K. Motomura, T. Terazono, H. Matuo and R. Matuura, J.Colloid Interface Sci. 57 (1976) 52.

33. K. Motomura, S. Yoshino, K. Fuju and R. Matuura, J.Colloid.Interface Sci. 60 (1977) 87.

34. H. Matuo, K. Motomura and R. Matuura, J. Colloid Interface Sci. 69 (1979) 192.

35. H. Matuo, K. Motomura and R. Matuura, Bull.Chem.Soc.Jpn. 52 (1979) 673.

36. H. Matuo, N. Yoshida, K. Motomura and R. Matuura, Bull.Chem.Soc.Jpn. 52 (1979) 667.

37. K. Motomura, M. Ikemotsu, Y. Hayami, H. Matuo and R. Matuura, Bull.Chem.Soc.Jpn. 53 (1980) 2217.

38. Y. Hayami, T. Yano, K. Motomura and R. Matuura, Bull.Chem.Soc.Jpn. 53 (1980) 3414.

39. H. Matuo, K. Motomura and R. Matuura, Bull.Chem.Soc.Jpn. 54 (1981) 2205.

40. H. Matuo, K. Motomura, and R. Matuura, Chem.Phys.Lipids 28 (1981) 385.

41. H. Matuo, T. Mitsui, K. Motomura and R. Matuura, Chem.Phys.Lipids 29 (1981) 55.

42. H. Matuo, D.K. Rice, D.M. Balthasar and D.A. Cadenhead, Chem.Phys.Lipids 30 (1982) 367.

43. H. Matuo, K. Motomura and R. Matuura, Chem.Phys.Lipids 30 (1982) 353.

C H A P T E R - IV

MIXED MONOLAYERS OF POLYMERS WITH n-LONG CHAIN COMPOUNDS

INTRODUCTION

The compounds that form insoluble monolayers fall readily into two main classes. The first are the typical saturated long hydrocarbon chains having a polar group at the end. Monolayers formed by such compounds have been extensively studied by many investigators. The second class of insoluble monolayer comprise substances in which an indefinite number of polar groups are distributed along a polymer chain. Monolayer properties of such compounds have also been studied in the literature. However, very little work has been carried out on the mixed monolayers of these two classes of compounds. This forms the main aim of the present study. Before we discuss on mixed monolayers, it is essential to know the work carried out on polymer monolayers.

Crisp [1,2] has given good reviews of the work on surface films of polymers. Before the World War II, the information on polymer monolayers was very scanty. Derivatives of cellulose had been studied by Katz and Samwel [3], Adam [4] and by Harding and Adam [5]. Sheppard and Keenan [6] showed that both proteins and cellulose nitrate formed very thin films of reproducible area on a clean mercury surface. Monolayers of synthetic

polymers were also studied by Katz and Samwel [7], Moss [8], Harkins et al.[9]. Adam [10] mentioned the possibility of spreading the methyl and ethyl methacrylate.

Singer [11] has developed an equation of state for two dimensional, insoluble linear polymers based on idealized quasi-lattice model, following Flory-Huggins treatment of thermodynamic behaviour of polymer solutions. The equation is given as follows:

$$\pi/\pi_o = [(x-1)Z'/2x].\ln [1-(Z/Z')(A_o/A)] - \ln[1-(A_o/A)] \quad (4.1)$$

A = area($\mathring{A}^2$) available per monomer unit in polymer molecule at film pressure π.

A_o = corresponding area in close-packed state

$\pi_o = kT/A_o$

x = number of monomer units in a molecule

Z' = nearly equal to coordination number (this varies from 2 to 4).

This equation of state represents the π-A relation for monolayers of synthetic polymers and protein monolayers both at air-water and oil-water interfaces. Davis and his co-workers [12,13] have introduced a factor ω as a measure of flexibility of a polymer chain in the interface.

$$\omega = Z' - 2$$

For a rigid molecule, $Z' = 2$; $\omega = 0$ and for a completely flexible molecule $Z' = 4$; $\omega = 2$.

However, Kawai [14] reports that the definition of ω lacks in theoretical background. The author says that the coordination number Z' has no connection with molecular flexibility of the polymer chain in nature and the quantitative discussion of ω would be impossible due to lack of its theoretical justification.

Hotta and co-workers [16-21] have studied the π-A and ΔV-A of various monolayers including polyvinyl acetate, polyvinyl stearate, polymethylmethacrylate undissociated polymethacrylic acids, copolymers of polymethacrylic acid and diethylaminoethyl vinyl ether, polyoctadecyl methacrylate, poly-ϵ-caproamide, polyethylene terphthalate, polyacrylonitrile, poly-N-vinyl pyrrolidone etc. at air-water and oil-water interfaces at different pH values. All polymers except polyvinyl acetate gave films of condensed type at air-water interface, whereas all polymers except polyethylene terphthalate and polyacrylonitrile give films of expanded type at oil-water interface. The presence of ring group in main chain makes the polymer molecule rigid even at oil-water interface, while that in the

side chain is not essentially different from the chain groups. The cohesion between nonpolar group is predominant in most of the cases at air-water interface and is absent at oil-water interfaces. The steric effect of side chains is very effective when they lie at the interface.

Parker and Shereshefsky [22] have studied the π-A isotherms of monolayers of polystyrene, cellulose acetate and polymethyl methacrylate at air-water interface. They have compared the molecular weights of the samples calculated from π-A isotherm and from conventional methods like viscosity. The authors found good agreement between the two molecular weights.

Llopis and Rebollo [23] have studied the effect of temperature on π-A isotherms of polyvinyl acetate, polyvinyl alcohol and dimethyl cellulose. The effect of temperature is insignificant on monolayers of dimethyl cellulose. The monolayers of polyvinyl acetate, for a given value of area per monomer unit, the surface pressure undergoes through a minimum with rise in temperature, whereas those of polyvinyl alcohol undergo through a maximum with rise in temperature. From the variation in surface pressure with temperature, the spreading entropy and enthalpy have been obtained. The partial penetration of macromolecule into substratum increases with the compression,this effect becomes

noticeable when temperature increases for polyvinyl alcohol.

Tachibana and Inokuchi [24] have studied the rheological properties of protein monolayers. The authors have presented a static method of measuring surface viscoelasticity of spread monolayers.

Motomura and Matuura [25] have criticized the Singer's equation of state for polymer monolayers. A new equation has been derived by the authors taking into account the cohesive forces. The π-A isotherms of polyvinyl acetate, polymethyl acrylate and polymethyl methacrylate are shown to be in good agreement with the equation of state. The influence of surface concentration of the monolayer and that of temperature on the equation of state has been discussed by Llopis and Subirana [26]. Huggins [27] has derived the equation of state for the polymer monolayers considering the effect of temperature and the partial submersion of the chains in the substrate.

Gabrielli and Puggelli [28] has studied poly(m-fluorostyrene) and poly(p-fluorostyrene) at oil-water (toluene-water) interface by measuuring π-A isotherms at 25, 30 and 35^{o}C. The authors report that the macromolecules studied differ not only in limiting areas but also in

the type of the bidimensional phase and in energies present in the monolayers even though the polymers have same steric configuration but the monomeric units are positional isomers.

Hammond et al.[29] have studied various polymers at air-water interface. The authors have reported significant increase in limiting area (23.0 to 26.5 $\AA^2$ / monomer unit) of polymethyl acrylate with the increase in molecular weight. Such a large increase in limiting area with the molecular weight has never been reported, however, on the other hand some investigators [1,8,9] have reported it to be almost independent of molecular weight.

Nakahara et al.[30] have studied the poly-n-nonyl methacrylate, poly-n-dodecyl methacrylate, poly-n-tetradecyl methacrylate, poly-n-hexadecyl methacrylate, poly-n-octadecyl methacrylate monolayers at air-water interface in the temperature range between 10 to 35°C by measuring π-A isotherms. The authors have reported phase transitions in all of the compounds studied. The transitions in poly-n-octadecyl methacrylate and poly-n-hexadecyl methacrylate are reported to be time dependent.

The effect of gamma radiations on the monolayers of synthetic polyamino acids has been studied by

Korgaonkar and Joshi [31]. In case of poly-L-tyrosine the authors report reduction in areas after irradiation, however, such reduction is not observed in case of poly-DL-alamine. This type of data has been used for the interpretation of polyamino acid structure.

Jarvis [32] has studied monolayers of homologous series of polydimethylsiloxanes on various substrates, viz. water, tricfesyl phosphate, propylene carbonate, diethylphthalate, bis(2-ethyl hexyl)adipate and hexadecane. The polydimethylsiloxanes can be spread as insoluble monolayers on all organic substrates mentioned above. The monolayer stability and insolubility were found to vary with the molecular weight of polydimethyl-siloxane and polarity of substrate liquids. However, the author has not commented regarding the orientation of the polymer at the interface.

Nakamae et al.[33] have studied monomolecular films of polymers having carboxylic groups at air-water interface by measuring π-A isotherms and collapse pressures. They have suggested that the polymer monolayer is a suitable model for polymers adsorbed on the surface of an inorganic powder. The interactions between an inorganic powder and polymer is one of the most important factors which controls the properties of composite

materials e.g. paint, ink, magnetic recording etc.

Breton [34] has reviewed the application and technique of formation of polymeric Langmuir-Blodgett films. Gabrielli and his co-workers [35-38] have studied the mechanism of collapse of various polymer monolayers. In the case of polyvinyl acetate [35], the collapse phenomenon involves the expulsion of small segment (approximately monomeric units) of polymer chains. In case of polymethyl methacrylate, cellulose acetate and poly(L, D and DL)alanine, the collapse occurs in two steps; the process of separation of polymeric chains from the substrate and the formation of the bi-layer. This type of mechanism is known as nucleation and growth.

The work of polymer monolayers has been carried out by many investigators [39-44]. Since polymer has been used in the present investigation as one of the components of the mixed monolayer, some of the mixed monolayer systems have been reviewed in the following paragraphs.

Gabrielli et al.[45-47] have put forth the idea of orientation and compatibility in mixed monolayers. According to these investigators, the compatibility between two components of a mixed monolayer will be observed only when both components have similar orientation

at the interface. This has been concluded from studies on various vertical-vertical (V-V), horizontal-horizontal (H-H) and horizontal-vertical (H-V) types of systems, viz. polymethyl methacrylate with stearic acid, myristic acid, oleic acid, polypropyl methacrylate, polyoctadecyl methacrylate and polyvinyl stearate with oleic acid, polyoctadecyl methacrylate, polyvinyl acetate and polyvinyl acetate with oleic acid. In all the above systems only V-V and H-H types are compatible and H-V types are incompatible. The mixed monolayers of polymethyl methacrylate with polyethyl methacrylate, polybutyl methacrylate and polyethyl methacrylate with polybutyl methacrylate have been studied by measuring film pressure and surface viscosity to determine the stability of these mixed monolayers [48]. The stability is attributed to cohesive energies between the macromolecular segments.

Wu and Huntsberger [49] have studied (i) polyvinyl acetate - poly-n-butyl methacrylate, (ii) polyvinyl acetate - poly-i-butyl methacrylate, (iii) polyvinyl acetate - poly-t-butylmethacrylate, (iv) polymethyl methacrylate - polyvinyl acetate and (v) poly-n-butyl methacrylate-poly-i-butyl methacrylate. All these polymers are of H-H type. Therefore all of the mixtures are

expected to be compatible; however, the systems (ii) and (iii) have been reported to be incompatible. The reason for this may be that the branched iso and tertary butyl side chains appears to possess very poor packing geometry with vinyl acetate segment.

Another interesting system has been studied by Puggelli and Gabrielli [50]. Here the authors have studied (i) polyvinyl butyrate - polyvinyl acetate system and compared with (ii) polyvinyl acetate - polymethyl methacrylate system. The polymers used in both the systems are oriented horizontally at the interface. Even though, both systems are compatible, the system "(i)" behaves non-ideally whereas system "(ii)" ideally. The authors explain this odd behaviour by considering spreading thermodynamic functions i.e. spreading entropy and enthalpy. In case of system "(ii)" both components have spreading entropies and enthalpies of the same sign while in the case of non-ideal mixtures (i.e. system "(i)") two components have opposite signs. The enthalpic contribution comes from polymer-polymer interaction and from polymer substrate interactions. The different behaviour of polymer-substrate interaction of polyvinyl butyrate with respect to polymethyl methacrylate may be the reason for the different behaviour of system "(i)".

Gabrielli and Baglioni [51] have studied the mixed monolayers of polydimethylsiloxane with cellulose acetate. Both polymers are horizontally oriented at the interface. Even though the two polymers are quite different from each other the bidimensional solubility is observed.

Mixed monolayers of polyvinyl acetate with stearic acid, n-hexacosanoic acid, methyl stearate, 1-octadecanol, etc. have been studied [52,53]. In these mixtures polymer is oriented horizontally whereas n-long chain compound vertically. Naturally all these mixtures are found to be incompatible. Similar behaviour is true for the mixed monolayers of poly-γ-benzyl-L-glutamate and arachidic acid [54].

Trapeznikov and Kolobov [55] have studied mixed monolayers of polydimethylsiloxane and polydimethyl phenylsiloxane with oleic acid at air-water interface. Both systems show a non-ideal compatibility.

Fukuda et al.[56] have done interesting measurements with polyvinyl stearate and n-long chain compound viz. 1-hexadecanol, 1-octadecanol and stearic acid. In this case, the polymer (polyvinyl stearate) is also vertically oriented and forms miscible mixture with the n-long chain compounds. The measurements on specific evaporation

resistance of the above systems indicate that mixed monolayers of polyvinyl stearate with 1-hexadecanol, 1-octadecanol and stearic acid can act as good evaporation retardant. Many other systems have been studied by Gabrielli et al. and other workers [57-61] to study the orientation and compatibility in mixed monolayers.

Recently Puggelli and Gabrielli [62] have reported some interesting results. They have studied poly-2-vinylpyridine (PVP) (which is horizontally oriented and has ionizable polar group) with vertically oriented compounds having non-ionizable polar groups, like stearic acid (SA), methyl stearate (MS), stearyl amine (SAm), polyvinyl stearate (PVS), polyoctadecylmethacrylate (POMA) and with horizontally oriented compounds (non-ionizable polar groups) like oleic acid (OA) and polymethyl methacrylate (PMMA) both at air-water and oil-water interfaces at 15°, 25° and 35°C. From the curves of A-x_1, K_s-x_1 and ΔG^E-x_1 the authors have shown complete miscibility in all the above systems at all mole fractions, at both air-water and oil-water interface, and at all the three temperatures. Visualization of physical picture of these mixed monolayers shows no scope for the hydrophobic chain-chain interaction in horizontal-vertical oriented mixed monolayers. Therefore, the authors have attributed the miscibility in unfavourably

oriented mixtures to the attraction between the polar groups. They have observed that the mixed monolayers of PVP-OA and PVP-PMMA are thermodynamically more stable than the other systems mentioned above (i.e. unfavourably oriented). This is because the interactions between hydrocarbon chains and the polar groups both are present in favourably oriented molecules. However, some further work needs to be done to understand the implications of the compatibility in mixed monolayers where one of the component is a polymer with ionizable polar group.

From the literature surveyed above it is clear that the monolayers of polymers and mixtures of polymers have been received wide attention. In continuation of search for a better water evaporation retardant, we have undertaken the work on mixed monolayers of polymers with n-long chain compounds. The literature revealed that the H-V type of systems, being incompatible, are not suitable water evaporation retardants. Therefore it is necessary to mix a vertically oriented polymer with n-long chain compounds to get homogeneous, compatible mixed film, as these are V-V type of mixtures, which may behave as better evaporation retardant in terms of stability and efficacy as compared to the pure components.

With this view in mind, we have selected polyvinyl stearate as a vertically oriented polymer to mix with n-long chain compounds. The π-A isotherms of following systems have been studied at 25°C.

System I : Polyvinyl stearate (PVS) with Eicosanol; $C_{20}H_{41}OH$ (C_{20}-OH)

System II: Polyvinyl stearate (PVS) with Hexadecoxy ethanol; $C_{16}H_{33}OC_2H_4OH$ (C_{16}-OC_2H_4OH)

System III: Polyvinyl stearate (PVS) with Octadecoxy ethanol; $C_{18}H_{37}OC_2H_4OH$ (C_{18}-OC_2H_4OH)

System IV: Polyvinyl stearate (PVS) with Docosanoxy ethanol; $C_{22}H_{45}OC_2H_4OH$ (C_{22}-OC_2H_4OH)

System V : Polyvinyl stearate (PVS) with Hexadecoxy propanol; $C_{16}H_{33}OC_3H_6OH$ (C_{16}-OC_3H_6OH)

System VI: Polyvinyl stearate (PVS) with Docosanoxy propanol; $C_{22}H_{45}OC_3H_6OH$ (C_{22}-OC_3H_6OH).

Along with above (V-V) systems, we have also done the study on a typical (H-V) type system to confirm the general rule of orientation and compatibility. The system selected is:

System VII: Polyvinyl acetate (PVAc) with Docosanoxy ethanol; $C_{22}H_{45}OC_2H_4OH$ (C_{22}-OC_2H_4OH).

The experimental technique for getting π-A isotherms and the purity of the compounds used has already been discussed in Chapter II. The surface viscosity measurements of polymer and its mixtures were not possible with the rotational surface viscometer constructed in the laboratory.

RESULTS AND DISCUSSIONS

The π-A isotherms of the mixed monolayers of PVS with various n-long chain compounds have been given in the Figs. 4.1 to 4.6. It is clear from the π-A isotherms that the mixed monolayers and the PVS do not show any sharp phase transition point. The miscibility in the mixed monolayers can be decided by considering following derived data from π-A isotherms.

Area-mole fraction curves (A-x_1)

All the polymer mixtures have been studied at five different mole fractions. The mole fractions of polymer component in mixed system are taken as the mole fractions based on the monomer unit. The area is expressed in terms of square angstroms per monomer unit.

Interactions in mixed monolayers can be best judged at low pressures. Therefore the A-x_1 curves have

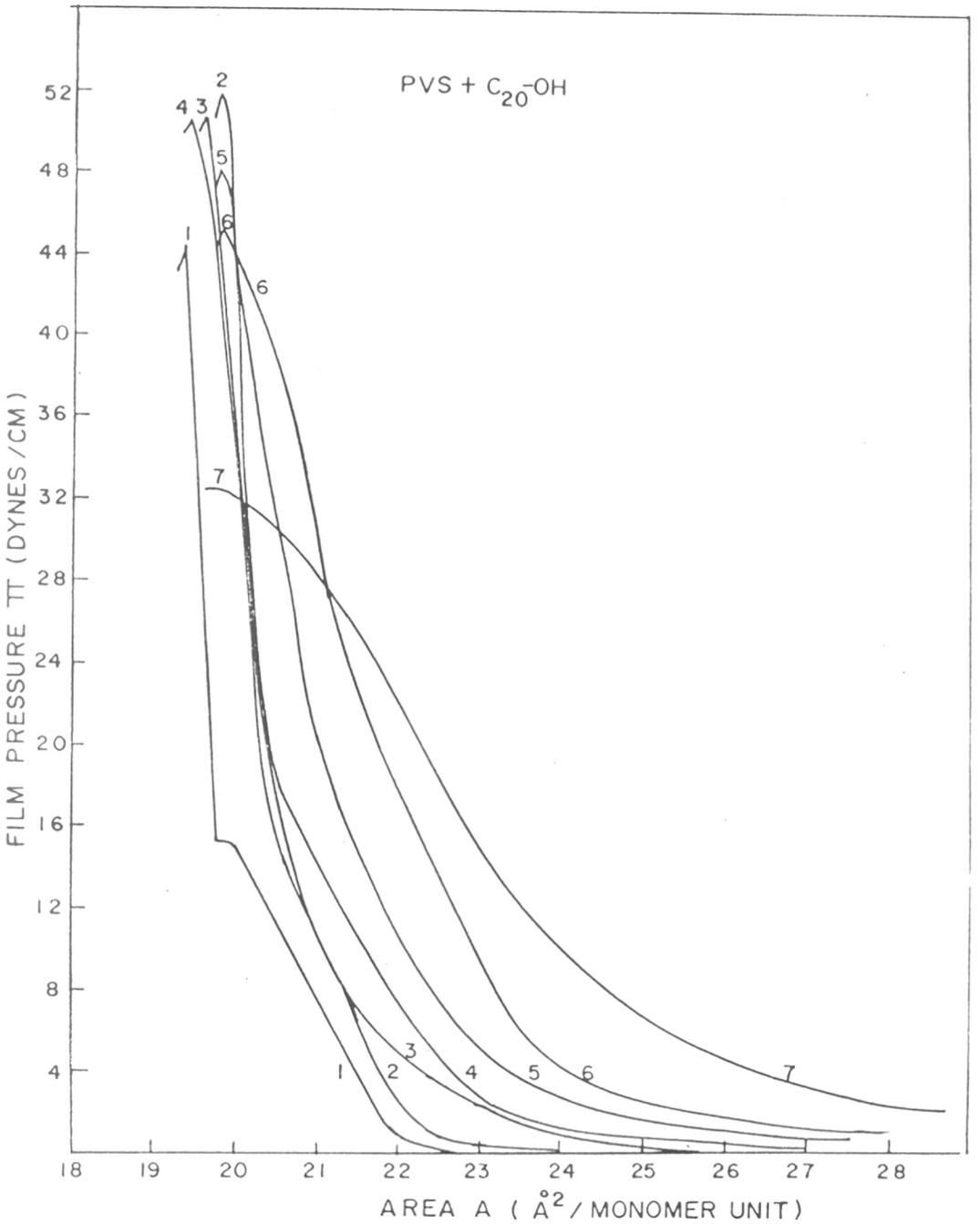

FIG. 4·1 : π-A ISOTHERMS OF PVS, C_{20}-OH AND THEIR MIXTURES AT 25°C. MOLE FRACTION OF PVS : CURVE 1 : 0·0 (C_{20}-OH) ; 2 : 0·20 ; 3 : 0·33 ; 4 : 0·50 ; 5 : 0·66 ; 6 : 0·80 ; 7 : 1·0 (PVS).

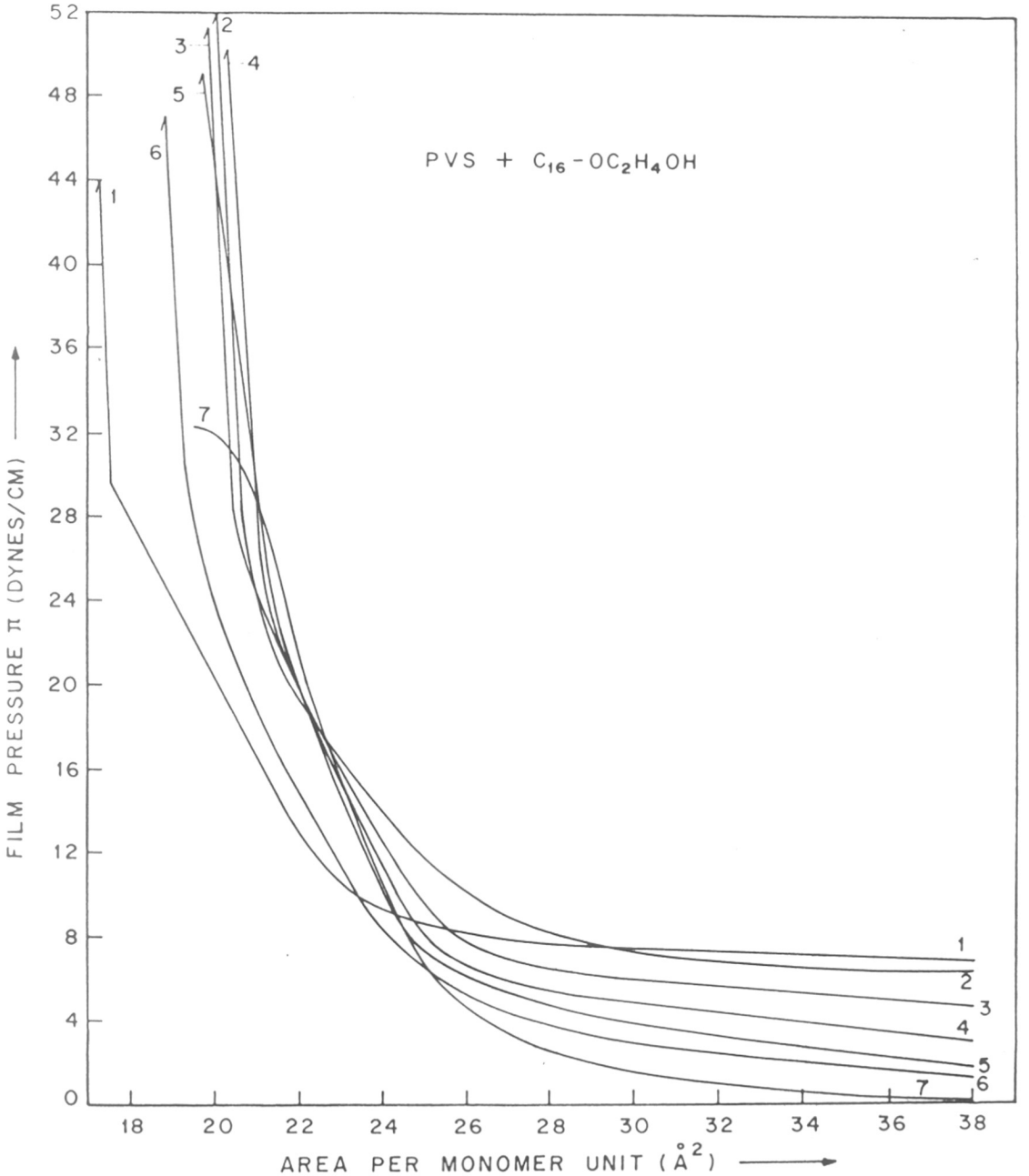

FIG. 4·2 : π-A ISOTHERMS OF PVS, C_{16}-OC_2H_4OH AND THEIR MIXTURES AT 25°C. MOLE FRACTION OF PVS : CURVE 1 : 0·0(C_{16}-OC_2H_4OH) ; 2 : 0·20 ; 3 : 0·33 ; 4 : 0·50 ; 5 : 0·66 ; 6 : 0·80 ; 7 : 1·0 (PVS).

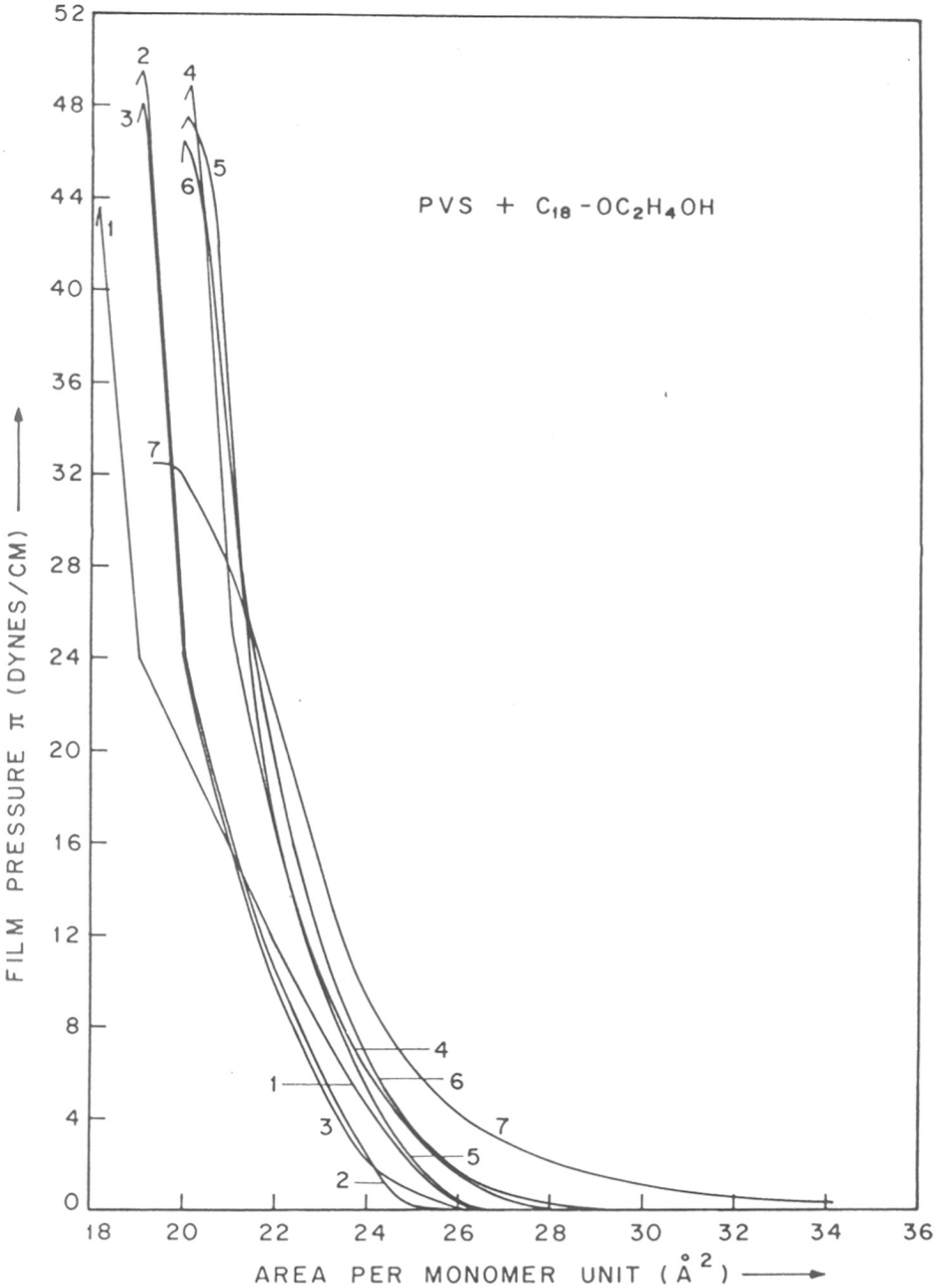

FIG. 4·3 : π – A ISOTHERMS OF PVS, C_{18}-OC_2H_4OH AND THEIR MIXTURES AT 25°C. MOLE FRACTION OF PVS : CURVE 1 : 0·0 (C_{18}-OC_2H_4OH) ; 2 : 0·20 ; 3 : 0·33 ; 4 : 0·50 ; 5 : 0·66 ; 6 : 0·80 ; 7 : 1·0 (PVS).

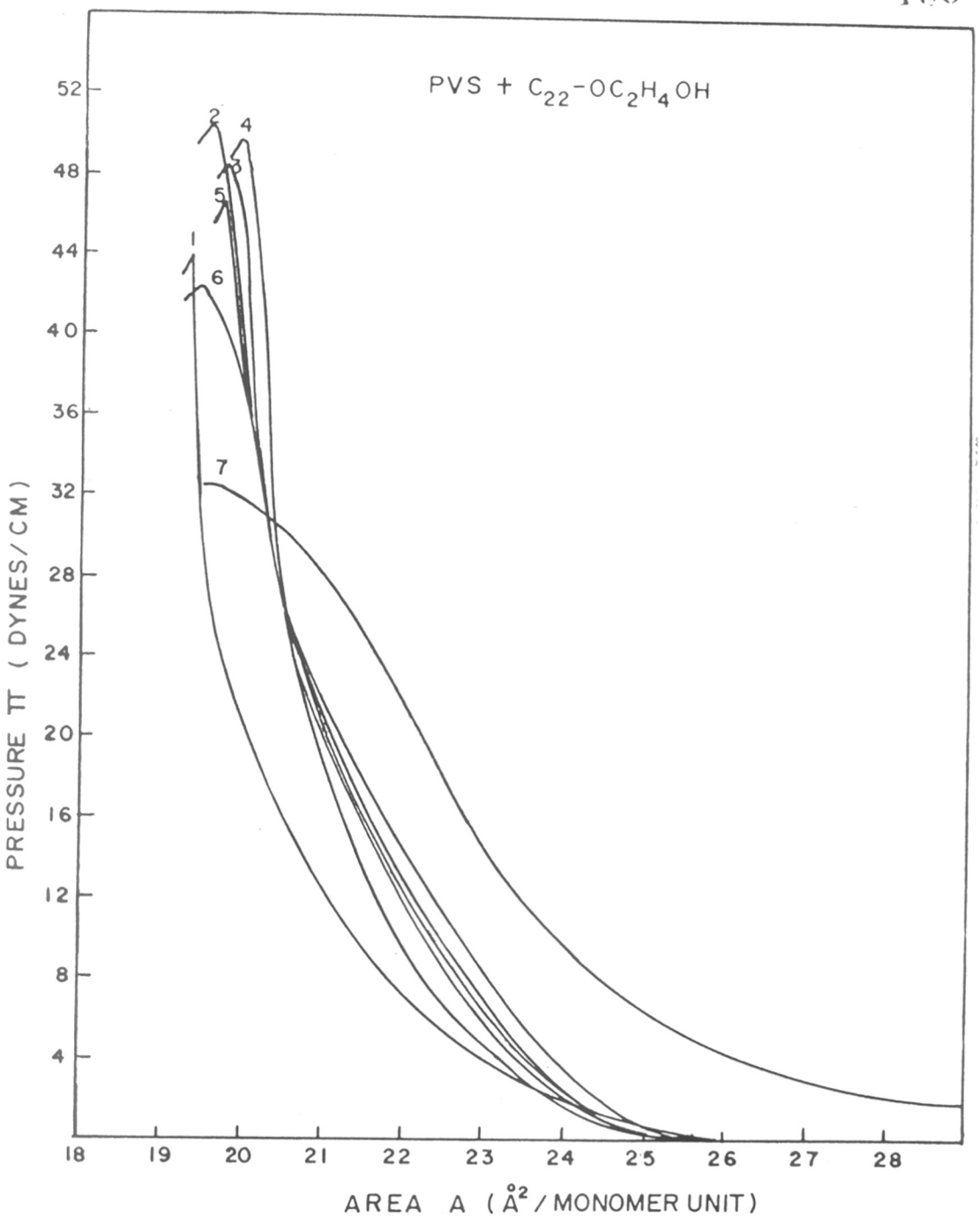

FIG. 4·4 : π-A ISOTHERMS OF PVS , C_{22}-OC_2H_4OH AND THEIR MIXTURES AT 25°C. MOLE FRACTION OF PVS : CURVE 1 : 0·0 (C_{22}-OC_2H_4OH) ; 2 : 0·20 ; 3 : 0·33 ; 4 : 0·50 ; 5 : 0·66 ; 6 : 0·80 ; 7 : 1·0 (PVS).

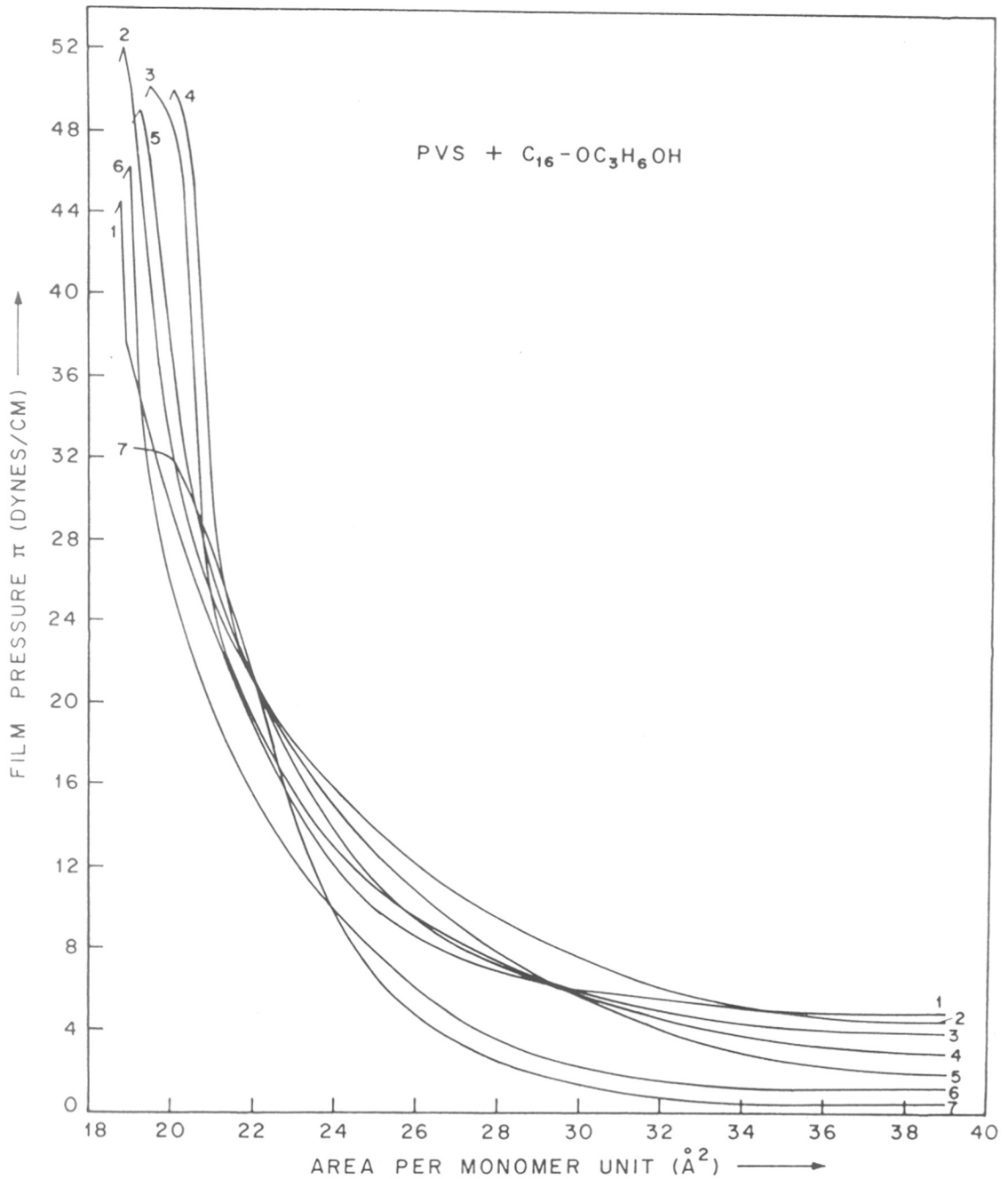

FIG. 4·5 : π-A ISOTHERMS OF PVS, C_{16}-OC_3H_6OH AND THEIR MIXTURES AT 25°C. MOLE FRACTION OF PVS : CURVE 1 : 0·0 (C_{16}-OC_3H_6OH) ; 2 : 0·20 ; 3 : 0·33 ; 4 : 0·50 ; 5 : 0·66 ; 6 : 0·80 ; 7 : 1·0 (PVS).

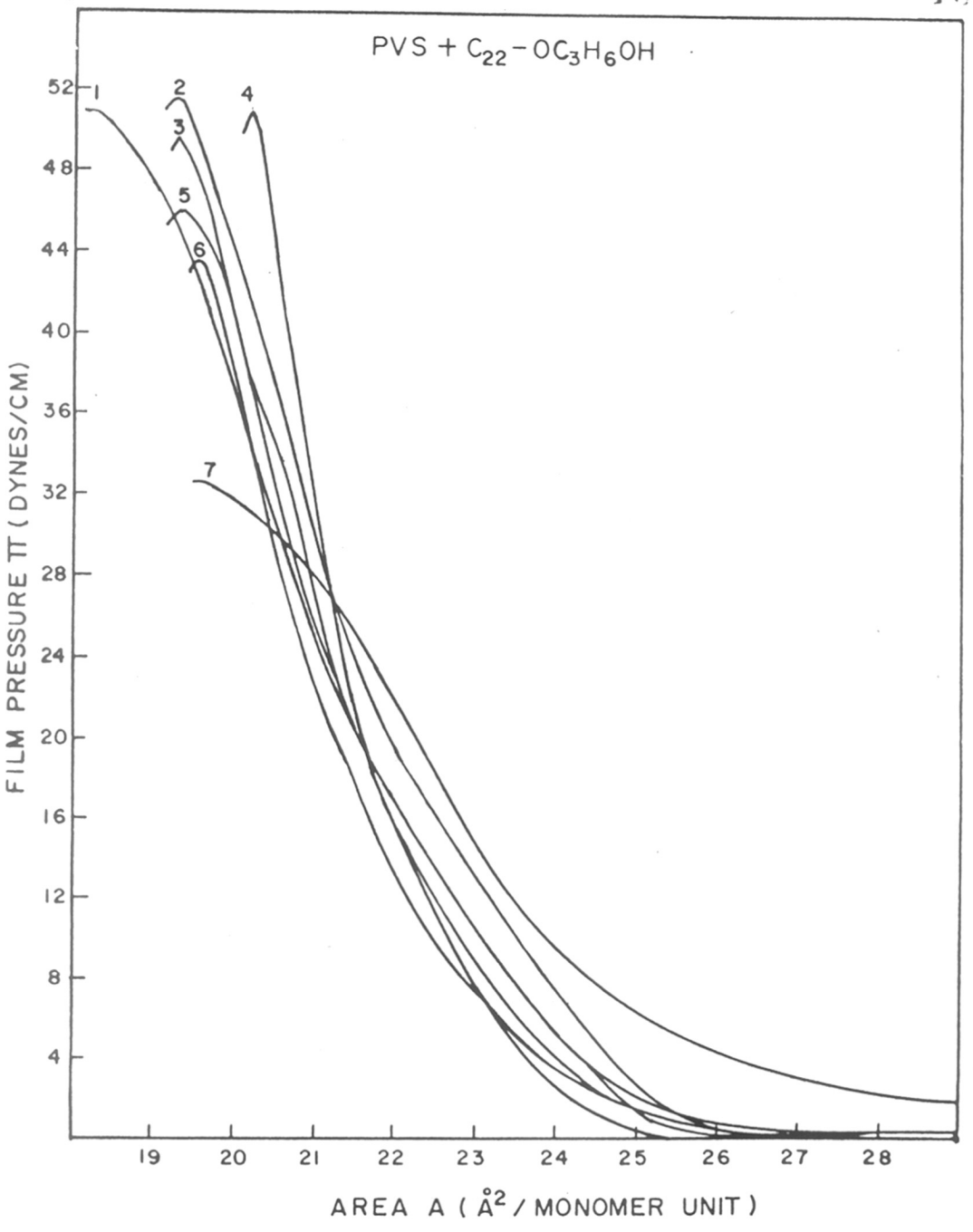

FIG. 4·6 : π-A ISOTHERMS OF PVS, C_{22}-OC_3H_6OH AND THEIR MIXTURES AT 25°C. MOLE FRACTION OF PVS: CURVE 1 : 0·0(C_{22}-OC_3H_6OH); 2 : 0·20 ; 3 : 0·33 ; 4 : 0·50 ; 5 : 0·66 ; 6 : 0·80 ; 7 : 1·0 (PVS).

been shown at only one suitable surface pressure i.e. at 8 dynes/cm in Fig. 4.7.

Systems I and III show complete negative deviations, whereas systems II, IV and VI show positive deviation at 0.20 mole fraction and then complete negative deviation, and system V shows complete positive deviation. These deviations can be explained based on Cadenhead-Muller-Landau [63] model. The positive deviations can be attributed to miscibility of the films when one of the components cannot be accommodated and disturbs the packing of the second component; the negative deviations arise due to miscibility of the components accompanied by geometrical rearrangement to accommodate the two types of molecules. Thus the A-x_1 curves of these mixed monolayer systems indicate strong intermolecular interaction between the two components.

Compression modulus - mole fraction (K_s - x_1) curves

The compression modolus against mole fraction have been plotted in Fig.4.8 for all the systems. Compression modolus at 8 dynes/cm was calculated using the formula [52]

$$K_s = \frac{A_o . f_1}{A_o - A_1} \qquad (4.2)$$

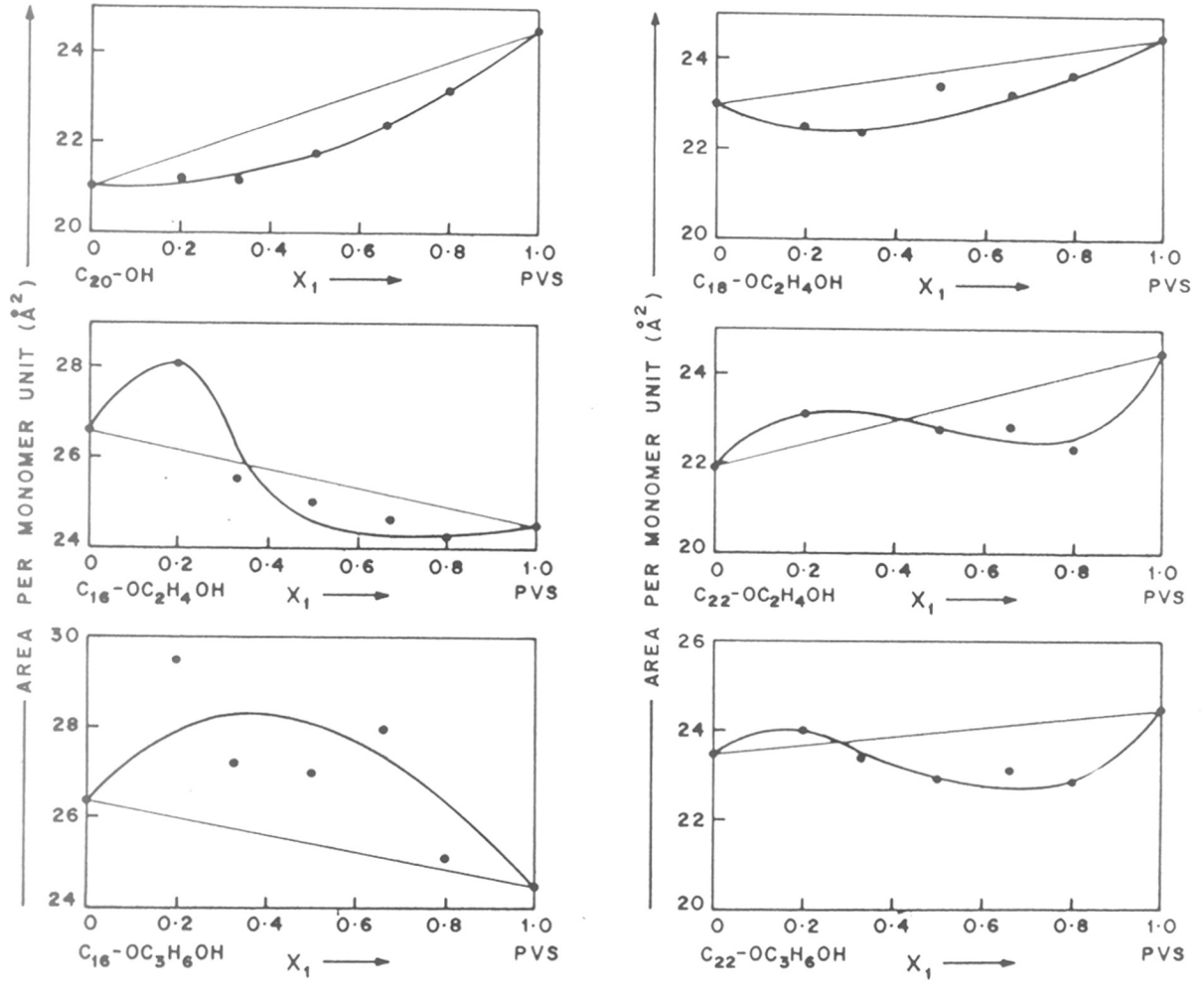

FIG. 4·7 : AREA PER MONOMER AGAINST MOLE FRACTION FOR DIFFERENT SYSTEMS AT 8 DYNES/CM.

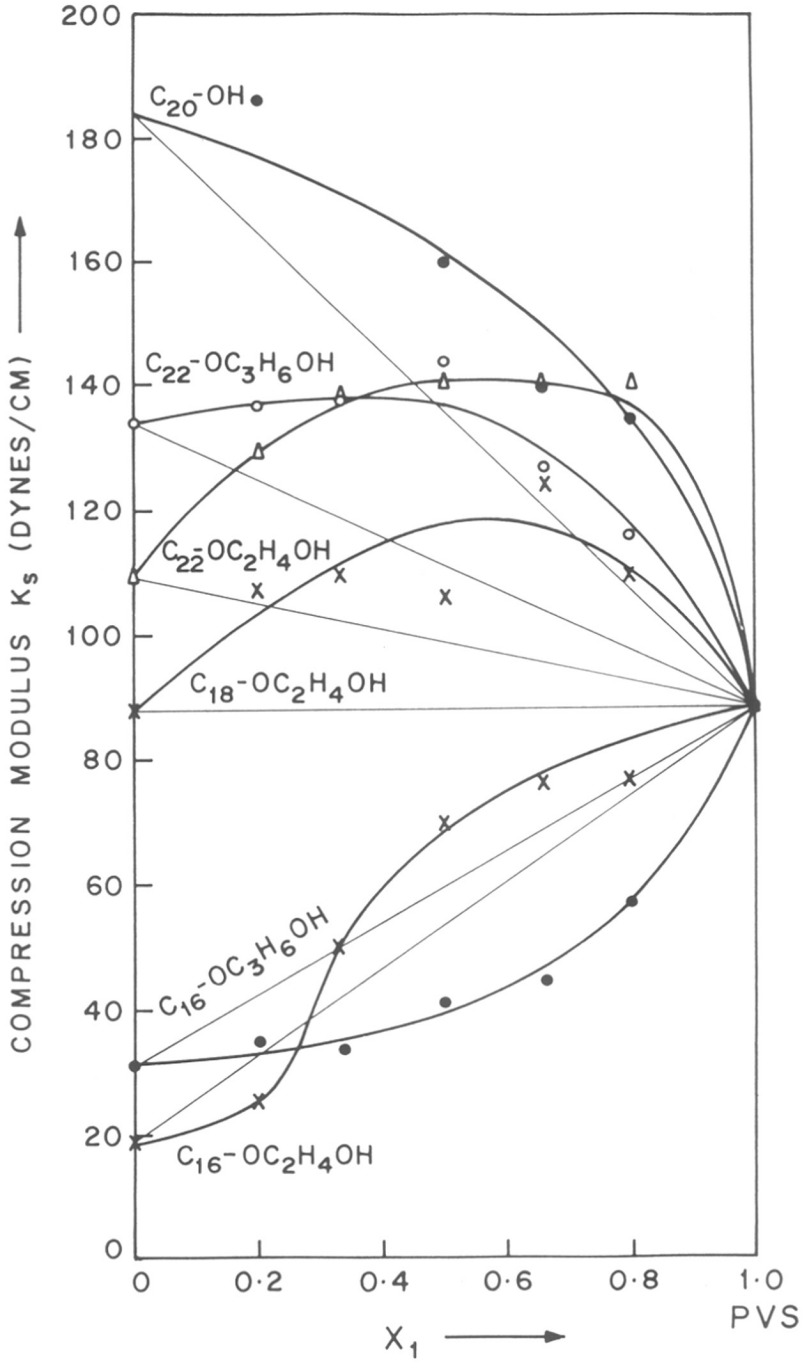

FIG. 4·8 : COMPRESSION MODULUS (K_s) AGAINST MOLE FRACTION.

where Ao is extrapolated area at zero pressure, A_1 is the smaller (than Ao) at surface pressure f_1. These curves show positive and negative deviations from ideal behaviour. The curves are complementary to A-x_1 curves; indicating mixing between the two components.

The values of compression modulus for PVS with n-long chain mixed monolayer systems are much lower as compared to those of mixed monolayers of n-long chain alcohols or alkoxy ethanol themselves. This means that polymer mixed monolayers are more compressible than those of only n-long chain mixed monolayers. This suggests that the polymer mixed films should be more stable than those of only n-long chain mixed monolayer towards the wind velocity. The miscibilities of n-long chain compounds with polymer monolayers may be explained as follows [56]: The PVS monolayer has low compression modulus even in condensed state as compared to long chain compounds (see Table I). This suggests that PVS monolayer has a large free area even in the condensed state. Therefore, when n-long chain compounds are mixed with PVS in monolayer state these molecules behave as solvents in two dimensional polymer solution and fill up the free areas of the polymer to achieve a homogeneous mixture.

TABLE I

Compression modulus and compressibilities of various n-long chain compounds and PVS in condensed state.

Compounds	Compression modulus K_s (dynes/cm)	Compressibility C_s (cm/dynes)
C_{20}-OH	1592.0	6.28×10^{-4}
C_{16}-OC_2H_4OH	500.0	2.00×10^{-3}
C_{18}-OC_2H_4OH	465.0	2.15×10^{-3}
C_{22}-OC_2H_4OH	4575.0	2.18×10^{-4}
C_{16}-OC_3H_6OH	675.0	1.48×10^{-3}
C_{22}-OC_3H_6OH	250.0	4.00×10^{-3}
PVS	112.8	8.86×10^{-3}

Excess free energy of mixing - mole fraction (ΔG^E-x_1) curves

The excess free energy of mixing (ΔG^E) has been calculated using Goodrich [64] treatment [Eqn.(3.9) in Chapter III]. The limitations of this treatment have already been discussed in Chapter III. However, in dealing with polymer mixed monolayers, the Goodrich theory gets more limitations. In the mixtures, one of the components being polymeric substance the equation cannot be directly used to evaluate the excess free energy of mixing. The mole fraction of the polymer component have been calculated based on molecular weight of the monomer unit. Therefore, as suggested by Fukuda et al.[56] the calculation of ΔG^E is only a rough approximation because it involves the assumption that each monomer unit behaves independently as a kinetic unit. However, many investigators have successfully interpreted the excess free energy of mixing values for such mixed monolayer systems [49,50,56,57,59].

In Fig. 4.9 the values of ΔG^E have been plotted against mole fraction, calculated by graphic integration of π-A isotherm upto 8 dynes/cm. All the systems show negative deviations from the ideal behaviour. The negativity is large in polymer rich region. This clearly indicates strong intermolecular interactions between the

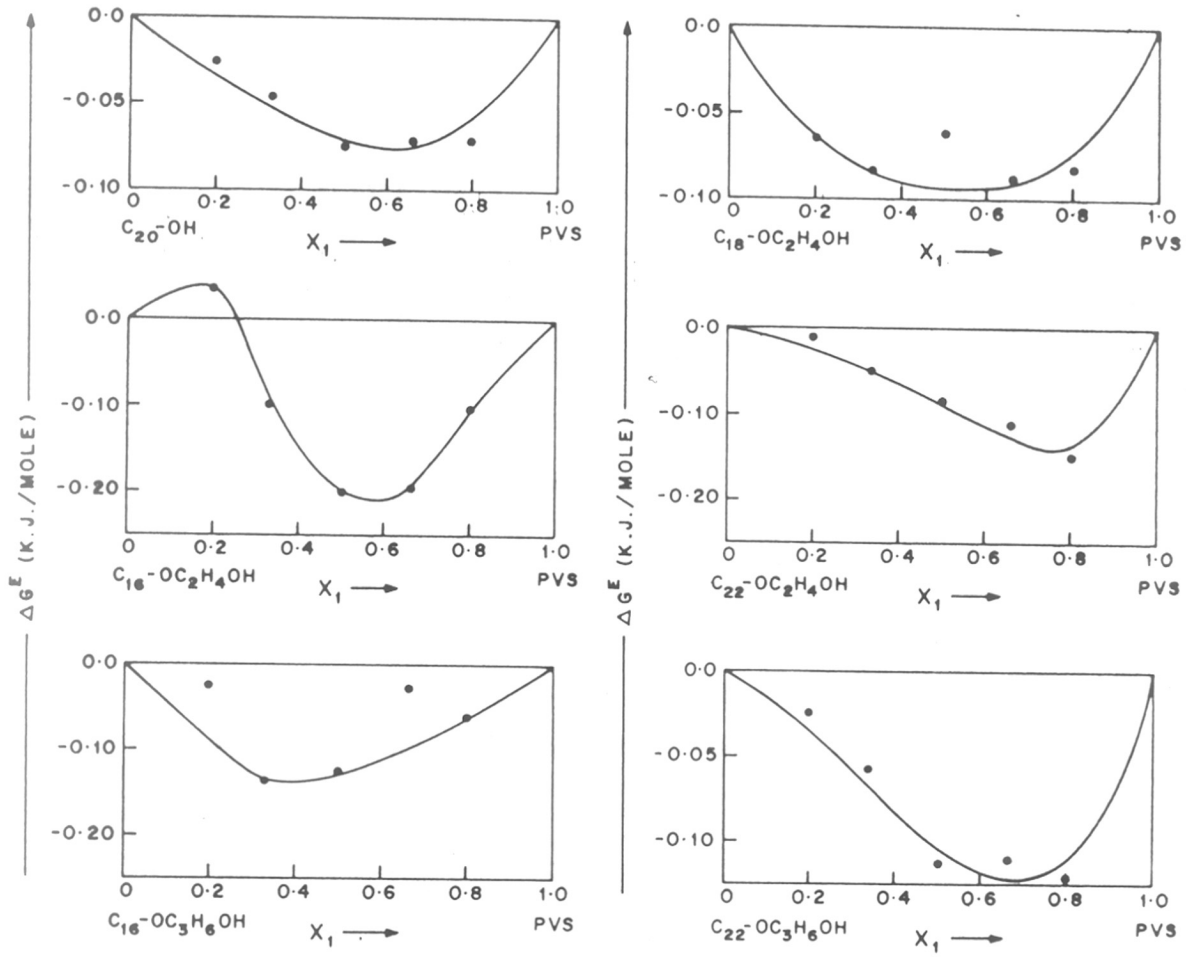

FIG. 4·9 : EXCESS FREE ENERGY OF MIXING FOR DIFFERENT SYSTEMS AT 8 DYNES / CM.

two components of the mixture; the resulting mixed monolayer is non-ideal and miscible at all the mole fractions.

The values of ΔG^{E} can be related to excess free energy of activation for a water molecule to escape through the monolayer ΔG^{*E} as suggested by Costin and Barnes [65].

$$\Delta G^{*E} = -K.\ \Delta G^{E} \qquad (4.3)$$

K being constant, depending on system to system.

The Eqn.(4.3) suggests that the mole fraction where maximum negative value of ΔG^{E} exist, should provide maximum resistance to a water molecule to escape through the monolayer. The mixed monolayers of PVS with n-alcohols, alkoxy ethanols and propanols are in fact, found to be good evaporation retardants in the semi-field experiments in our laboratory.

Collapse pressure-mole fraction curves (π_c-x_1)

The collapse pressures of all the mixed monolayers and the pure components were determined simultaneously with π-A isotherm. The collapse pressures have been plotted against mole fraction in Fig.4.10. The collapse pressures of all mixed monolayers are higher than the pure components indicating non-ideal behaviour and strong intermolecular

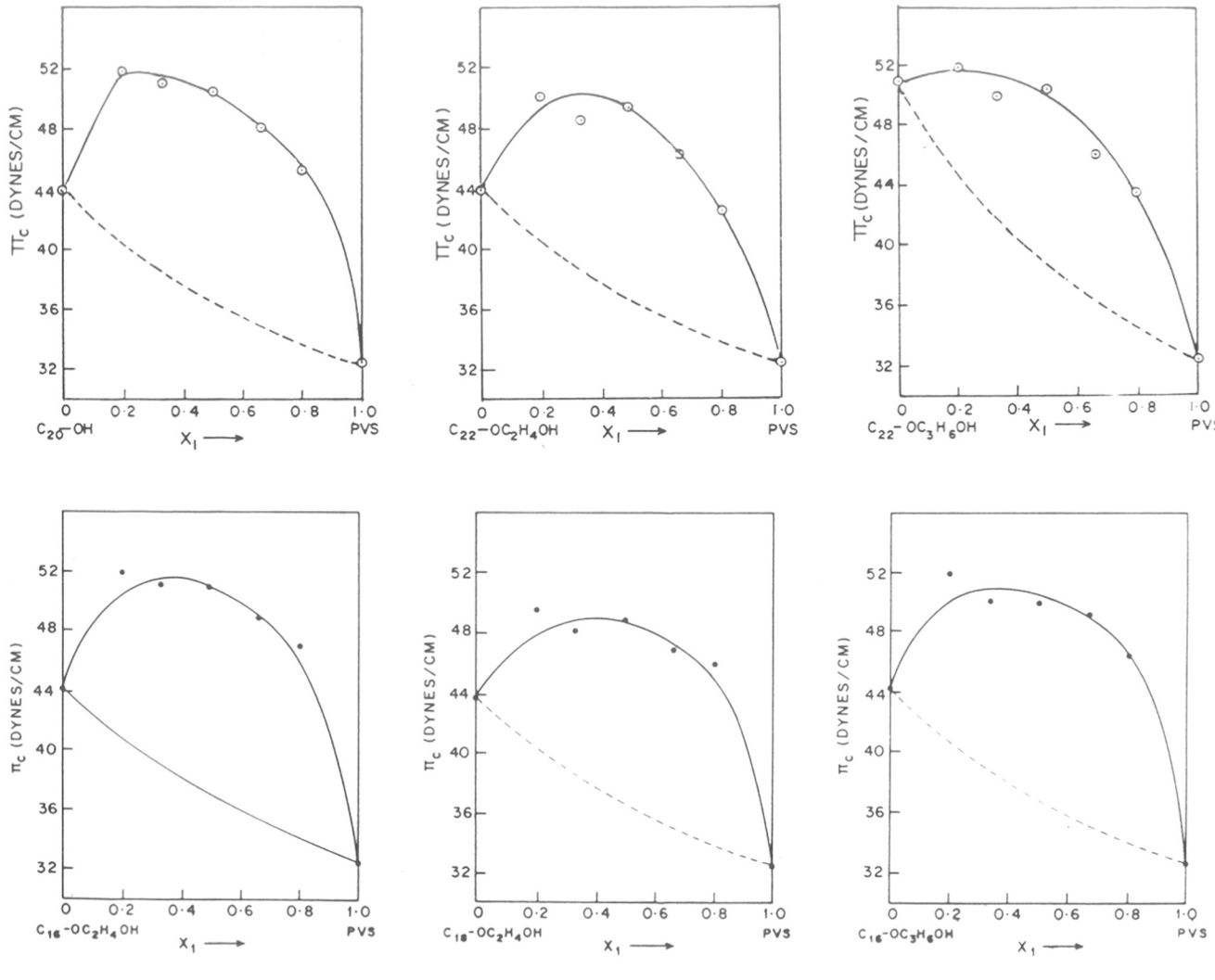

FIG. 4·10 : COLLAPSE PRESSURE (π_c) AGAINST MOLE FRACTION FOR VARIOUS SYSTEMS. THE DOTTED CURVE SHOWS IDEAL BEHAVIOUR FOR THE SYSTEMS ACCORDING TO JOOS THEORY.

interactions between the two components. In order to confirm non-ideal behaviour observed in these systems, we have adopted Joos [66] treatment and calculated $\pi_{c,m}$ values using equation (3.12) given in Chapter III. The calculated values of $\pi_{c,m}$ have been represented by broken curve in Fig. 4.10. It is very clear from the Fig. 4.10 that the mixed monolayers are miscible and non-ideal.

The various derived data from π-A isotherms considered above indicate that the mixed monolayers of PVS and n-long chain compounds exhibit miscibility and non-ideality. This observation is also supported by considering the thickness of the monolayer films.

If the density of the compound, mass* and area in which the film is spread are known then by considering the following simple relations, the thickness of film formed can be calculated.

Volume of the compound = mass/density

The above volume of compound is being spread in certain area

Volume = Area x thickness

Therefore, Area x thickness = mass/density

---

* Mass of the compound being spread can be known accurately by knowing the amount of solution delivered through Agla micrometer syringe.

Thus the thickness of the n-long chain compounds in condensed state have been obtained and tabulated in Table II along with that of PVS in condensed state. From the Table II it is seen that the thickness of PVS is comparable with that of n-long chain compounds. This indicates that there is scope for the interaction between PVS and n-long chain compounds.

From the Table II it is clear that the thickness of n-long chain compound is 6 to 7 times more than that of PVA_c indicating no scope for the mutual interactions between the two components. Thus the study of mixed monolayers of PVS with various n-long chain compounds form miscible and non-ideal films. These mixed monolayers are expected to act as stable water evaporation retardants because of higher collapse pressure.

The π-A isotherms of pure PVAc, C_{22}-OC_2H_4OH and the 1:1 molar ratio mixture have been plotted in the Fig.4.11. It is clear from the figure that the mixture shows two distinct collapse pressures indicating complete immiscibility of the two components. When surface pressure of the mixture reaches to collapse pressure of polymer component, it is completely squeezed out;what remains above that surface pressure is only the long chain component. However, Ries et al [52,53] have reported

TABLE II

Thickness of various monomolecular films in condensed state.

No.	Compound	Thickness (Å)
1	C_{20}-OH	30
2	C_{16}-OC_2H_4OH	30
3	C_{18}-OC_2H_4OH	32
4	C_{22}-OC_2H_4OH	36
5	C_{16}-OC_3H_6OH	30
6	C_{22}-OC_3H_6OH	36
7	PVS*	26
8	PVA_c*	5

* Ref. [47]

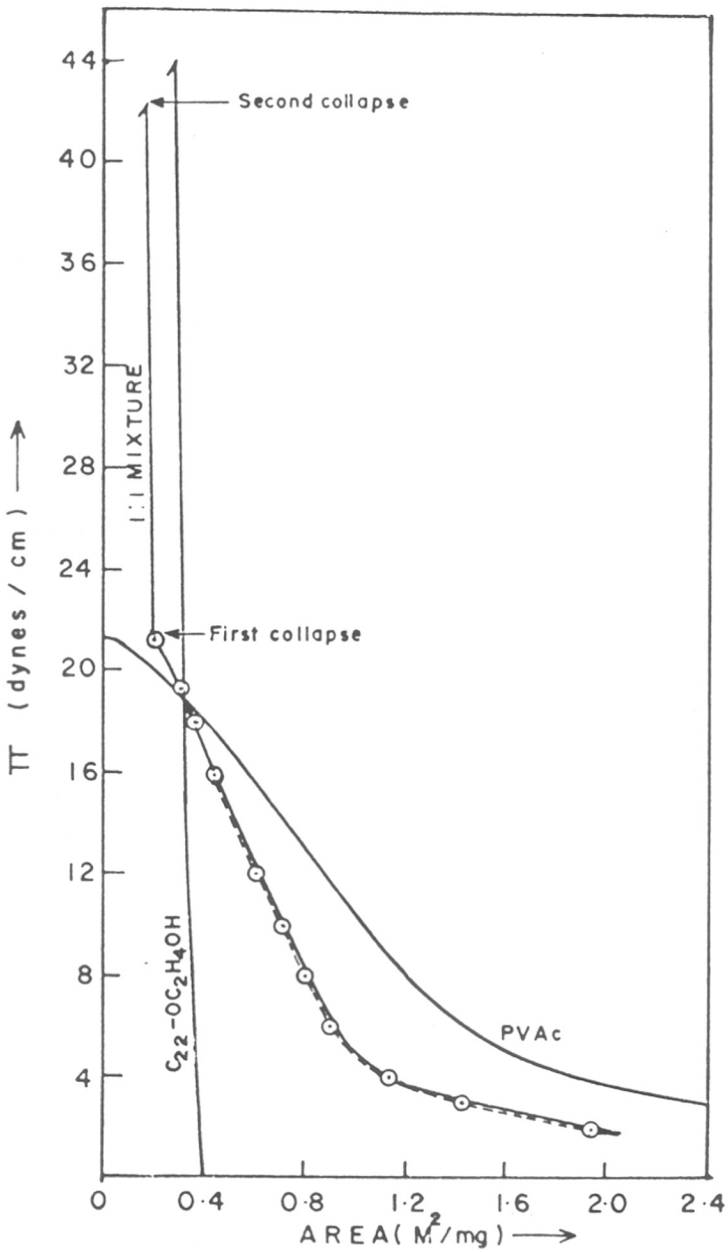

FIG. 4·11 : π – A ISOTHERMS OF PVA_c , C_{22}-OC_2H_4OH AND THEIR 1 : 1 RATIO MIXTURE. THE DOTTED CURVE SHOWS THE IDEAL BEHAVIOUR.

extremely high collapse pressure for the mixed monolayers of PVAc with stearic acid, n-hexacosanoic acid, n-hexatriacontanoic acid and 2-hydroxy stearic acid. The higher collapse pressures may be due to intermolecular hydrogen bonding which is possible between -COOH groups. The mixed monolayers of PVA_c with methyl stearate, 1-octadecanol, cholesterol [52] and in the present study with C_{22}-OC_2H_4OH, the collapse pressures are of the same order since intermolecular hydrogen bonding is not possible with -OH groups.

As discussed earlier, the comparison of thickness of PVA_c with n-long chain compounds indicate no scope for the intermolecular interactions. Therefore, the mixed monolayers of PVA_c with n-long chain compounds are immiscible.

The thread like polymers lie flat on the water surface; the polar groups are hydrogen bonded with water molecules. Such type of polymers are called as "horizontally oriented" e.g. polyvinyl acetate, polymethyl acrylate, polymethyl methacrylate etc. If a polymer has a n-alkyl long chain in the monomer unit; the polymer chain lies flat on the water surface but the n-alkyl long chain orients itself vertical to the interface, such polymers are called as "vertically oriented" e.g. polyvinyl stearate, polyoctadecyl methacrylate etc. The orientation of polyvinyl

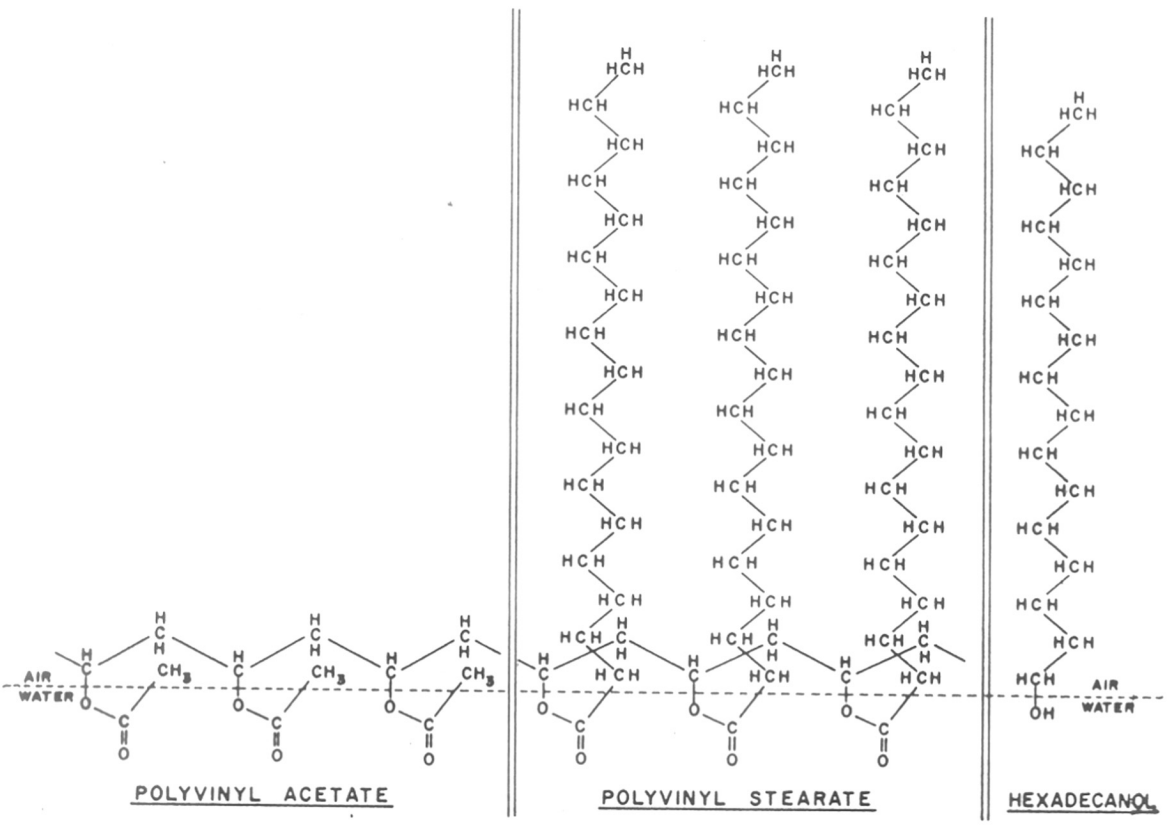

FIG. 4·12 : MOLECULAR ORIENTATION AT AIR-WATER INTERFACE.

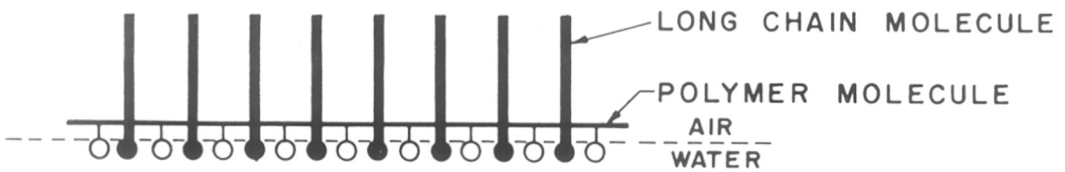

HORIZONTAL - VERTICAL ORIENTATION

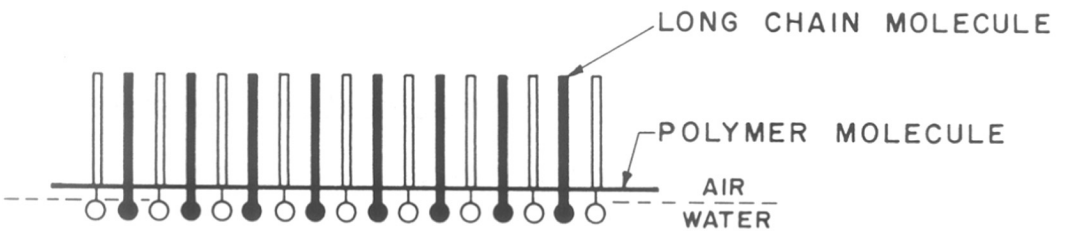

VERTICAL - VERTICAL ORIENTATION

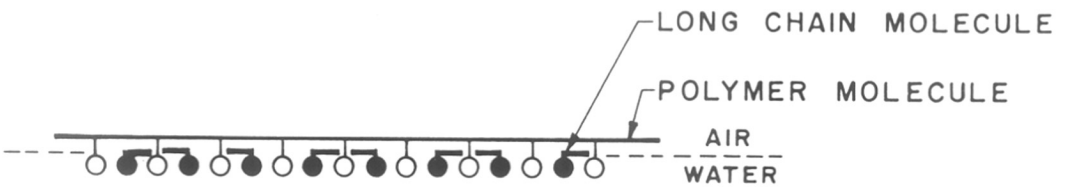

HORIZONTAL - HORIZONTAL ORIENTATION

FIG. 4·13 : SCHEMATIC REPRESENTATION OF DIFFERENT TYPES OF MIXED MONOLAYERS AT AIR - WATER INTERFACE.

acetate, polyvinyl stearate and hexadecanol at the air-water interface has been shown in Fig. 4.12. The schematic representation of orientation and compatibility in mixed monolayers of vertical-vertical, vertical-horizontal and horizontal-horizontal has been shown in Fig. 4.13. Thus our data also supports Gabrielli et al.[45-47] about the compatibility in mixed monolayers due to different orientations.

Comments on units of area

During the study on mixed monolayers of polymers with n-long chain compounds we have done some interesting observations on the units of area in π-A isotherms. In plotting the π-A isotherms (and therefore A-x_1 plots) the area can be expressed in two ways (i) square meters per milligram (M^2/mg) and (ii) square angstroms per monomer unit ($\AA^2$/monomer unit). If A-x_1 of a mixed monolayer system in both units are compared, the systems which look ideal compatible or incompatible in M^2/mg may become completely non-ideal and compatible in the $\AA^2$/monomer unit. A H-V type of system; which in fact should show incompatibility* in A-x_1 plots, shows complete compatibility and non-ideality if the area in A-x_1 plots are expressed

---

* while saying "compatible" or "incompatible" it is assumed that we are referring to only those systems where the film forming molecules have non-ionizable polar groups. In such systems rule of similar orientation for compatible systems is valid.

in $\mathring{A}^2$/monomer unit. These observations have been noticed from the present data and from the literature as well (see Fig. 4.14).

The figures 4.15 and 4.16 give the π-A isotherms of PVA_c + C_{22}-OC_2H_4OH system and PVA_c + stearic acid (SA) at 1:1 ratio along with pure components in two different plottings corresponding to area expressed in M^2/mg and $\mathring{A}^2$/ monomer unit. The dotted curves in both figures indicate the ideal behaviour of the system calculated from pure components using following equation.

$$A_{12} = x_1A_1 + x_2A_2 \qquad (4.4)$$

When area are expressed in M^2/mg, the calculated ideal curve and the experimental curve match exactly; indicating the system is either ideal compatible or incompatible. However, if the areas are expressed in $\mathring{A}^2$/monomer unit the experimental curve shows considerable deviation from the calculated ideal curve. Naturally, one should conclude that the system is non-ideal and miscible. The same fact is observed if the system PVA_c + SA reported by Ries et al.[53] is converted into $\mathring{A}^2$/monomer unit. However, the fact that two collapse pressures are observed in both plottings; which gives clear indication of immisible behaviour. The

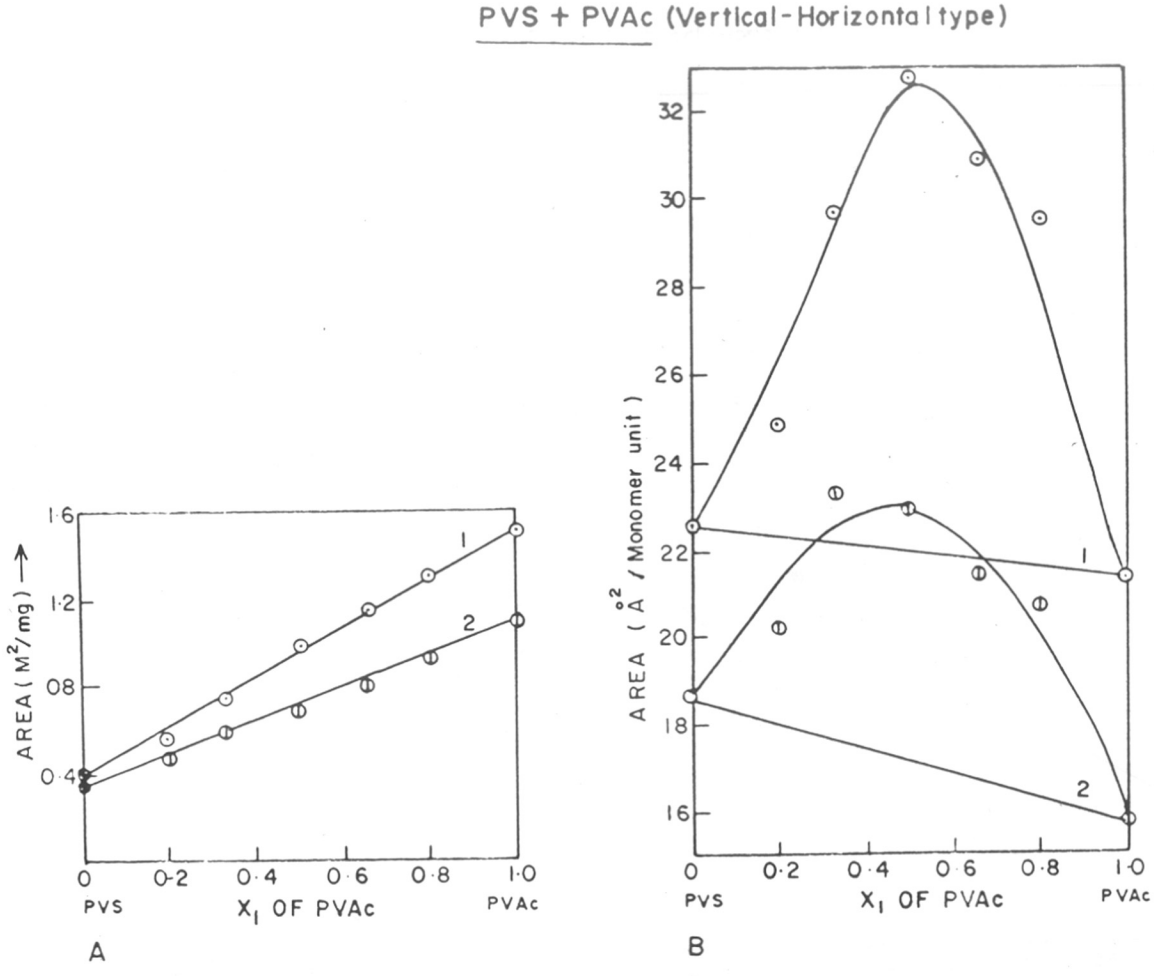

FIG. 4·14 : AREA AGAINST MOLE FRACTION PLOTS FOR PVS + PVAc SYSTEM. PART A : AREA IN M^2/MG. PART B : AREA IN $Å^2$/MONOMER UNIT. CURVE 1 & 2 AT 3 & 8 DYNES/CM. DATA HAVE BEEN TAKEN FROM REF. [47].

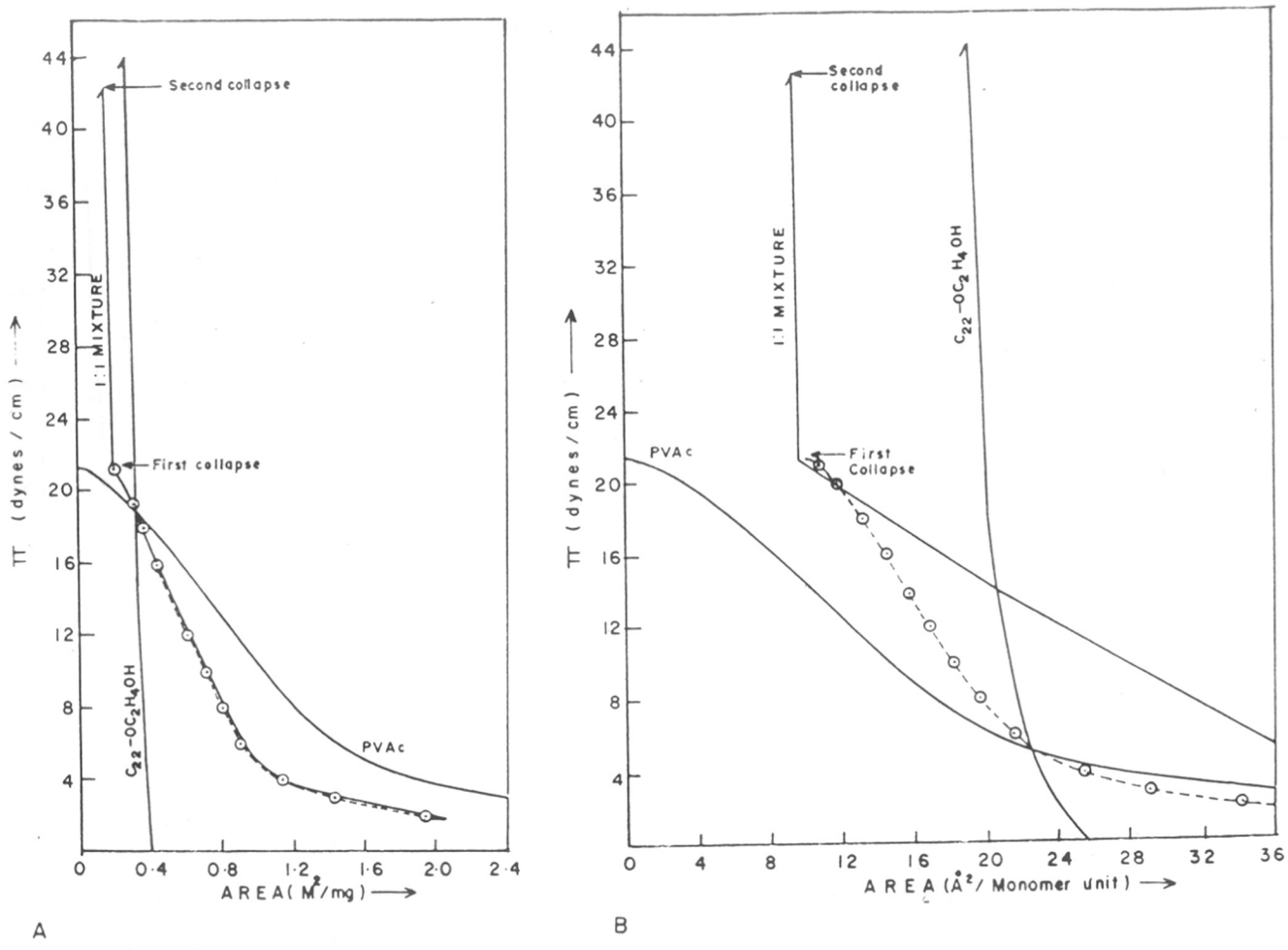

FIG. 4·15 : π - A ISOTHERMS OF $C_{22}-OC_2H_4OH$, PVAc AND 1 : 1 MIXTURE AT 25°C. THE DOTTED CURVE INDICATE THE IDEAL BEHAVIOUR. PART A : AREA IN M^2/MG. PART B : AREA IN Å^2 PER MONOMER UNIT.

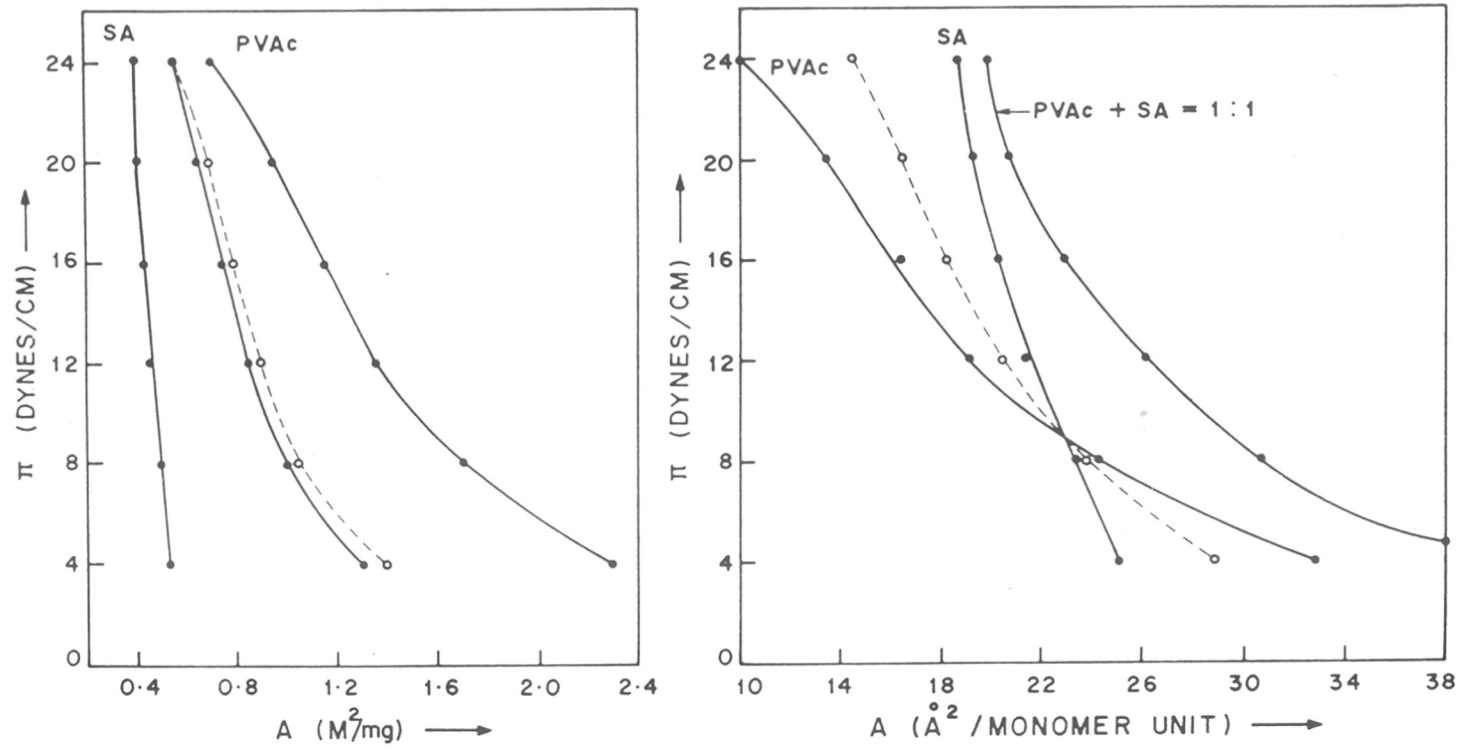

FIG. 4·16 : π-A ISOTHERMS OF STEARIC ACID, POLYVINYL ACETATE AND THEIR MIXTURE IN TWO DIFFERENT UNITS OF AREA DATA FROM REF. [53].

following points will help to understand the apparent increase in area when area is expressed in $\AA^2$/monomer unit.

The polymer component is horizontally oriented and the n-long chain is vertically oriented, therefore there is no chance for chain-chain interactions between two components (Compare the thickness of two films from Table II and also see Figs. 4.12 and 4.13). The Figs. 4.15 and 4.16 indicate that the apparent deviation from ideal behaviour is more at low pressures than at high pressures. At low pressures, the polymer chains and long chain molecules are randomly oriented at the interface. Because of the hindrance of polymer chains, the long chain molecules cannot come closer and the average area per monomer unit increases. Such type of apparent increase due to steric hindrance of bulky molecules has been pointed out by Shah and Capps [67]. As the surface pressure increases the difference in area (between expected and observed) decreases. At the collapse pressure of polymer component (first collapse), the experimental area equals to the calculated average area.

In case of V-V and H-H types of mixtures also, in some systems, the observer is confused when the A-x_1 plots in two different units are compared.

The Fig. 4.17 gives the plots of A-x_1 curves for PVS + C_{20}-OH (V-V) system at three surface pressures in

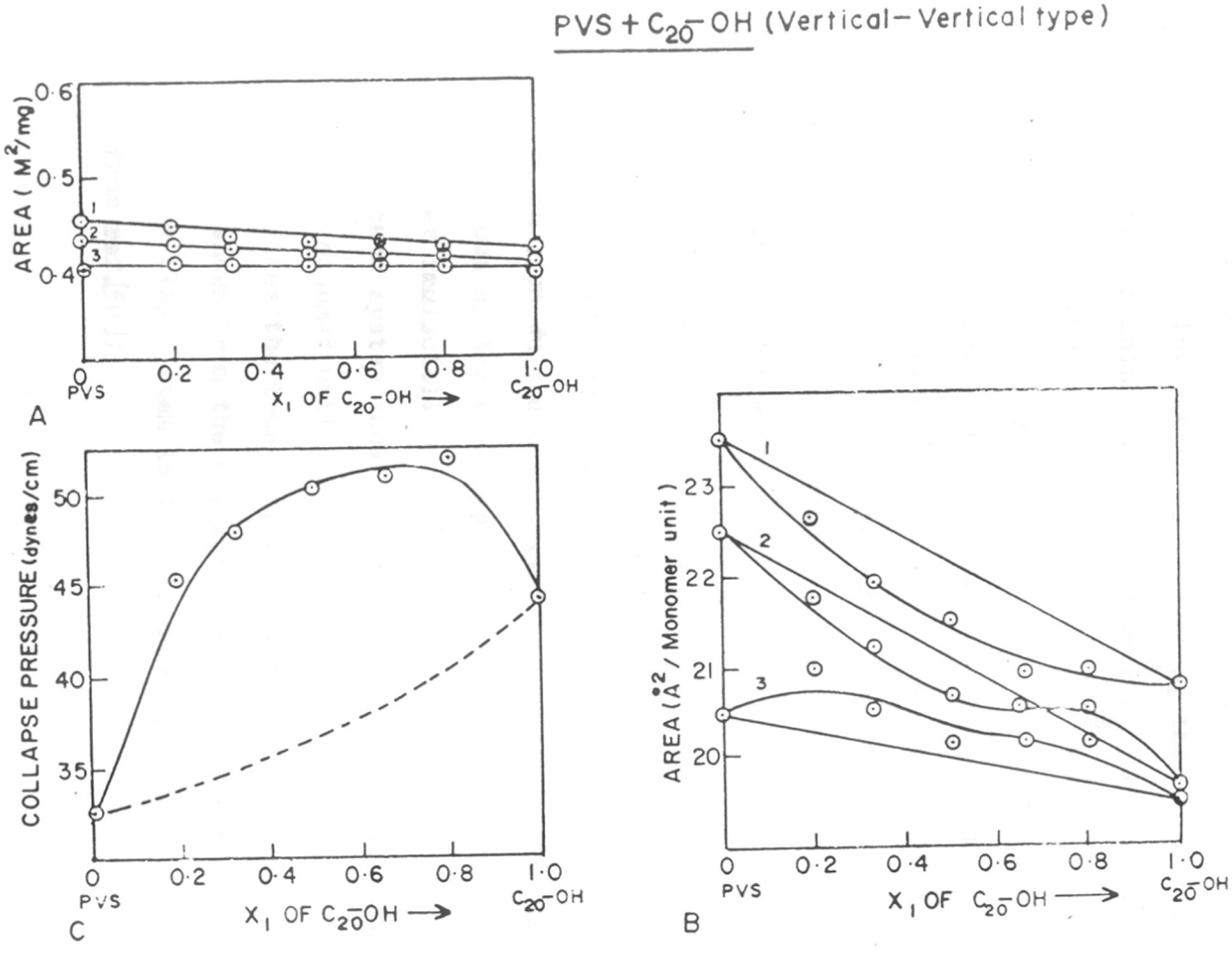

FIG. 4·17 : AREA AGAINST MOLE FRACTION PLOTS FOR PVS + C_{20}-OH SYSTEM. PART A : AREA IN M^2/MG . PART B : AREA IN $Å^2$/MONOMER UNIT . PART C : $\pi_c - X_1$. CURVE 1, 2 & 3 AT 12 , 18 & 30 DYNES/CM .

M^2/mg and in $\mathring{A}^2$/monomer unit. The A-x_1 curves in M^2/mg are seen to be additive at all mole fractions and at all the pressures, suggesting that the system is either immiscible or ideal miscible. On the other hand, when the same system is plotted in $\mathring{A}^2$/monomer unit the A-x_1 plots clearly show negative and positive deviations from ideal behaviour indicating non-ideal and miscible behaviour. Therefore, to avoid the confusion one has to consider the collapse pressure data, which clearly differentiates between immiscible, ideally miscible and non-ideal systems.

In Fig. 4.18 the A-x_1 plots for the mixed monolayers of polymethyl methacrylate (PMMA) + PVA_c (H-H) in two different plottings is shown. The data has been taken from Wu and Hutsberger [49]. As observed in previous system (V-V type), the plots in M^2/mg suggest either immiscible or ideal miscible behaviour, however, the same system shows non-ideal and miscible behaviour in $\mathring{A}^2$/monomer unit plots. Here also the collapse pressure data gives the true picture. Puggelli and Gabrielli [50] have shown from the collapse pressure data that the PMMA + PVA_c system is ideally miscible (see Fig.1 from ref.[50]).

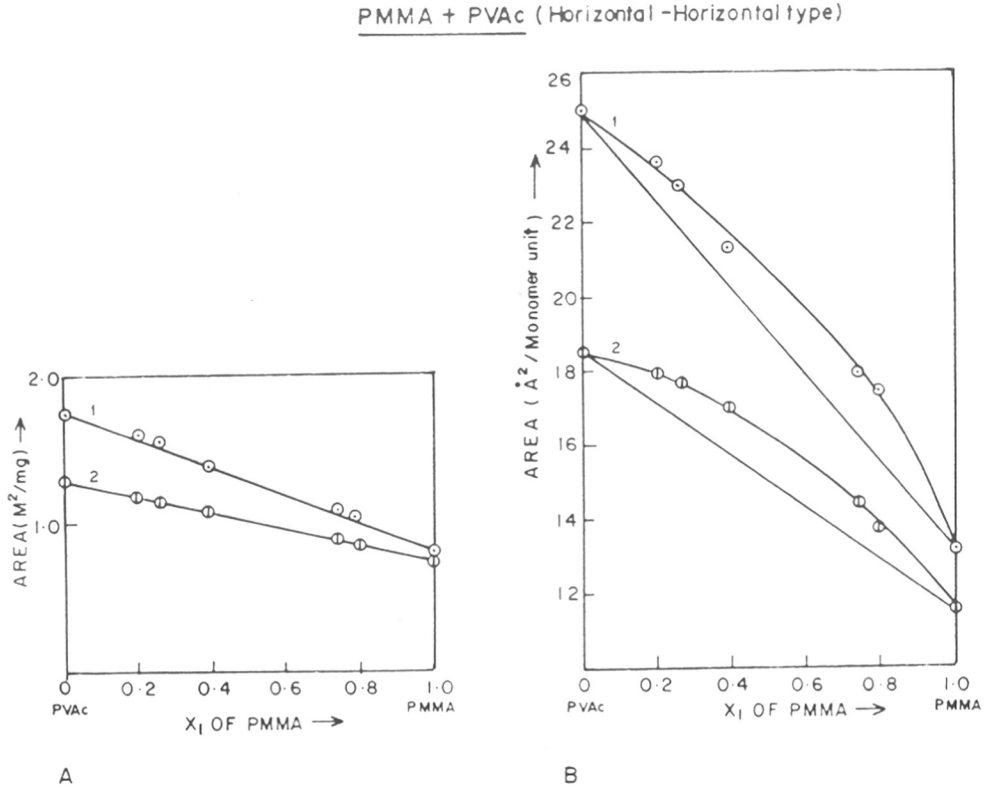

FIG. 4·18 : AREA AGAINST MOLE FRACTION PLOTS FOR PMMA + PVAc SYSTEM. PART A : AREA IN M^2/MG. PART B : AREA IN $Å^2$/MONOMER UNIT. CURVE 1 & 2 AT 5 & 10 DYNES/CM. DATA HAVE BEEN TAKEN FROM REF. [49].

All the above discussion suggest that the $A\text{-}x_1$ curves do not give the true picture of the behaviour of the system. In polymer mixed monolayers, the phase transitions are not observed, therefore, one has to have the measurements on the collapse pressures of mixed monolayers to get the exact idea about the behaviour of the system. The importance of collapse pressure has also been recognized by Gabrielli and his co-workers [68,69].

CONCLUSIONS

1) The mixed monolayers of polyvinyl stearate with n-long chain alcohol, alkoxy ethanols and propanols are found to be miscible and non-ideal. On the other hand the mixed monolayer of polyvinyl acetate with n-long chain compound is found to be immiscible. Thus our study supports the views of Gabrielli and his co-workers regarding the orientation and compatibility in mixed monolayers where both the components have non-ionizable polar groups.

2) The mixed monolayers of polyvinyl stearate with various n-long chain compounds are expected to be better water evaporation retardants than pure components because of strong intermolecular interactions.

3) It is shown that the collapse pressure against mole fraction curves give the correct behaviour of the system (miscible, immiscible) rather than the area against mole fraction curves.

REFERENCES

1. D.J. Crisp, J.Colloid Sci. 1 (1946) 49 and 161.

2. D.J. Crisp, Surface Phenomena in Chemistry and Biology, eds. J.F. Danielli, K.G.A. Pankhurst and A.C. Riddiford, Pergamon Press (1958) p.23.

3. See the cross ref. "Katz and Samwell (1929a, 1929b)" from ref. 2

4. N.K. Adam, Trans.Faraday Soc. 29 (1933) 90.

5. J.B. Harding and N.K. Adam, Trans.Faraday Soc. 29 (1933) 837.

6. S.E. Sheppard and R.L. Keenan, Nature (London) 121 (1928) 982.

7. See the cross ref. "Katz and Samwel (1928)" from ref .2

8. S.A. Moss, J.Am.Chem.Soc. 56 (1934) 41.

9. W.D. Harkins, E.F. Carman and H.E. Ries, J.Chem.Phys. 3 (1935) 692.

10. N.K. Adam, The Physics and Chemistry of Surfaces 3rd ed., Oxford (1941).

11. S.J. Singer, J.Chem.Phys. 16 (1948) 872.

12. J.T. Davies and J. Llopis, Proc.Roy.Soc.(London) A227 (1955) 537.

13. J.T. Davies, J.Colloid Sci. 9 Suppl.1 (1954) 9.

14. T. Kawai, J.Polym.Sci. 35 (1959) 401.

15. H.L. Frisch, R. Simha and F.R. Eirich, J.Chem.Phys. 21 (1953) 365.

16. T. Isemura, H. Hotta and T. Miwa, Bull.Chem.Soc.Jpn. 26 (1953) 380.

17. H. Hotta, Bull.Chem.Soc.Jpn. 26 (1953) 386.

18. H. Hotta, Bull.Chem.Soc.Jpn. 27 (1954) 80 and 412.

19. T. Isemura, H. Hotta and S. Otsuka, Bull.Chem.Soc.Jpn. 27 (1954) 93.

20. H. Hotta, Bull.Chem.Soc.Jpn. 28 (1955) 64.

21. H. Hotta, J.Colloid Sci. 9 (1954) 504.

22. J. Parker and J.L. Shereshefsky, J.Phys.Chem. 58 (1954) 850.

23. J. Llopis and D.V. Rebollo, J.Colloid Sci. 11 (1956) 543.

24. T. Tachibana and K. Inokuchi, J.Colloid Sci. 8 (1953) 341.

25. K. Motomura and R. Matuura, J.Colloid Sci. 18 (1963) 52.

26. J. Llopis and J.A. Subirana, J.Polym.Sci. 60 (1962) 113.

27. M.L. Huggins, Macromol Chem. 87 (1965) 119.

28. G. Gabrielli and M. Puggelli, J.Appl.Polym.Sci. 16 (1972) 2427.

29. J.M. Hammond, M.H. Williams and W.G.P. Robertson, Nature (London) 189 (1961) 549.

30. T. Nakahra, K. Motomura and R. Matuura, Bull.Chem.Soc.Jpn. 40 (1967) 495.

31. K.S. Korgaonkar and S.V. Joshi, Radiation Res. 35 (1968) 213.

32. N.L. Jarvis, J.Colloid Interface Sci. 29 (1969) 647.

33. K. Nakamae, T. Takeya, Y. Fujimura, I. Sakai and T. Matsumoto, J.Macromol.Sci.-Phys. B21 (1982) 157.

34. M. Breton, J.Macromol.Sci.-Rev.Macromol Chem. C21 (1981) 61.

35. G. Gabrielli and M. Puggelli, J.Colloid Interface Sci. 37 (1971) 503.

36. G. Gabrielli and G.G.T. Guarini, J.Colloid Interface Sci. 64 (1978) 185.

37. P. Baglioni, G. Gabrielli and G.G.T. Guarini, J.Colloid Interface Sci. 78 (1980) 347.

38. G. Gabrielli, P. Baglioni and E. Ferroni, J.Colloid Interface Sci. 81 (1981) 139.

39. J.C.H. Hwa and H.E. Ries Jr. J.Polym.Sci. Part B. Polym.Lett. 2 (1964) 389.

40. H.C. Saraswat and A. Kalyansundaram, J.Polym.Sci. Z (1951) 325.

41. A. Blumstein and H.E. Ries Jr. J.Polym.Sci. Part B. Polym.Lett. 3 (1965) 927.

42. T. Nakahara, K. Motomura and R. Matuura, J.Polym.Sci.A-2 4 (1966) 649.

43. G. Gabrielli, M. Puggelli and E. Ferroni, J.Colloid Interface Sci. 33 (1970) 133.

44. W.M. Lee, J.L. Shereshefsky and R.R. Stromberg, J.Res.Natl.Bur.Stand A65 (1961) 51.

45. G. Gabrielli and A. Maddii, J.Colloid Interface Sci. 64 (1978) 19.

46. G. Gabrielli, P. Baglioni and A. Maddii, J.Colloid Interface Sci. 79 (1981) 268.

47. G. Gabrielli, M. Puggelli and P. Baglioni, J.Colloid Interface Sci. 86 (1982) 485.

48. G. Gabrielli, M. Puggelli and E. Ferroni, J.Colloid Interface Sci. 48 (1974) 145.

49. S. Wu and J.R. Huntsberger, J.Colloid Interface Sci. 29 (1969) 138.

50. M. Puggelli and G. Gabrielli, J.Colloid Interface Sci. 61 (1977) 420.

51. G. Gabrielli and P. Baglioni, J.Colloid Interface Sci. 73 (1980) 582.

52. H.E. Ries Jr. and D.C. Walker, J.Colloid Sci. 16 (1961) 361.

53. H.E. Ries Jr., R.A. Ahlbeck and J. Gabor, J.Colloid Sci. 14 (1959) 354.

54. G. Gabrielli, J.Colloid Interface Sci. 53 (1975) 148.

55. A.A. Trapeznikov and M.A. Kolobov, Colloid J.USSR 44 (1982) 244.

56. K. Fukuda, T. Kato, S. Machida and Y. Shimizu, J.Colloid Interface Sci. 68 (1979) 82.

57. G. Gabrielli, M. Puggelli and R. Faccioli, J.Colloid Interface Sci. 37 (1971) 213.

58. A. Labbauf, J.Appl.Polym.Sci. 10 (1966) 865.

59. G. Gabrielli, M. Puggelli and R. Faccioli, J.Colloid Interface Sci. 41 (1972) 63.

60. G. Fabrielli and P. Baglioni, J.Colloid Interface Sci. 83 (1981) 221.

61. A. Labbauf and J.R. Zack, J.Colloid Interface Sci. 35 (1971) 569.

62. M. Puggelli and G. Gabrielli, Colloid Polym.Sci. 261 (1983) 82, 166 and 667.

63. D.A. Cadenhead and F. Muller-Landau, J.Colloid Interface Sci. 78 (1980) 269.

64. F.C. Goodrich, Proc.2nd.Int.Congr.Surf.Activity, Butterworth, London, 1 (1957) 85.

65. I.S. Costin and G.T. Barnes, J.Colloid Interface Sci. 51 (1975) 122.

66. P. Joos, Bull.Soc.Chim.Belges 78 (1969) 207.

67. D.O. Shah and R.W. Capps, J.Colloid Interface Sci. 27 (1968) 319.

68. G. Gabrielli, P. Baglioni and A. Fabbrini, Colloids and Surfaces 3 (1981) 147.

69. P. Baglioni, E. Gallori, G. Gabrielli and E. Ferroni, J.Colloid Interface Sci. 88 (1982) 221.

APPENDIX I

PREPARATION AND PURIFICATION OF n-LONG CHAIN ALCOHOLS, ALKOXY ETHANOLS AND PROPANOLS.

Monolayer properties are very sensitive to the purity of the compounds used. It is therefore, necessary to make sure that the compounds used are pure of the order of 99%. With this view, the preparation and purification procedures followed have been described in the following:

1) n-LONG CHAIN ALCOHOLS

a) Hexadecanol and eicosanol:

Commercially available, Fluka make, best quality alcohols have been rigorously purified by repeated crystallizations from dry acetone. Further, the samples were subjected to acetylation using 2 moles of pure acetic anhydride in the presence of 1.5 moles of unhydrous sodium acetate (BDH). The acetate of the alcohol was purified by fractional distillation in an efficient column. The middle fraction which distilled at constant temperature and gave a single peak on gas chromatogram was deacetylated by refluxing with 2N alcoholic KOH and distilled under vacuum. The purity of these compounds was checked after several crystallizations on gas chromatogram and was found to be better than 99.8%.

b) Docosanol (Behenyl alcohol)

It was obtained by alcoholysis of refined mustered oil,

using ethyl alcohol containing sulfuric acid as catalyst to convert fatty acid to ethyl esters. These esters were fractionated by vacuum distillation and the last fraction comprised of ethyl behenate was hydrolised at 250°C in the presence of copper chromite catalyst and hydrogen pressure greater than 200 kg/cm^2. The alcohol obtained was hot filtered and distilled under vacuum. This alcohol was found to be 95% pure. Further purification was carried out as mentioned above for other alcohols. The final product obtained after following the purification procedure was found to be better than 99.8%.

2) n-LONG CHAIN ALKOXY ETHANOLS AND PROPANOLS

The method consists of condensing the alkyl bromide with mono-sodium glycolate. The dry and pure HBr was bubbled into pure alcohol heated to 110°C. The bromide was extracted with petroleum ether and was made free from unreacted alcohol by sulphation followed by washing of alcohol sulphate with methanol and subsequently with distilled water, after neutralising the reaction mixture with aqueous ammonia. The bromide was removed by stripping with petroleum ether and was purified by vacuum distillation. The pure alkyl bromide, thus obtained, was condensed with mono-sodium glycolate obtained by adding requisite amount

of sodium to large excess of ethylene glycol. The reaction temperature was varied from 140 to 180°C and reaction time from 70 to 100 hours depending on the chain length of the alkyl bromide. The product was extracted with petroleum ether. The part of the reaction product soluble in petroleum ether contained ethylene glycol mono-alkyl ether (i.e. n-alkoxy ethanol) along with dialkyl ether and 1-alkenes. The alkenes distilled over as a first liquid fraction, middle fraction contained the major component i.e. monoether while diether remained as residue in the reaction flask. The monoethers were crystallised several times from petroleum ether (60-80°C). The purity of the compounds were checked on gas chromatogram and were found to be 99.9% pure.

The procedure for n-alkoxy propanols remains the same as described above except that mono-sodium salt of 1,3-propane diol should be used instead of monosodium glycolate. Here again the purity obtained for the final product viz. n-long chain propanols was found to be 99.9%.

TABLE

Compounds	Melting points °C
C_{16}-OH	49.6
C_{20}-OH	64.1
C_{22}-OH	71.0
C_{16}-OC_2H_4OH	42.7
C_{18}-OC_2H_4OH	51.0
C_{22}-OC_2H_4OH	64.3
C_{16}-OC_3H_6OH	41.7
C_{22}-OC_3H_6OH	62.8

APPENDIX II

Dimensions of the various equipments needed for the Langmuir film pressure balance (all dimensions are in mm.)

	Description		Quantity
1)	Wooden table (heaviest possible) of the size 1250 (L) X 750(W) X 750(H)	..	One
2)	Angle iron stands of the size		
	i) 900(L) X 900(W) X 1400(H)	..	Two
	ii) 1400(L) X 600(W) X 850(H)	..	One
3)	Langmuir trough of perspex or teflon size: 700(L) X 170(W) X 30(H) outer dimensions 680(L) X 150(W) X 20(H) inner dimensions	..	One
4)	A suitable wooden case for the trough	..	One
5)	Glass casing with one side sliding door all glasses should be easily removable size: 1100(L) X 600(W) X 540(H)	..	One
6)	Langmuir film balance (see the Fig.2.1)	..	One
7)	Mica or teflon sheets of the size: (to cut float and rings of viscometer) 300(L) X 300(W) X 0.15 (thickness)	..	Six
8)	Reflecting mirror (diameter 7 mm)	..	Six
9)	Barriers of perspex or teflon 220(L) X 10(W) X 10(H)	..	Six

10)	Rectangular brass rods (220(L) X 10(W) X 10(H) (to be fixed to barriers for getting rigidity)	..	Six
11)	Teflon ribbon roll of 20 mm width	..	Two
12)	Thermometer of the range 0-50°C with 0.1°C accuracy.	..	Two
13)	Thermostat having constant temperature water.	..	One
14)	Water circulating pump of 1/8th H.P.	..	One
15)	Glass serpentine coil of suitable size of the trough (3-5 mm inner diameter)	..	One
16)	Brass levelling screws	..	Three
17)	Lamp and scale arrangements	..	Four
18)	Rubber tubes of various diameters	..	1 mtr.each

Surface Viscometer (dimensional details with respect to the Fig. 2.2). (All dimensions are in mm.)

1)	Length of the stainless steel tube (p)	=	400.0
2)	Length of the stainless steel tube (F)	=	370.0
3)	Diameter of stainless steel tube (id) (F)	=	35.0
4)	Diameter of stainless steel tube (id) (p)	=	15.0
5)	Length of brass rods (b')	=	57.0
6)	Length of brass rods (a')	=	34.0
7)	Diameter of brass disc (K)	=	64.0
8)	Diameter of brass disc (K')	=	39.0

9) Brass strips at right angles; $x_1x_2 = y_1y_2$ = 118.0

10) Length of the phosphor bronze wire (e) = 650.0

11) Diameter of phosphor bronze wire (e) = 0.17

12) Diameter of the reflecting mirror (m) = 7.0

13) Inner diameter of outer mica ring (d) = 103.0

14) Outer diameter of inner mica ring (b) = 63.0

15) Diameter of mica disc (unwaxed) (c) = 96.0

16) Diameter of mica disc (waxed) (a) = 42.0

17) Thickness of the mica disc/ring = 0.15

Refer the Fig. 2.3

Top portion of the viscometer

The inner stainless steel tube (p) is levelled with the help of three levelling screws resting on a triangular brass platform (T). The height of triangular brass platform (T) from the angle iron stand = 90.0; Length of the triangular platform (all sides equal) X = 100.0; The phosphor bronze wire is suspended from a screw (S) at the top. This screw has been fixed to another threaded screw (L) on a stand for adjusting the height of the wire.

The outer stainless steel tube (F) is fixed through worm gear (w) to a synchronous motor having gear system (14). The gear system enables to vary the speed of the outer stainless steel tube (F) (and therefore of the inner mica ring (b)) from 1 RPM to 12 RPM.

BIBLIOGRAPHY

1. N.K. Adam, "The Physics and Chemistry of Surfaces" 3rd edn. Oxford University Press, London, 1941.

2. W.D. Harkins, "The Physical Chemistry of Surface Films" Reinhold, New York, 1952.

3. J.T. Davies and E.K. Rideal, "Interfacial Phenomena", Academic Press, New York, 1961.

4. L.I. Osipow, "Surface Chemistry" Theory and Industrial Applications, Reinhold, New York, 1962.

5. M. Joly, in "Recent Progress in Surface Science", (Eds: J.F. Danniellli, K.G.A. Pankhurst and A.C. Riddiford) Vol.1, p.1. Academic Press, New York 1964.

6. M. Joly, in "Surface & Colloid Science" (Ed. E. Matijevic) Vol.5, p. 1 and 79, John Wiley & Sons, 1972.

7. G.L. Gaines Jr. "Insoluble Monolayers at Liquid-Gas Interfaces", Interscience Publishers, New York, 1966.

8. G.T. Barnes in "A Specialist Periodical Reports : Colloid Science" Vol.2, p. 182 and 1975, Vol.3, p.150, 1979.

9. A.W. Adamson, "The Physical Chemistry of Surfaces" 2nd Edn. Interscience Publishers, New York, 1967.

10. Monolayers: Advances in Chemistry Series, 144 (Ed. E.D. Goddard), American Chemical Society, Washington D.C., 1975.

11. N.L. Gershfeld, in "Methods in Membrane Biology" Vol.1, Chap.2, Plenum Press, New York, 1974.

12. J.H. Fendler, "Membrane Mimetic Chemistry" John Wiley & Sons, 1982.

LIST OF PUBLICATIONS

1) Surface viscosity and pressure area isotherms of mixed monolayers of hexadecanol with docosanol and hexadecoxy ethanol with docosanoxy ethanol at 25°C.
V.S. Kulkarni and S.S. Katti
J.Colloid Interface Sci. 89 (1982) 40.

2) Surface viscosity, pressure area isotherms of mixed monolayers of hexadecoxypropanol with docosanoxy-propanol at air-water interface
V.S. Kulkarni and S.S. Katti
Indian J.Chem. In press.

3) Comments on orientation and compatibility in mixed monolayers of polymers and low molecular weight compounds
V.S. Kulkarni and S.S. Katti
Colloids and Surfaces. In press.

4) Mixed monolayers of polyvinyl stearate with eicosanol, docosanoxyethanol and docosanoxypropanol
V.S. Kulkarni and S.S. Katti
Colloids and Surfaces. In press.